METABOLIC REGULATION OF QUIESCENCE ENTRY AND EXIT IN *SACCHAROMYCES CEREVISIAE*

APPROVED BY SUPERVISORY COMMITTEE

Jennifer Kohler, Ph.D

Melanie Cobb, Ph.D

Hongtao Yu, Ph.D

Benjamin Tu, Ph.D

METABOLIC REGULATION OF QUIESCENCE ENTRY AND EXIT IN *SACCHAROMYCES CEREVISIAE*

by

LEI SHI

DISSERTATION

Presented to the Faculty of the Graduate School of Biomedical Sciences

The University of Texas Southwestern Medical Center at Dallas

In Partial Fulfillment of the Requirements

For the degree of

DOCTOR OF PHILOSOPHY

The University of Texas Southwestern Medical Center

Dallas, Texas

December, 2014

METOBOLIC REGULATION OF QUIESCENCE ENTRY AND EXIT IN *SACCHAROMYCES CEREVISIAE*

LEI SHI

The University of Texas Southwestern Medical Center at Dallas, 2014

BENJAMIN TU, Ph.D

Unicellular microorganisms often enter a state called quiescence when they encounter harsh environmental conditions. They stop growth and proliferation until conditions improve. In

quiescence, the budding yeast slows down transcription three- to five-fold, while its translation rate drops to 0.3% of that in growth phase. Importantly, yeast quiescent cells have remarkably higher stress resistance than growing cells. Once conditions improve, they readily re-enter the cell cycle. Though quiescence is an important phase of cell life, its understanding has been limited.

Previously, Allen *et al.* reported the isolation of quiescent yeast cells from stationary phase culture by cell density fractionation (Allen et al., 2006). Cells of high density, which they termed quiescent cells, were more stress-resistant and had more growth potential when conditions improved. However, it remained unknown how quiescent cells became dense and what mechanism allowed cells to enter quiescence. I report the intracellular glycogen and trehalose accumulation leads to increased density of quiescent yeast cells. Glycogen and trehalose are two carbon reserves yeast cells accumulate during entry into quiescence. Cells unable to produce glycogen and trehalose exhibit no density change during the entry of quiescence. Furthermore, yeast cells lacking trehalose dramatically slowed down the adaptation and growth in fresh nutrients. Thus, trehalose is a key determinant of the quiescent state and possibly fuels rapid cell cycle progression in the presence of fresh nutrients.

When conditions improve, quiescent yeast cells readily re-enter growth. The proper regulation of quiescence exit in response to the environment is of vital importance to balance cell growth and quiescence. In budding yeast, *CLN3* is one of the G1 cyclins that govern cell cycle entry and transition from G1 to S phase. *CLN3* is the first activated G1 cyclin that subsequently induces the other G1 cyclins. Notably, *CLN3* deletion slows down yeast cell cycle entry. Thus, studying *CLN3* expression in response to nutrients may reveal the key mechanism of quiescence

exit. I report acetyl-CoA induces immediate *CLN3* transcription in quiescent yeast cells. Acetate derived surge of acetyl-CoA promotes extensive histone H3 acetylation at *CLN3* promoter mediated by the SAGA complex, a histone H3 acetyltransferase. The acetylated histones loosen the chromatin at *CLN3* promoter and facilitate rapid *CLN3* transcription. Thus, acetyl-CoA is sensed by the SAGA complex to induce *CLN3* transcription that promotes quiescence exit and regrowth.

Altogether, my studies have revealed insights into how yeast cells enter and exit quiescence metabolically. In addition to yeast cell quiescence regulation, my studies may also aid in understanding the key mechanisms of quiescence regulation in higher eukaryotic systems.

TABLE OF CONTENTS

PRIOR PUBLICATIONS

Lei Shi, Benjamin P. Tu. Protein acetylation as a means to regulate protein function in tune with metabolic state. *Biochem. Soc. Trans. 2014 42:4 1037-1042*

Lei Shi, Benjamin P. Tu. Acetyl-CoA induces transcription of the key G1 cyclin *CLN3* to promote entry into the cell division cycle in *Saccharomyces cerevisiae. PNAS 2013 110 (18) 7318-7323*

Lei Shi, Benjamin M. Sutter, Xinyue Ye, and Benjamin P. Tu. Trehalose Is a Key Determinant of the Quiescent Metabolic State That Fuels Cell Cycle Progression upon Return to Growth. *Mol. Biol. Cell 2010 21:12 1982-1990*

List of Figures

List of Tables

List of abbreviations

ABF2	ARS-Binding Factor 2
Acetyl-CoA	Acetyl-Coenzyme A
ACS1/2	Acetyl-CoA Synthetase 1/2
ACT1	Actin 1
ADA2/3	transcriptional ADAptor 2/3
ATP	Adenosine TriPhosphate
ATP1/2	ATP synthase 1/2
AZF1	Asparagine-rich Zinc Finger 1
cAMP-PKA	cyclic Adenosine MonoPhosphate – Protein Kinase A
CDC28	Cell Division Cycle 28
ChIP-Seq	Chromatin Immunoprecipitation – Sequencing
CLB5/6	Cyclin B 5/6
CLN1/2/3	Cyclin 1/2/3
CoA	Coenzyme A
COR1	Core protein of QH2 cytochrome c reductase 1
dO2	dissolved Oxygen

DS	Diauxic Shift
ER	Endoplasmic Reticulum
FHL1	Fork Head Like 1
GCN5	General Control Nonderepressible 5
GFP	Green Fluorescent Protein
GLC3	Glycogen branching enzyme 3
GRE	Glucose Responsive Element
HAT	Histone Acetyltransferase
HPA2	Histone and other Protein Acetyltransferase 2
HygroR	Hygromycin Resistant
ICL1	IsoCitrate Lyase 1
IGO1/2	Initiation of G zerO 1/2
KanR	Kanamycin Resistant
KGD1	alpha-KetoGlutarate Dehydrogenase 1
LSM1	Like SM 1
MCM1	MiniChromosome Maintenance 1
MPT5	Multicoy suppressor of Pop Two 5

mRNA	messenger RNA
mRNP	messenger RNA
mtDNA	mitochondrial DNA
NatR	Nourseothricin Resistant
nonQ cells	non-quiescent cells
NTH1	Neutral Trehalase 1
OD600	Optical Density at 600 nm
OX	OXidative
PBS	Phosphate Buffered Saline
PET	Positron Emission Tomography
PKA	Protein Kinase A
Q cells	quiescent cell
QCR7	ubiQuinol-cytochrome C oxidoReductase 7
RAP1	Repressor Activator Protein 1
RB	Reductive Building
RC	Reductive Charging
RGT2	Restores Glucose Transport 2

Rho0	Strain lacking mtDNA
Ribi	ribosome biogenesis
RIM15	Regulator of IME2 15
RIP1	Rieske Iron-sulfur Protein 1
ROS	Reactive Oxygen Species
RP	Ribosomal Protein
RPD3	Reduced Potassium Dependency 3
RPL33B	Ribosomal Protein of the Large subunit 33B
RPS11B	Ribosomal Protein of the Small subunit 11B
SAGA	Spt-Ada-Gcn5 Acetyltransferase
SAS2/3	Something About Silencing 2/3
SDH4	Succinate DeHydrogenase 4
SGal	Synthetic medium with Galactose
SGF73	SAGA associated Factor 73
SNF2/3	Sucrose NonFermentable 2/3
SP	Stationary Phase
SPT7	Suppressor of Ty's 7

SSD1	Suppressor of SIT4 Deletion 1
SWI/SNF	Switch/Sucrose NonFermentable
TCA	TriCarboxylic Acid cycle
TORC1	Target Of Rapamycin Complex 1
TPS1	Trehalose-6-Phosphate Synthase 1
UDP	Uridine DiPhosphate
WHI3/5	Whiskey 3/5
WT	Wild Type
YDJ1	Yeast DnaJ 1
YMC	Yeast Metabolic Cycle
YP	Yeast Extract
YPD	Yeast Extract with Glucose
YPGal	Yeast Extract with Galactose
YPGal-T	Yeast Extract with Galactose minus Trehalose

I. INTRODUCTION

Quiescence, also called G0 in the cell cycle, is a state where cells do not grow or proliferate in response to stress conditions, such as nutrient starvation, heat and cold shock, oxidative stress, etc. Post-mitotic cells employ the G1 cell cycle checkpoint to assess the extracellular environment and determine whether to proceed with another cell division. If the condition is not favorable, cells will alternatively stop and enter quiescence. Quiescence is the most common cell state on earth. Most microbes on earth exist in a dormant but viable state and are often unculturable in limited laboratory conditions (Lewis, 2007). In multicellular eukaryotes, quiescence is also the most common cellular state after organismal maturity, such as quiescent stem cells and terminally differentiated cells. Features of quiescence are essential for stem cell maintenance (Suda et al., 2005), as well as activating cells for wound healing (Chang et al., 2002). Thus, understanding the regulation of quiescence will be relevant to diverse biological processes including the life cycle of pathogens, the development of cancer, and the survival and reproduction of all living organisms.

Saccharomyces cerevisiae, or the budding yeast, undergoes quiescence in response to a variety of stresses. It is the most studied unicellular eukaryote, with the most complete set of experimental tools available. The basic cellular processes (e.g. cell cycle, metabolism, nutrient sensing) of the budding yeast are largely conserved among the eukaryotes. Thus, using budding yeast as a model system of quiescence would likely provide key insights in basic cellular mechanisms used by eukaryotes.

Yeast quiescence is usually triggered by waning supplies of nutrients in common laboratory conditions. After rapid logarithmic growth in rich media, yeast cells exhaust glucose

and reprogram their metabolism for the transition from fermentation to respiration. The reprogramming is known as the diauxic shift (DS). In post-DS phase, or stationary phase (SP), yeast cells rely on nonfermentable carbon sources from the spent media to complete the last round of cell division. Once all carbon sources are depleted, they arrest growth completely and enter the quiescent state. Quiescent cells adopt completely different traits from rapidly growing cells including: thickened cell wall, decreased metabolic rate, accumulation of storage molecules, such as glycogen and trehalose, acquired resistance to stresses (Werner-Washburne et al., 1993), three- to five- fold decreased transcription (Choder, 1991), decreased translation at 0.3% of that in logarithmic phase (Fuge et al., 1994), and condensed chromosomes (Pinon, 1978). Many of these traits are common among various eukaryotic systems, including human quiescent cells. Thus, it will be of significant interest to understand how these traits are regulated and how they contribute to quiescence.

Although yeast quiescence is usually established by depletion of nutrients, work over the past few decades has shown that these cells are not starved. Before nutrients are exhausted, yeast cells redirect their resources and metabolism to conserve and stockpile critical provisions, including glucose, phosphate, and fatty acids (De Virgilio, 2012; Francois and Parrou, 2001; Lillie and Pringle, 1980). Glucose is stored in the form of trehalose and glycogen. These carbohydrates provide a ready energy source when cell division resumes (Sillje et al., 1999).

Trehalose is a natural alpha-linked disaccharide formed from two glucose molecules. Trehalose synthesis has been found in many eukaryotic systems, including fungi, crustaceans, insects and plants. With its hydroxyl groups, trehalose forms hydrogen bonds with proteins and membrane lipids in a manner similar to the water effect during hydration (Crowe et al., 1992).

Thus, trehalose has been proposed to stabilize and protect proteins and membranes (Elbein et al., 2003) from dehydration (Gadd et al., 1987), heat shock (De Virgilio et al., 1994; Hottiger et al., 1994; Ribeiro et al., 1997), and oxidative damage (Benaroudj et al., 2001). When stress is alleviated, trehalose-protected molecules can resume their normal function and allow rapid exit of quiescence. The tardigrade, commonly called water bear, is a micro-animal that can resist complete dehydration due to tremendous accumulation of trehalose (Hengherr et al., 2008). When they receive water, tardigrades revive and return to their metabolic state. Trehalose has also been found essential for the acquired viability in near-freezing temperature (Kandror et al., 2004). Yeast strains are commonly stored in refrigerator in laboratories. While yeast cells adapt to the cold temperature, trehalose synthesis enzymes increased concomitantly with trehalose accumulation. Mutants lacking trehalose synthesis did not survive in cold. Consequently, trehalose has been used in preserving various biological materials in research and industry (Erdag et al., 2002; Zhou et al., 2010). In addition, trehalose has been proposed as a rapid energy source to fuel the cell cycle entry. Unlike glycogen, the degradation of trehalose can instantly generate two glucose molecules upon re-initiation of growth. Interestingly, insects use trehalose instead of glucose in the blood as the major energy source for flight (Becker et al., 1996).

ISOLATION OF QUIESCENT CELLS FROM STATIONARY PHASE CULTURE

Yeast “stationary phase” has mistakenly been considered identical to “quiescence”. Previous investigations of quiescence had used stationary phase cultures, assuming all cells in stationary phase were quiescent. However, stationary phase cultures were heterogeneous with mixed cell types (Allen et al., 2006). By density fractionation, cells in stationary phase culture were separated into two cell populations. After rapid growth in rich media, yeast cells exhausted

the glucose and entered diauxic shift to prepare for the transition into stationary phase. During the transition, a population of yeast cells gradually became dense while the other population remained light. The dense cells were more tolerant to stresses, such as heat shock. When nutrients were repleted, they could readily enter cell cycle synchronously. Thus, these cells were called quiescent cells (Q cells) (Allen et al., 2006). In contrast, the light cells appeared less resistant to stresses and did not respond uniformly to the repletion of nutrients. They were termed non-quiescent cells (nonQ cells).

The two cell populations have distinct morphological characteristics (Allen et al., 2006). By light microscopic examination, Q cells were uniformly unbudded, most of which (90%) were virgin daughter cells. They were also quite light refractive, suggestive of their fortified cell walls. Under electron microscopy, Q cells contained a single, electron-dense vacuole, but no other apparent organelles, such as mitochondria or endoplasmic reticulum. With phosphotungstic acid staining, a large number of glycogen granules were observed in Q cells. In contrast, nonQ cell population contained both budded and unbudded cell types. They were comprised of cells at various replicative ages, ranging from virgin daughter cells to old mother cells. Their cell walls were not as thick as Q cells. Interestingly, nonQ cells contained massive amounts of mitochondria and ER under electron microscope, and their vacuoles contained numerous vesicles. In stark contrast to Q cells, nonQ cells did not contain glycogen granules.

In addition, Q cells tended to be more viable (assessed by vacuolar accumulation of a fluorescent dye that depends on active metabolism) and more capable of reproduction (assessed by colony forming capability). They also displayed very few signs of ROS accumulation or apoptosis. In contrast, though most nonQ cells appeared viable, only ~40% of nonQ cells formed

colonies. nonQ cells also displayed signs of ROS accumulation and apoptosis (Allen et al., 2006).

Microarray analysis also revealed differences between the two cell populations (Allen et al., 2006). Q cells expressed transcripts encoding proteins for water stress, fatty acid oxidation, membrane integrity and some metabolic pathways, such as coenzyme metabolism. These transcripts indicate Q cells were prepared to resist environmental stresses and might use fatty acid oxidation to meet their energy need to maintain quiescence. In nonQ cells, most abundant transcripts were associated with DNA recombination and transposition, indicating nonQ cells did not arrest their growth in the absence of nutrients.

The isolation of pure quiescent yeast cells from stationary phase may substantially facilitate the progression of yeast quiescence research. Compared to studying quiescence in stationary phase culture, this method potentially minimizes interfering phenotypes from nonQ cell population and helps to uncover the mechanism of quiescence regulation within Q cells.

YEAST METABOLIC CYCLE – A HIGHLY COORDINATED AND MORE NATURAL SYSTEM UNDER LIMITED NUTRIENT AVAILABILITY

In our laboratory, the yeast metabolic cycle (YMC) has been extensively characterized and utilized as a powerful culture system. When a prototrophic yeast strain such as CEN.PK is grown to high density, starved for glucose, and then fed with limited continuous glucose, they display robust oscillations of dissolved oxygen consumption (Figure I-1). By microarray analysis, more than half of the yeast genes are periodically expressed as a function of the YMC (Tu et al., 2005). Genes of similar function are expressed coordinately in the same temporal

window, while different functional gene groups have distinct temporal expression. Although the nutrient-rich batch culture system has been used extensively to uncover many basic cellular mechanisms, it may not always be representative of the natural environment that wild yeast lives in. Compared to the nutrient-rich conditions, the YMC more resembles the nutrient-poor state that yeast cells might encounter in nature. Under such challenging conditions, yeast cells deploy regulatory strategies that are fundamentally different from their behaviors in rich media. Many genes that are not expressed significantly in rich media are expressed during the YMC, such as genes involved in mitochondrial and peroxisomal function, autophagy, and ubiquitination. More importantly, these genes are activated precisely according to the temporal phase of the YMC. Thus, YMC may facilitate the elucidation of fundamental mechanisms of yeast cellular response to the environment.

Based on clustering analysis of the YMC transcriptome, three distinct phases can be discerned as OX (oxidative), RB (reductive building), and RC (reductive charging) phase (Figure I-2). The OX phase is a phase where oxygen consumption suddenly increases with a sharp decrease in dissolved oxygen. The rapid oxygen consumption indicates that yeast cells in this phase dramatically increase their respiration for energy. Consistent with this prediction, transcripts encoding ribosome biogenesis and amino acid biosynthesis that consume the majority of cellular energy increase sharply. These transcripts suggest the OX phase may be devoted to the establishment of protein synthesis machinery for growth and subsequent cell division. Transcripts of *CLN3*, the first activated G1 cyclin to initiate cell cycle, also peak precisely with ribosome biogenesis transcripts. To enter the cell cycle, Cln3p activates the cyclin-dependent kinase Cdc28p and induces transcription of over 200 downstream effectors including *CLN1* and *CLN2* to transition from G1 to S phase (Ferrezuelo et al., 2010). Toward the end of the OX phase

and after *CLN3* transcription peaks, *CLN1* and *CLN2* mRNAs increase sharply, confirming the role of the OX phase in cell growth for the preparation of the subsequent cell division.

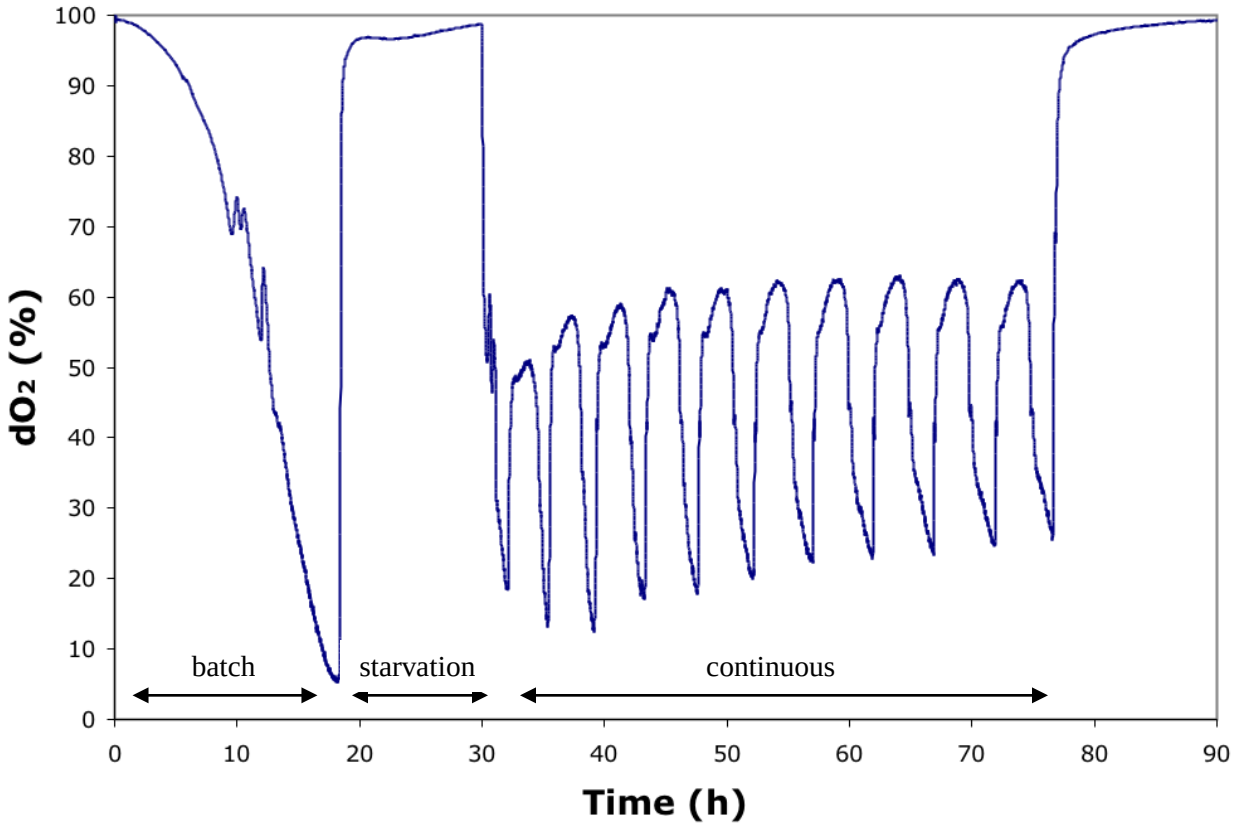

Figure I-1 The metabolic cycle of yeast. During batch mode, the cells are grown to a high density and then starved for at least 4 hours. During continuous mode (arrow), media containing glucose is introduced to the culture at a constant dilution rate (~0.09 to 0.1 per hours). dO2 refers to dissolved oxygen concentrations (% saturation) in the media

In the RB phase following the OX phase, yeast cells slow down respiration and transition to a reductive phase characterized by reduced rates of oxygen consumption. As visualized using light microscopy, 40-50% of yeast cells initiate budding synchronously. Consistently, transcripts encoding proteins involved in DNA replication, histones, and spindle pole body components can be observed. Furthermore, the majority of mitochondria biogenesis transcripts also peak in this phase, indicating cells may rebuild their mitochondria in response to the intense respiration from the previous phase. Notably, cells gate their DNA replication and mitosis strictly to the RB phase but none in the OX phase. Cell cycle mutants that forced cell division during the OX phase were found to accumulate spontaneous mutations (Chen et al., 2007). Thus, the RB phase is a phase for cells to divide and replenish their mitochondria.

The RC phase is typically the longest of the three phases and immediately follows the RB phase. This phase is characterized by steady rates of low oxygen consumption. Many gene products for metabolism of carbon sources other than glucose are elevated during this temporal window, including peroxisomal functions, metabolism of carbohydrate storage and ethanol utilization. These indicate that cells in the RC phase rely on alternative metabolic strategies for energy production. Furthermore, many genes associated with stress response and starvation are highly expressed, including proteasome proteins, vacuole and autophagy components. These observations predict cells are actively recycling and recharging for the preparation to enter the OX phase again.

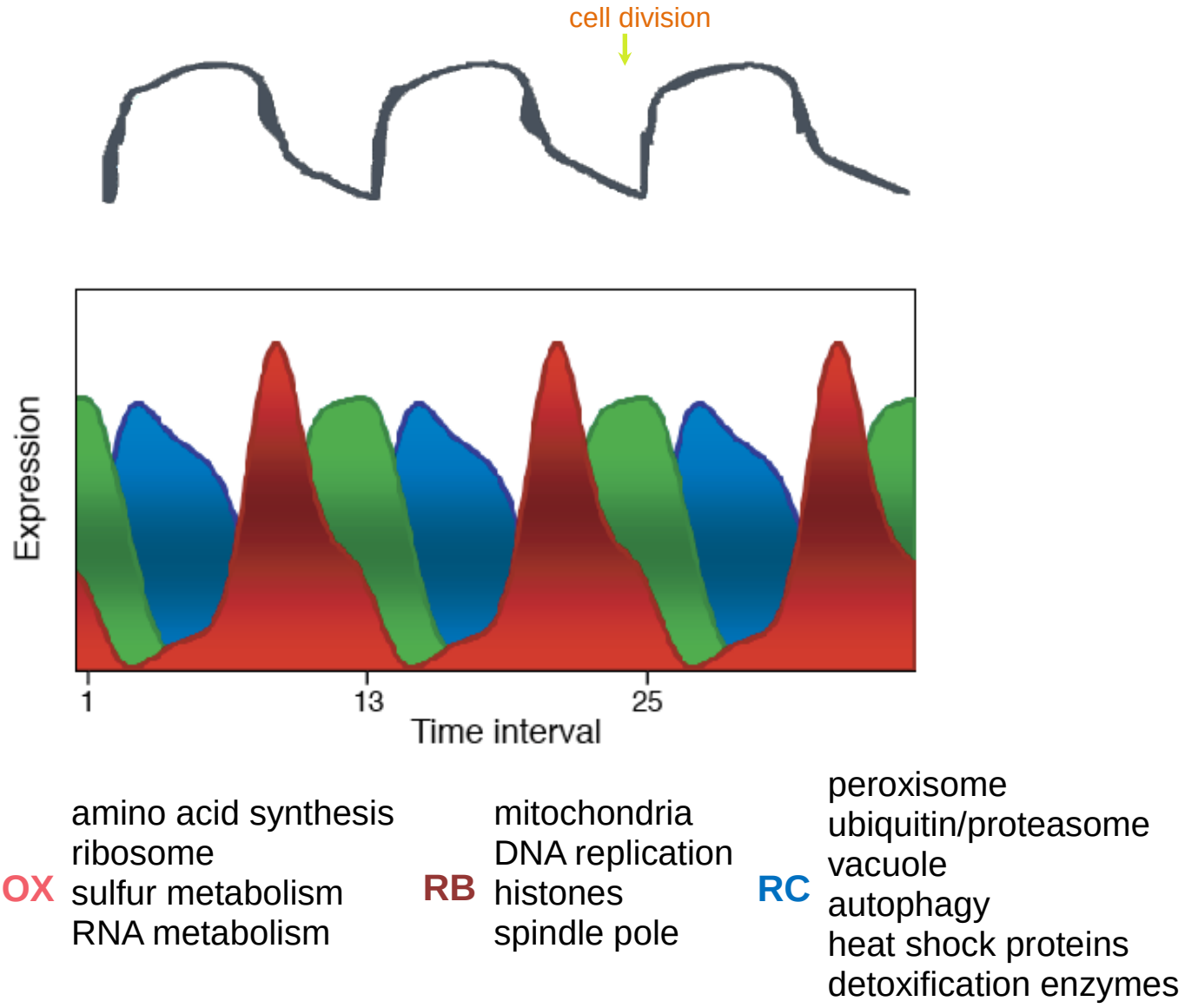

Figure I-2 Gene expression cluster during the metabolic cycle. Average profiles for the three superclusters of gene expression during the metabolic cycle: OX (oxidative), RB (reductive, building), and RC (reductive, charging). The OX supercluster (1023 genes) peaks roughly during time intervals 8 to 12, 20 to 24, and 32 to 36; the RB supercluster (977 genes), during time intervals 10 to 14 and 22 to 26; and the RC supercluster (1510 genes), during time intervals 2 to 7, 14 to 19, and 26 to 31. Examples of classes of genes in each supercluster are listed.

Beyond the highly coordinated periodic mRNA fluctuations, the YMC also displays cyclic changes of metabolites. As monitored by both liquid chromatography tandem mass spectrometry and two-dimensional gas chromatography/time-of-flight mass spectrometry, common intracellular metabolite concentrations were profiled across the YMC (Tu et al., 2007). These surveys reveal that many metabolites oscillated their abundance precisely as a function of the YMC, such as carbohydrates, amino acids and nucleotides. According to these data, the logic of the metabolic oscillations largely matches the prediction from the transcriptome analysis, indicating many metabolic activities are regulated differently in distinct YMC phases. Retrospectively, the YMC metabolome may also extend the understanding of the regulation of YMC beyond the transcriptome data. Certain metabolites may inherently exhibit cyclic changes and in turn, have a reciprocal role in regulating the YMC. Thus, many cellular processes are intimately coupled to cyclic changes in metabolism or redox homeostasis to be executed efficiently and optimally.

ACETYL-COA AS A CUE TO INITIATE CELL GROWTH AND PROLIFERATION

Acetyl-CoA is a central metabolite in cellular energy metabolism. Acetyl-CoA is compartmentalized between mitochondrial and nucleo-cytosolic pools (Takahashi et al., 2006). Typically, glucose is a major source of acetyl-CoA. Glucose is converted to pyruvate through glycolysis in the cytoplasm. Pyruvate then is transported into mitochondria and converted to acetyl-CoA by the pyruvate dehydrogenase complex. Alternatively, mitochondrial pools of acetyl-CoA can be generated from fatty acid oxidation, CoA transferases (Fleck and Brock, 2009), or mitochondrial acetyl-CoA synthetase enzymes (Fujino et al., 2001; Perez-Chacon et al., 2009). Cells can also produce acetyl-CoA from available amino acids, such as glutamine and

leucine (Hensley et al., 2013). Cytosolic acetyl-CoA can be produced from mitochondrial-derived citrate via the enzyme ATP citrate lyase, or from acetate by the nucleo-cytosolic acetyl-CoA synthetase enzymes (Luong et al., 2000; Wellen et al., 2009). Once generated, acetyl-CoA has multiple fates. Acetyl-CoA can be coupled to oxaloacetate for entry into the TCA cycle as citrate, which then through a series of transformations is used for synthesis of ATP or particular amino acids and cofactors. Acetyl-CoA in the cytosol can be carboxylated to form malonyl-CoA, the initial step in fatty acid synthesis. Acetyl-CoA is also used as a substrate in the biosynthesis of numerous other metabolites. In addition, as discussed below, acetyl-CoA is the acetyl group donor for numerous acetylation modifications that occur on proteins (Cai et al., 2011; Takahashi et al., 2006; Wang et al., 2010; Zhao et al., 2010).

Beyond its role in energy metabolism and biosynthesis, acetyl-CoA also functions as the acetyl group donor for protein acetylation modifications. Recently, my lab colleague Ling showed that intracellular acetyl-CoA levels oscillate as a function of the growth status of yeast cells and can in turn influence the abundance of certain protein lysine acetylation modifications (Cai et al., 2011). That is, particular acetylation modifications could in fact be regulated by the availability of this acetyl donor.

During the YMC, yeast cells can become highly synchronized and undergo robust oscillations in oxygen consumption (as discussed above) (Tu et al., 2005). Metabolite profiling studies revealed that acetyl-CoA levels oscillate periodically as a function of the YMC (Tu et al., 2007). Upon exit of the RC quiescent-like phase and entry into the OX growth phase, intracellular trehalose and glycogen reserves rapidly decrease which is accompanied by an increase in glucose. Shortly after this rise in glucose, acetyl-CoA level sharply increases,

precisely correlating with the temporal window of growth gene induction (Tu et al., 2005; Tu et al., 2007). Acetyl-CoA level decreases as cells enter the RC phase, whereupon stress and survival genes are induced. Intracellular acetyl-CoA in batch culture-grown cells also increases substantially upon nutrient repletion (Cai et al., 2011). However, prior to these observations, a role for acetyl-CoA in growth regulation was perhaps not considered because of its abundance and ease of synthesis in cells grown in glucose-rich medium.

Thus, acetyl-CoA may function as a metabolic cue to induce cell growth upon carbon source repletion. Consistently, various carbon sources, including glucose, ethanol and acetate, stimulated cells in the RC phase to enter growth in the OX phase. Following addition of 13C-labeled acetate, 13C-acetyl-CoA levels increased rapidly within a minute, and further induced synthesis of unlabeled 12C-acetyl-CoA, likely from other carbon sources to further promote growth (Cai et al., 2011). By surveying acetylated proteins following addition of 13C-acetate, beside histones, Spt7p, Sgf73p and Ada3p were identified to be acetylated precisely upon growth entry, in tune with the increase in intracellular acetyl-CoA. These proteins are components of the transcriptional coactivator complex SAGA, which harbors histone acetyltransferase activity (Grant et al., 1997; Grant et al., 1999). It was further observed that numerous sites on histone H3 (K9, K14, K18, K23, K27) and H4 (K5, K8, K12) linked to gene activation were also acetylated precisely in tune with the spike in acetyl-CoA levels in the OX phase. Subsequent ChIP-Seq analysis revealed that the acetylated histones were present primarily at a distinctive set of more than 1,000 genes important for cell growth that are induced during the OX phase. Thus, the increase in acetyl-CoA may induce SAGA to acetylate histones at each of these genes, in turn activating their transcription and enabling cells to commit to growth (Figure I-3). Acetylation of

histones at these genes is dependent on Gcn5p, the acetyltransferase enzyme within SAGA, and mutation of GCN5 or these components of SAGA disrupts the YMC (Cai et al., 2011).

These studies using the YMC have revealed that acetyl-CoA plays a key role in regulating particular acetylation events that are important for cell growth. They suggest that the acetyltransferase Gcn5p present within SAGA has the distinctive ability to acetylate its substrates in concert with surges in acetyl-CoA. Consistent with this idea, additional Gcn5p substrates, including the transcriptional co-activator of ribosomal subunit genes Ifh1p and the subunit of the SWI/SNF chromatin remodeling complex Snf2p (Cai et al., 2013; Kim et al., 2010), were also dynamically acetylated in tune with acetyl-CoA. Interestingly, proteins that are acetylated but which are not Gcn5p substrates, were not dynamically acetylated in tune with the acetyl-CoA fluctuations that occur in the YMC (Cai et al., 2011). Taken together, these data suggest that in budding yeast, the acetylation of Gcn5p substrates is driven by intracellular acetyl-CoA.

The quiescent state is common to all organisms on earth and understanding the metabolic basis of quiescence may provide key insights into multiple types of human diseases, such as cancer, pathogenic infection and neurodegenerative diseases. During my graduate work, I have uncovered mechanisms governing yeast quiescence entry and exit mediated by the cellular metabolic state. When yeast cells enter quiescence in response to nutrient starvation, trehalose and glycogen accumulate significantly, which causes an increase in cellular density. During the maintenance of quiescence, trehalose is preferentially maintained over glycogen by quiescent cells. Upon quiescence exit, yeast cells rapidly degrade the stored trehalose, possibly to fuel the initiation of cell cycle. To exit quiescence, yeast cells must sense the presence of sufficient

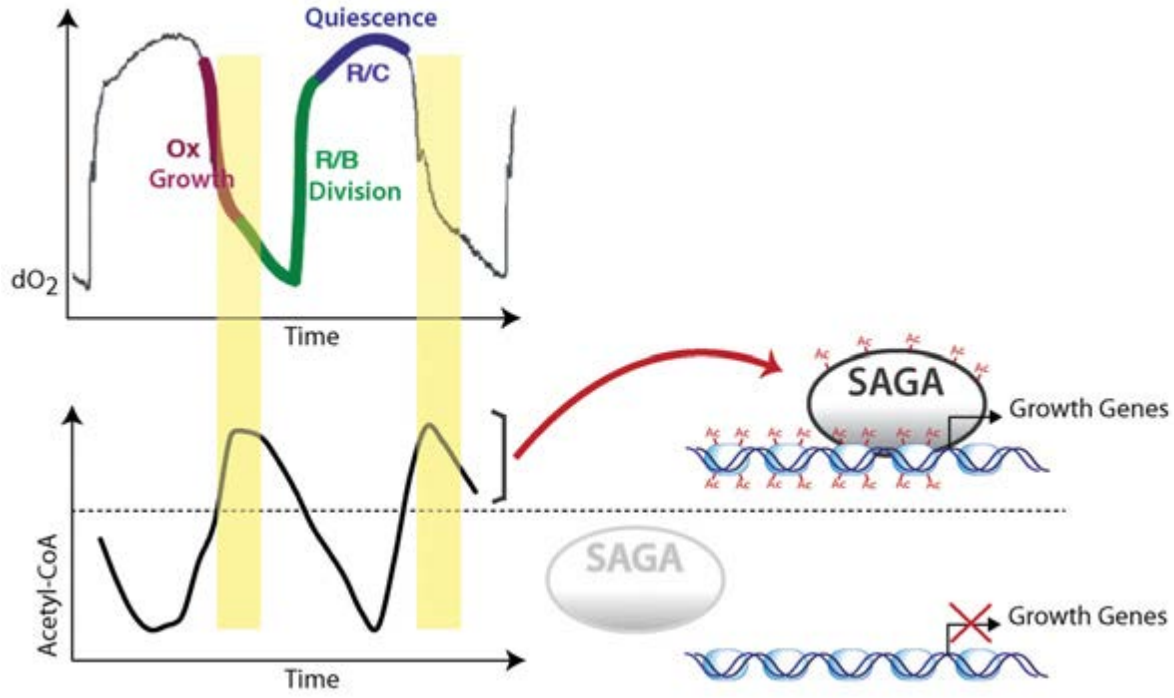

Figure I-3. Acetyl-CoA increase stimulates transcription of growth genes. Yeast cells undergo robust oscillations in oxygen consumption during continuous glucose-limited growth. Each YMC can be divided into three phases: the oxidative (Ox) growth phase, reductive/building (R/B) phase where cells divide and reductive charging (RC) phase reminiscent of quiescence. During the oxidative growth phase, a burst of acetyl-CoA induces the autoacetylation of the transcriptional co-activator complex SAGA and its subsequent recruitment to the promoters of more than 1000 growth genes to acetylate histone H3. The acetylated histones enable transcription of these growth genes to support growth entry.

nutrients to initiate cell cycle entry. CLN3 is the first G1 cyclin that is expressed and activated to initiate the cell cycle. The lack of CLN3 leads to slower entry of cell cycle. Despite numerous studies of CLN3 regulation, the mechanism underlying its transcriptional induction by glucose remained elusive. I have found that the metabolite acetyl-CoA downstream of glycolysis is the direct metabolic inducer of CLN3 transcription upon quiescence exit. The elevated acetyl-CoA availability, derived from either glucose or acetate, can be sensed by the histone H3 acetyltransferase SAGA complex that acetylates histone H3 at the CLN3 promoter region. The acetylated histones then support rapid CLN3 transcription. Cln3 can then activate over 200 downstream genes for continued entry into the cell division cycle.

II. TREHALOSE IS A KEY DETERMINANT OF QUIESCENT METABOLIC STATE THAT FUELS CELL CYCLE PROGRESSION UPON RETURN TO GROWTH

When conditions are not favorable, virtually all living cells have the capability of entering a resting state termed quiescence or G0. Many aspects of the quiescence program as well as the mechanisms governing the entry and exit from quiescence remain poorly understood. Previous studies using the budding yeast *Saccharomyces cerevisiae* have shown that upon entry into stationary phase, a quiescent cell population emerges that is heavier in density than nonquiescent cells. Here, we show that total intracellular trehalose and glycogen content exhibits substantial correlation with the density of individual cells both in stationary phase batch cultures and during continuous growth. During prolonged quiescence, trehalose stores are often maintained in favor over glycogen, perhaps to fulfill its numerous stress-protectant functions. Immediately upon exit from quiescence, cells preferentially metabolize trehalose over other fuel sources. Moreover, cells lacking trehalose initiate growth more slowly and frequently exhibit poor survivability. Together, our results support the view that trehalose, which is more stable than other carbohydrates, provides an enduring source of energy that helps drive cell cycle progression upon return to growth.

INTRODUCTION

When environment becomes unfavorable, all living cells exit mitosis and enter a state called quiescence. Once the environment improves, they readily re-enter growth and proliferation, thus exiting quiescence. The budding yeast *Saccharomyces cerevisiae* is commonly used to study quiescence due to its advantages, including the highly conserved basic cellular processes, the tractability to all levels of experimentation and the capability of entering the quiescence that shares characteristics with quiescent mammalian cells.

In the laboratory, yeast is usually cultured in nutrient-rich medium. After glucose exhaustion, yeast cells transition into diauxic shift and then enter stationary phase to grow on nonfermentable carbon sources. The survivability of the cell population in such conditions has been used as one of the important measures of quiescence, called chronological lifespan (Fabrizio and Longo, 2007; Powers et al., 2006). However, stationary phase is not identical to quiescence. Cells in stationary phase cultures are a mixture of budded and unbudded cells (Gendron et al., 2003; Werner-Washburne et al., 2002), suggesting there is differentiation in the stationary phase cell population. Recently, pure quiescent cells were separated from nonquiescent cells in the stationary phase culture by density fractionation (Allen et al., 2006). During stationary phase, a population of cells gradually became heavy while the other population remained light. The heavy cells displayed more reproductive potential and more tolerance to heat shock, thus being termed quiescent cells. Furthermore, they were mostly unbudded and could enter mitosis synchronously. In distinction, the light cells were heterogeneous with both budded and unbudded cells. They were less resistant to heat stress and did not readily grow and proliferate upon nutrient repletion so they were termed nonquiescent cells (Allen et al., 2006).

Morphological examination revealed that quiescent cells did not contain obvious mitochondria and endoplasmic reticulum but showed high levels of glycogen accumulation. Numerous transcripts were enriched in either quiescent or nonquiescent cell populations (Aragon et al., 2008). However, the determinant of increased density of quiescent cells as well as the mechanism establishing quiescence still remains unclear.

Here, we describe how our studies of metabolic cycles in budding yeast lead to the finding that the carbohydrate trehalose is a key determinant of the quiescent metabolic state and moreover functions as an energy reserve that helps fuel the exit from quiescence.

RESULTS

Cells in the RC phase of the yeast metabolic cycle become dense and resemble stationary phase quiescent cells

During continuous growth under nutrient-poor conditions, budding yeast exhibit robust oscillations in oxygen consumption (Kaspar von Meyenburg, 1969; Parulekar et al., 1986; Porro et al., 1988; Satroutdinov et al., 1992; Tu et al., 2005). Such cycles are characterized by phases of rapid oxygen consumption that alternate with phases where the rate of oxygen consumption is substantially lower. Numerous cellular and metabolic processes, including cell division, were found to be precisely orchestrated about these "yeast metabolic cycles" (YMCs) to defined temporal windows. Three phases of the YMC were defined by analysis of periodic gene expression patterns: an oxidative (OX) growth phase that coincides with a burst of mitochondrial respiration; a reductive, building phase (RB) where cells divide and up-regulate transcription of mitochondrial gene products; and a reductive, charging phase (RC) where many genes associated with starvation, stress-associated responses, and slow growth are induced (Brauer et al., 2008; Tu et al., 2005; Tu and McKnight, 2006). Yeast cell populations repeatedly undergo these three phases during continuous growth, and so the YMC can be interpreted to represent the life of a yeast cell under glucose-poor growth conditions (Tu and McKnight, 2006, 2007).

Metabolic cycles occur under glucose-poor conditions that to a first approximation might parallel those encountered by batch cultures sometime upon entry into stationary phase. Moreover, because in every metabolic cycle approximately half of the cell population divides (Tu et al., 2005), we wondered whether cycling cells might transiently segregate into quiescent and nonquiescent populations that resemble those observed previously in rich medium stationary

phase cultures (Allen et al., 2006).

To test this possibility, we collected cells at 16 time points across one metabolic cycle and subjected them to centrifugation through density gradients to assess whether there were any differences in the density of individual cells as a function of the YMC (Figure II-1). Interestingly, we observed that during the late RC phase (time points 5–10), the majority of cells became noticeably heavier in density. As they entered the OX growth phase (time points 11–14), a portion of the cell population became lighter in density. We estimated the average density of the entire cell population by comparing the sedimentation patterns of cells with those of marker beads with known, predetermined density (Materials and Methods). These calculations confirm that the average density of the cell population increases during the RC phase and subsequently decreases upon entry into the OX, growth phase. Thus, during late RC phase of the YMC, the majority of cells are reminiscent of stationary phase quiescent cells based on the criteria of individual cell density.

The precise determinants of the increased density of quiescent cells have been somewhat unclear (Allen et al., 2006). However, we noticed that the oscillating pattern of density changes that occurs as a function of the YMC correlates well with trehalose levels that were determined previously from metabolite profiling studies of the YMC (Tu et al., 2007). Trehalose, as well as glycogen, can constitute a large percentage of the mass of a yeast cell, up to 20% dry weight, and so the abundance of these two glucose-storage molecules could influence the apparent density of cells (Francois and Parrou, 2001; Lillie and Pringle, 1980). These carbohydrates, which are derived from glucose, are known to accumulate as growth rate decreases and as cells enter stationary phase (Boer et al., 2010; Lillie and Pringle, 1980; Sillje et al., 1999; Sillje et al., 1997).

We measured trehalose and glycogen content over the same 16 time points by using well established enzymatic assays, and we confirmed that the levels of these carbohydrates oscillate during the YMC, peaking during the end of RC phase (Figure II-1). Moreover, the pattern of trehalose and glycogen oscillation showed significant correlation to the observed density changes, with the time intervals where trehalose and glycogen were most abundant corresponding to the time intervals of highest cell density. These observations suggest that the total abundance of these storage carbohydrates might contribute to the overall apparent density of cells. The rapid decrease in trehalose and glycogen during the OX phase of the YMC suggests that stores of these carbohydrates are being metabolized to fuel a round of growth and proliferation. Thus, under such continuous culture conditions, yeast cells tend to accumulate trehalose and glycogen after the division process and then liquidate these carbohydrates during a subsequent round of growth (Futcher, 2006; Tu et al., 2007; Xu and Tsurugi, 2006).

Changes in cell density upon entry into stationary phase can be explained by changes in total intracellular glycogen and trehalose content

We next wondered whether total intracellular trehalose and glycogen content also would correlate with changes in cell density observed previously in stationary phase batch cultures (Allen et al., 2006). To test this possibility, we determined individual cell densities and trehalose and glycogen content of batch-cultured cells at a variety of times after entry into stationary phase. We also asked whether cells that cannot synthesize either trehalose (Δ*tps1*), glycogen (Δ*glc3*), or both trehalose and glycogen (Δ*glc3*Δ*tps1*) could still become dense and form quiescent populations. Because mutants that cannot synthesize trehalose (Δ*tps1*) are known to

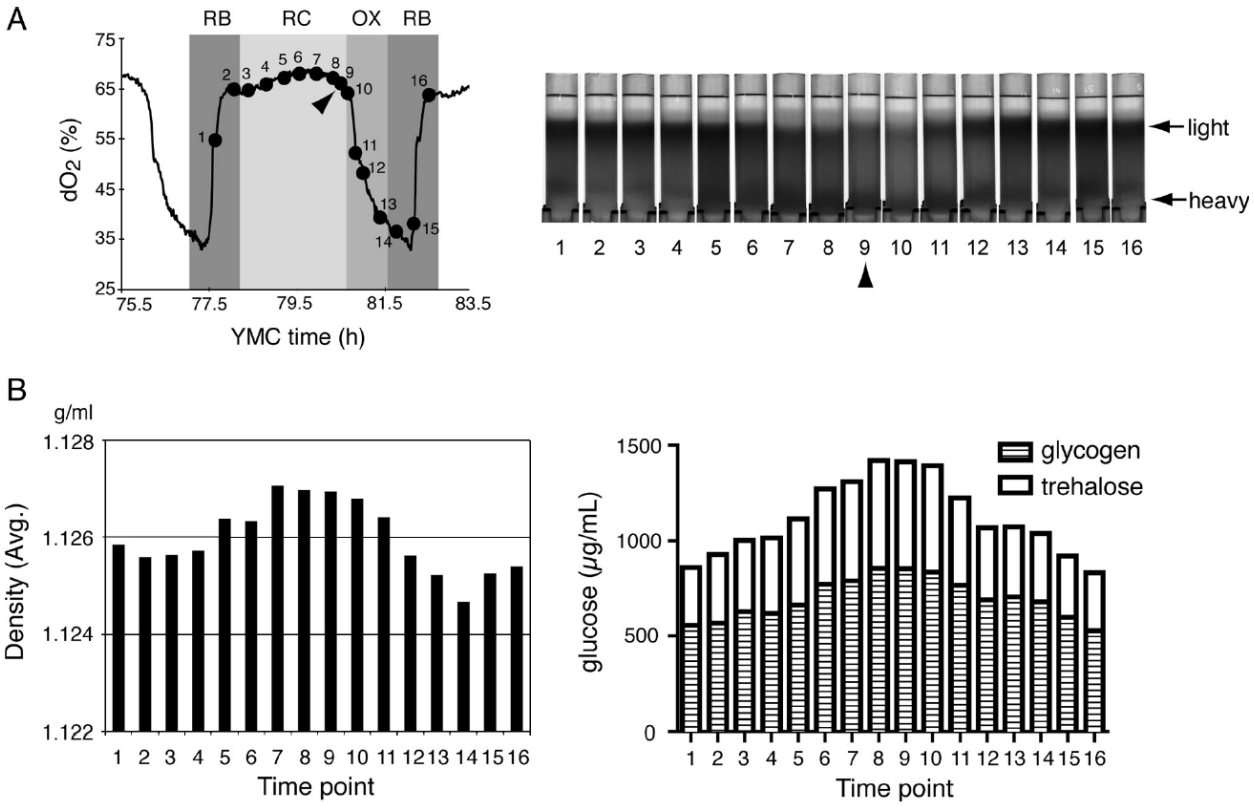

Figure II-1 Cyclic changes in individual cell density during the yeast metabolic cycle. (A) WT cells were collected at 16 time points spanning one complete metabolic cycle and fractionated according to density using Percoll gradients. “Light” refers to a population of cells at the top of the gradient that are lighter in density, whereas “heavy” refers to a population of cells at the bottom of the gradient that are heavier in density. Note that at time point 9 (arrow) in RC phase, the majority of the cells are heavy. (B) The average individual cell density of the entire population at each time point was estimated. Cell samples collected in parallel were assayed for trehalose and glycogen content. The bar graphs display the sum of glucose equivalents derived from intracellular trehalose (open) and glycogen (barred). Data are the means of three measurements from each time point. We confirmed that cells in the bottom fraction (heavy) indeed contained more trehalose and glycogen than cells in the top fraction (light)

have defects in their ability to uptake and metabolize glucose (Thevelein and Hohmann, 1995), we grew cells in rich medium containing galactose (YPGal) instead of glucose as the carbon source to minimize experimental complications due to growth deficiencies of Δ*tps1* mutants in glucose.

During such experiments, we observed that Δ*tps1* cells unexpectedly contained trehalose when grown in YPGal medium (Figure II-2). We subsequently confirmed that trehalose present in the yeast extract and peptone of rich medium might explain the presence of intracellular trehalose detected in Δ*tps1* cells after growth in such medium. Thus, we performed the majority of our growth and density measurements in either YPGal medium that had been pretreated with the enzyme trehalase (YPGal-T) to remove trehalose from the medium (Materials and Methods) or synthetic defined minimal medium (SGal) that does not contain trehalose.

These four strains were cultured in YPGal-T medium to log phase, diluted into fresh YPGal-T medium, and then grown for 7 d, conditions under which cells have entered stationary phase. Cells that cannot synthesize glycogen (Δ*glc3*) grew comparably to wild-type (WT) cells (Figure II-3). However, cells that cannot synthesize trehalose (Δ*tps1*), and cells that cannot synthesize both trehalose and glycogen (Δ*glc3*Δ*tps1*) exhibited significant defects in growth (Figure II-3). All strains eventually saturated at a similar high cell density ($OD_{600} > 15$) after 72 h.

On exit from exponential phase in YPGal-T ($OD_{600} = 2–5$), cells from all four strains tested were light in density. Beginning at ~20 h, we noticed that a fraction of the WT cell population became heavier in density, similar to quiescent populations reported previously

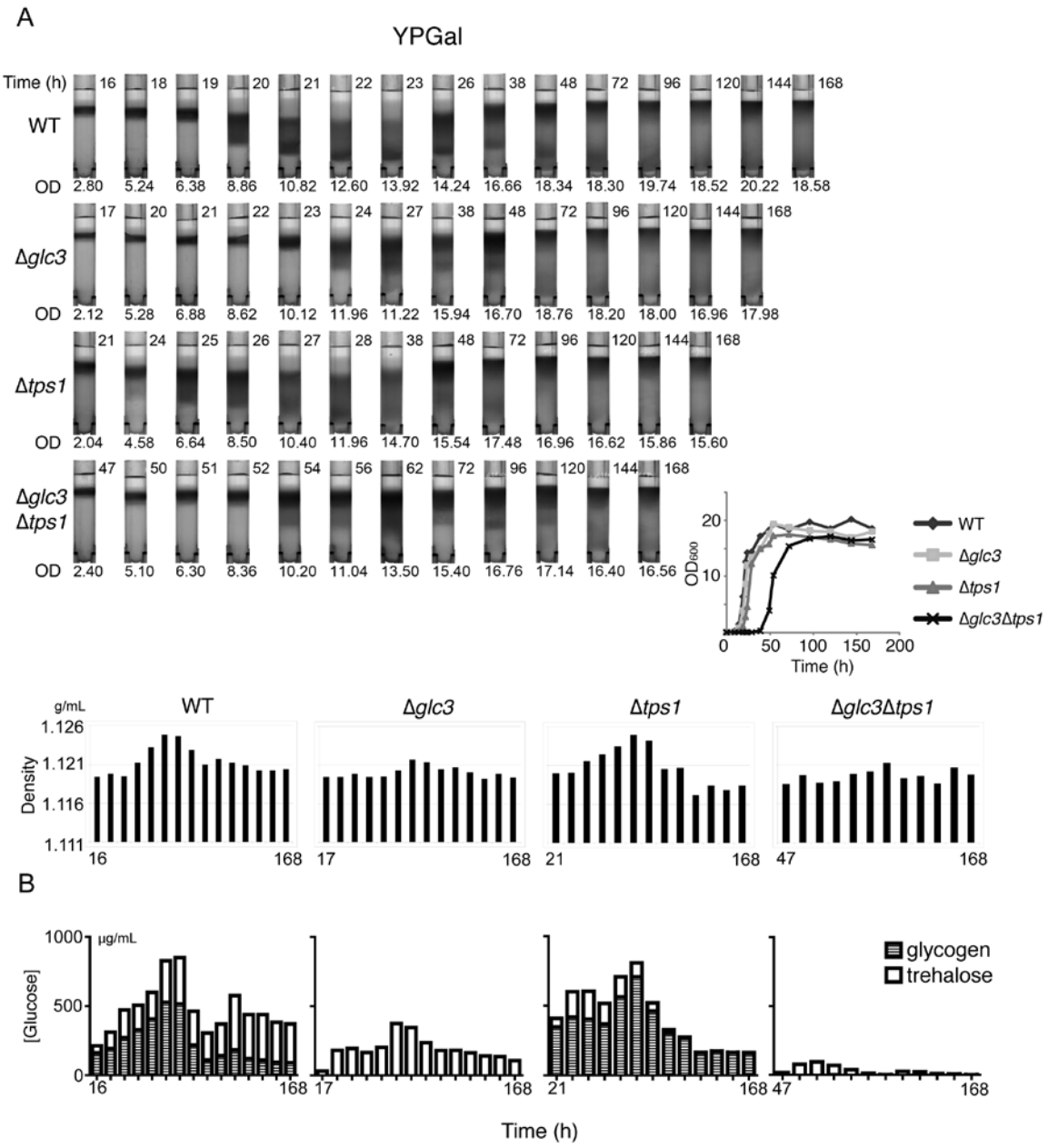

Figure II-2 Changes in cell density during growth in YPGal medium exhibit significant correlation with total intracellular trehalose and glycogen content. (A) Density gradients of WT, *Δtps1*, *Δglc3* and *Δglc3Δtps1* cultures as they enter stationary phase. Cells were collected at various times according to the growth curve, and were subsequently density fractionated. Average individual cell density of the population at each time point was estimated for comparison. For the density fractionation images, time (h) of collection is indicated at the top right corner of each tube and optical density of the culture (OD600) at the bottom. All the bar graphs only contain time labels for the first and last time points, the time points in between correspond to the time labels in the top panel. (B) Cell samples collected in parallel were assayed

for trehalose and glycogen content. Results of trehalose and glycogen content are the means of three measurements from each time point, represented by glucose equivalents. Note the unexpected presence of trehalose in *Δtps1* cells, from either yeast extract or peptone.

(Allen et al., 2006) (Figure II-3). Both heavy and light populations of cells were observable until ~72 h after inoculation. Beyond this point, the majority of cells were light up until 168 h. We observed that cells that cannot synthesize trehalose (Δ*tps1*) also could become dense upon entry into stationary phase, whereas cells that cannot synthesize either glycogen (Δ*glc3*) or both trehalose and glycogen (Δ*glc3*Δ*tps1*) also became dense but not nearly to the same extent as WT cells (Figure II-3).

We then measured the abundance of both trehalose and glycogen during the same time points that cell densities were determined for all four strains. The sum of trehalose and glycogen in terms of glucose equivalents showed significant correlation with average cell density (Figure II-3) for all strains tested. In WT cells, although both trehalose and glycogen levels initially increased during early stationary phase as expected, later on in stationary phase glycogen levels actually decreased whereas trehalose levels were maintained. After 7 days of growth, >3 times as much trehalose as glycogen was typically present within cells (Figure II-2 and II-3), indicating that trehalose is preferentially retained upon entry into long-term stationary phase, or quiescence, after growth in YP rich medium.

In Δ*tps1* cells, which can become dense to the same extent as WT cells upon entry into stationary phase, the concentration of glycogen was much greater than in WT cells, suggesting that glycogen synthesis is up-regulated to compensate for the inability of cells to synthesize trehalose (Figure II-3). In the absence of Tps1p, UDP-glucose equivalents that are a precursor for both trehalose and glycogen synthesis may be directed solely toward glycogen. In Δ*glc3* cells, as expected, no glycogen was detected. Similar to WT cells, trehalose levels increased upon entry into stationary phase and then decreased but were maintained (Figure II-3). However, due to the

lack of glycogen, these cells contained fewer total glucose equivalents than WT cells, which may explain why they do not become as dense (Figure II-3). In Δ*glc3*Δ*tps1* cells, which barely increased in density upon entry into stationary phase, there was almost no detectable glycogen or trehalose.

We then repeated the same experiments by growing the set of four strains in synthetic defined minimal medium with galactose as the carbon source (SGal). Again, for all strains tested, we observed a substantial correlation between total glucose equivalents in the form of trehalose and glycogen and the overall density of cells (Figure II-4). Together, these results strongly suggest that changes in individual cell density can largely be explained by the changes in glucose equivalents in the form of glycogen and trehalose within cells. However, under such synthetic minimal medium conditions, trehalose stores were not preferentially maintained compared with glycogen (Figure II-4).

Trehalose is a key determinant of the quiescent metabolic state

Because we observed a delay in the growth of cells lacking trehalose but not glycogen (compare Figure II-2 with Figures II-3 and II-4), we next asked whether addition of trehalose to Δ*tps1* strains could rescue growth of these cells upon dilution into fresh medium. Significantly, we observed that prior growth of Δ*tps1* cells in SGal medium that had been supplemented with trehalose partially improved growth upon dilution into SGal medium (Figure II-5). In contrast, for WT cells, there was no difference in growth when trehalose was supplemented to the medium. We also tested whether Δ*tps1* cells grown in SGal medium lacking trehalose altogether would benefit from the presence of trehalose in the new growth medium. In this scenario,

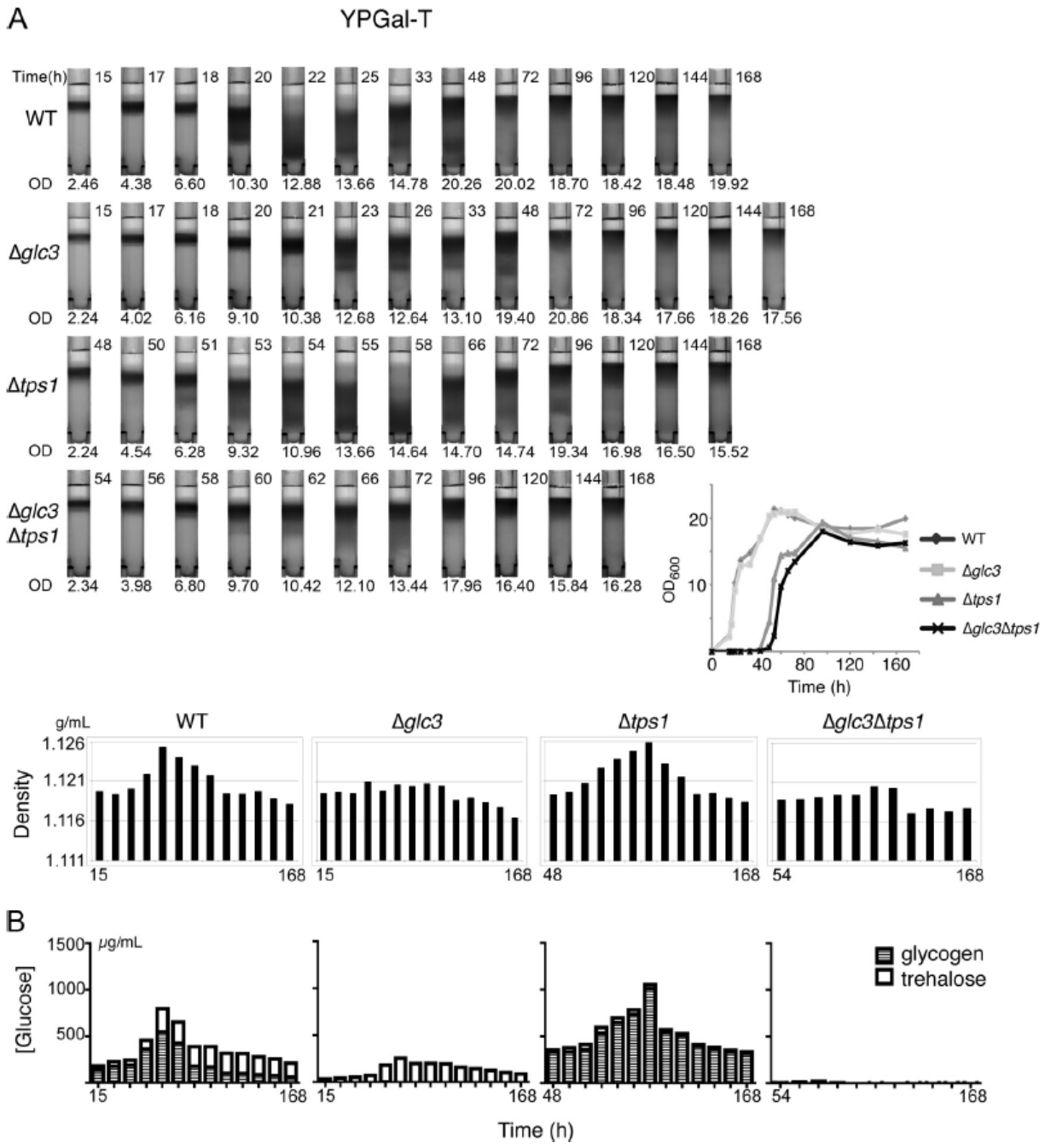

Figure II-3 Changes in cell density during growth in YPGal-T medium exhibit significant correlation with glucose equivalents in the form of glycogen and trehalose. (A) Density gradients of WT, *Δglc3*, *Δtps1*, and *Δglc3Δtps1* cultures as they enter stationary phase in YPGal minus trehalose medium. Cells were collected at various times according to the growth curves (inset) and were subsequently density fractionated. The average density of the population at each time point was estimated for comparison. For density fractionation, time (hours) of collection is indicated at the top right corner of each tube and optical density of the culture (OD600) at the

bottom. All the bar graphs only contain time labels for the first and last time points, the time points in between correspond to the time labels in the top panel. Time 0 of the growth curve refers to the time when cells were diluted into fresh medium. (B) Cell samples collected in parallel were assayed for trehalose and glycogen content. Results of trehalose and glycogen content are the means of three measurements from each time point, represented by glucose equivalents

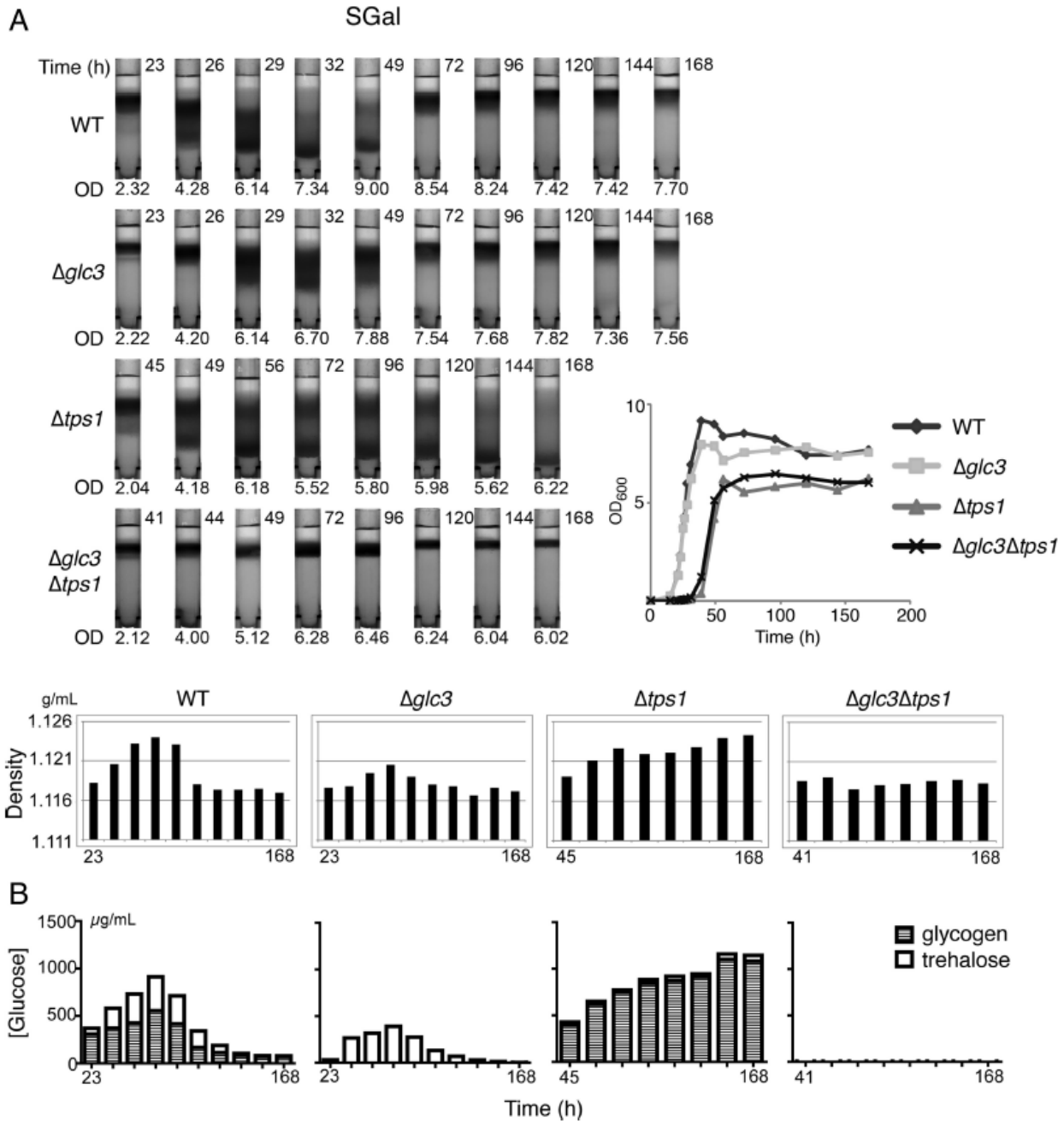

Figure II-4 Changes in cell density during growth in SGal medium exhibit significant correlation with glucose equivalents in the form of glycogen and trehalose. (A) Density gradients of WT, *Δglc3*, *Δtps1*, and *Δtps1Δglc3* cells as they enter stationary phase in SGal medium. Cell samples were collected according to the growth curves (inset) and were subsequently density fractionated. Average density of the population at each time point was estimated for comparison. (B) Cell samples collected in parallel were assayed for trehalose and glycogen content.

although there was not a detectable difference in the initial rates of growth, eventually these cells grew at a faster rate compared with Δ*tps1* cells that were diluted into regular SGal medium (Figure II-5). In contrast, there was no difference in the growth rates of WT cells if trehalose was supplemented to the new growth medium. Thus, the presence of trehalose can partially rescue the overall growth rates of Δ*tps1* cells lacking trehalose. Moreover, we observed an increased number of heavy, quiescent cells after 7 d of growth in medium containing trehalose, compared with medium lacking trehalose (Figure II-6).

The trehalase enzyme is activated to metabolize trehalose upon exit from quiescence

The growth defect exhibited by *Δtps1* strains and the retention of trehalose during long-term starvation or quiescence (Figure II-3) suggest there might be a specialized role for trehalose in fueling metabolic demands of a cell upon exit from quiescence. We grew WT cells for 7 d in rich medium, conditions under which they enter a quiescent state, and then diluted them into fresh rich medium to induce growth. We then measured glycogen, trehalose, and triglyceride content of cells at several time points immediately after dilution into fresh medium. We observed that trehalose stores were depleted rapidly, whereas glycogen stores initially increased during the first 30 min of regrowth (Figure II-8). Triglyceride levels remained largely constant, whereas free glycerol levels increased significantly (Figure II-8). We observed previously an increase in intracellular glycerol during the OX, growth phase of the YMC, which might be required for up-regulation of lipid synthesis needed to build a new cell (Tu et al., 2007). As growth progressed, total trehalose and glycogen stores decreased to levels expected of cells in exponential growth.

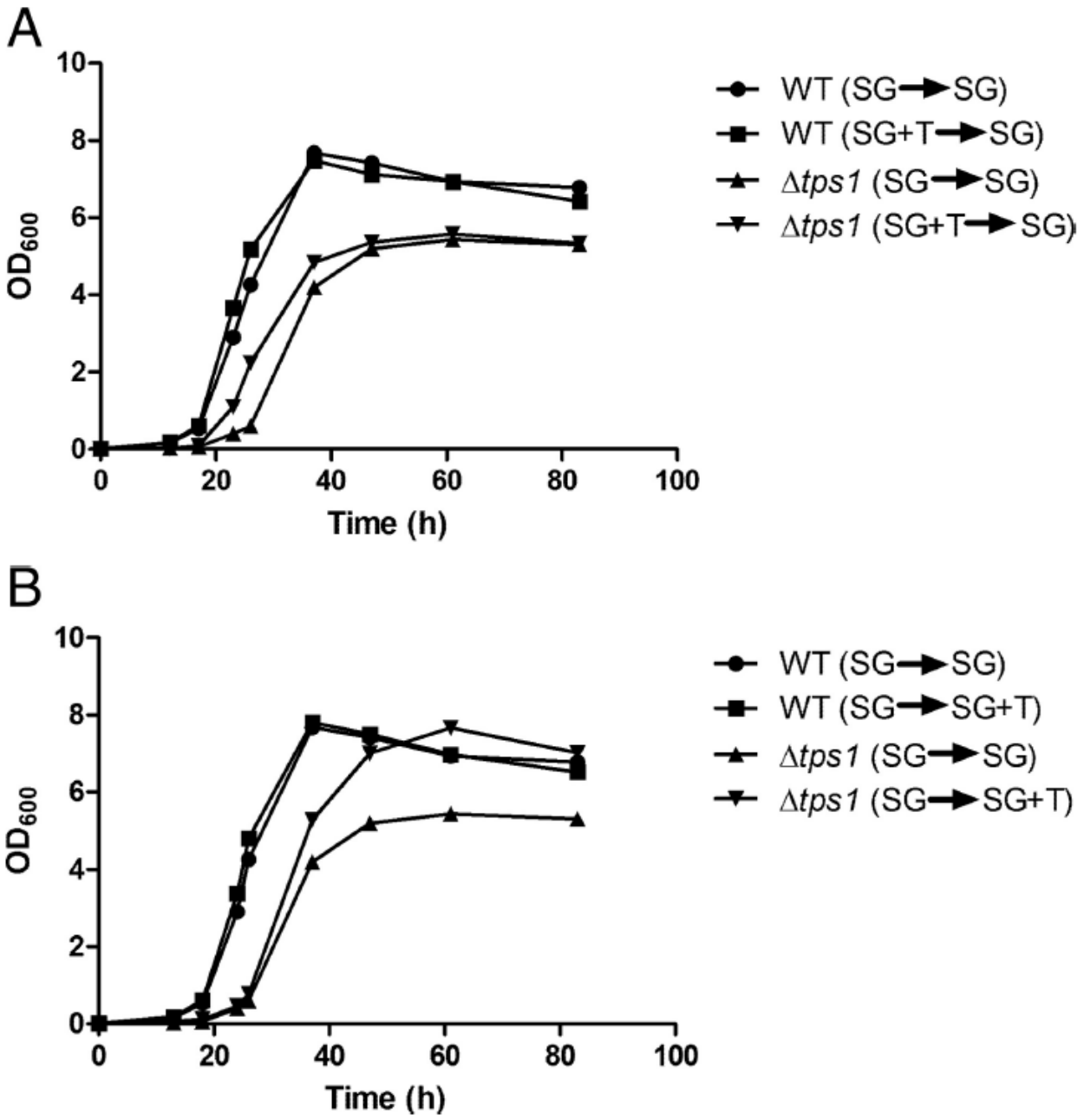

Figure II-5 Trehalose partially rescues growth of *Δtps1* cells. (A) To test whether prior growth in medium containing trehalose can partially rescue growth of *Δtps1* cells, WT and *Δtps1* cells were grown in SGal or SGal plus trehalose medium to log phase and then diluted into fresh SGal medium. OD600 was measured at the indicated time points. (B) To test whether subsequent growth in medium containing trehalose can improve growth of *Δtps1* cells, WT and *Δtps1* cells were grown in SGal medium to log phase and then inoculated into either fresh SGal or SGal plus trehalose medium. OD600 was measured at the indicated time points.

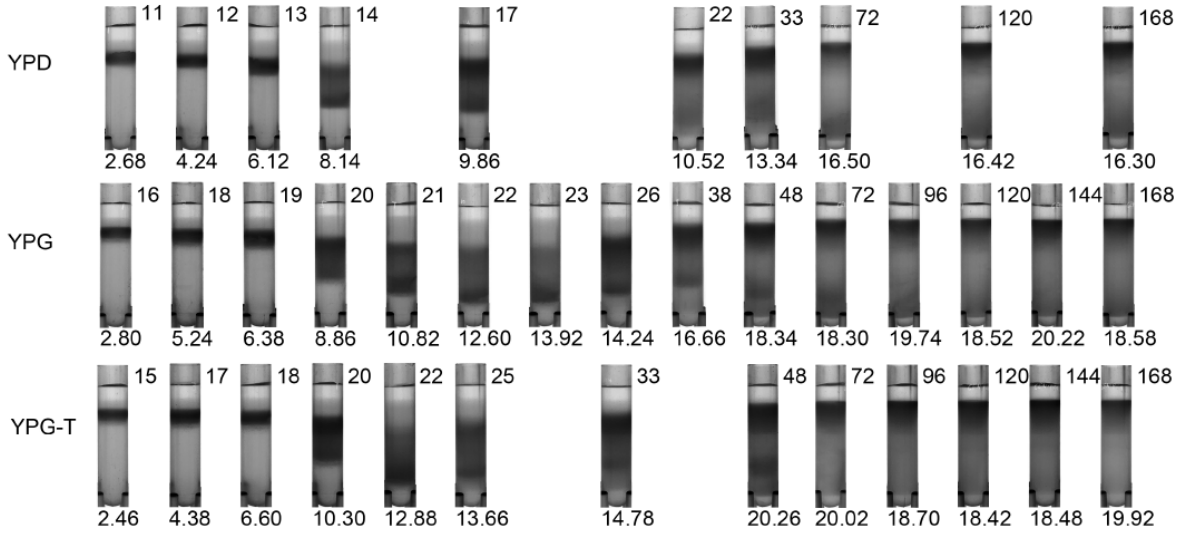

Figure II-6 WT cells grown in medium lacking trehalose show fewer dense/quiescent cells at later time points following long-term batch culture growth. WT yeast were grown in YPD, YPGal and YPGal-T media starting from log phase and the density of individual cells was resolved as described. Time (h) of collection is indicated at the top right corner of each tube and optical density of the culture (OD600) at the bottom. Density tubes from the three different media conditions are aligned according to the relative growth stage for comparison. Note that there are fewer dense/quiescent cells in the YPGal-T sample starting at 72 h of growth

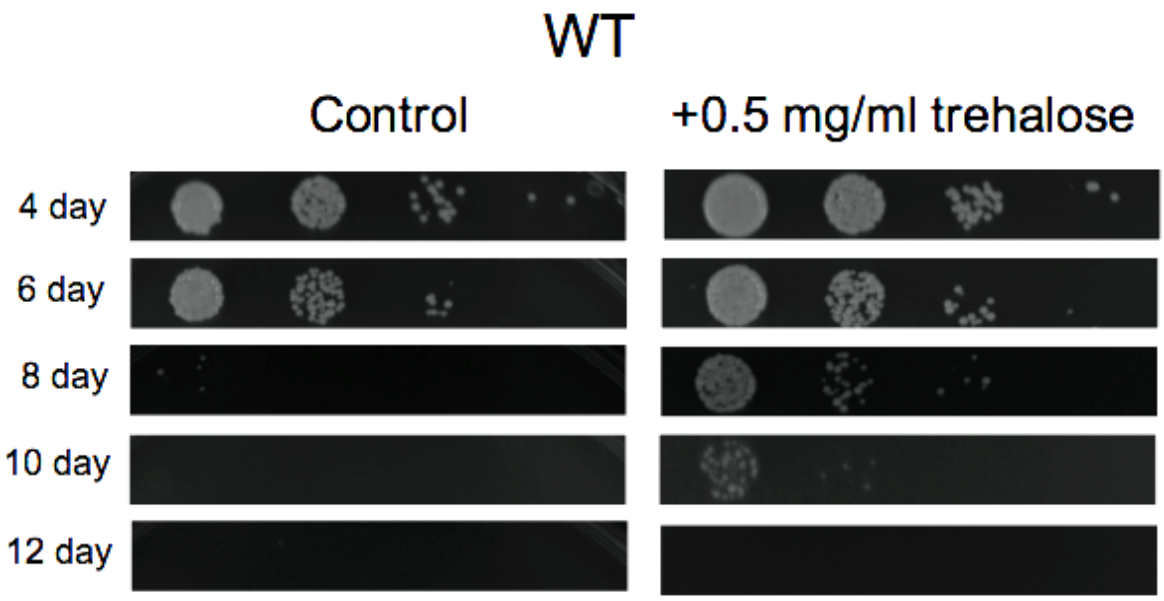

Figure II-7 Trehalose addition prolongs the chronological lifespan of WT cells grown in SGal medium lacking trehalose. WT yeast were grown in SGal and SGal+T media starting from log phase and the survivability of cells in each condition were measured by spotting 10,000, 1000, 100 and 10 cells on YPGal agar plate from left to right. The plate was incubated at 30 ºC for 2 days to assess the viability.

Cells lacking glycogen (*Δglc3*), which do not exhibit growth defects, also rapidly metabolized trehalose stores upon exit from quiescence (Figure II-9). However, cells lacking trehalose (*Δtps1*) did not rapidly metabolize their glycogen stores. The inability of these cells to metabolize trehalose stores could explain why they exit quiescence more slowly (Figures II-2, II-3, II-4, II-5 and II-9). These data support the idea that intracellular trehalose stores play an important role in fueling cell cycle progression upon exit from quiescence.

The observation that trehalose stores are metabolized preferentially upon exit from quiescence predicts that the trehalase enzymes will be specifically activated during the switch to growth. We used the YMC system to immunoprecipitate the major trehalase enzyme Nth1p from cells to assay its activity during either the quiescent-like (RC) or growth and division (OX and RB) phases of the YMC. We observed a significant increase in trehalase activity at a single time point in the midst of the OX growth phase, just after the exit from the RC phase that can be likened to quiescence (Figure II-8C). Similarly, we found a significant up-regulation of trehalase activity upon regrowth after 7 d in stationary phase using a normal batch culture model of quiescence (Figure II-8D). Moreover, because Nth1p has been reported to be a substrate of the cAMP-dependent protein kinase A (Uno et al., 1983; van der Plaat, 1974), we tested whether the activity of Nth1p would be dependent on phosphorylation. Prior treatment of immunoprecipitated Nth1p with general phosphatases significantly decreased its activity especially in the OX phase (Figure II-8C), indicating that phosphorylation events play an important role in regulating Nth1p activity. Although we observed that the *NTH1* gene is up-regulated significantly in RC phase, the Nth1p protein levels do not change significantly between the quiescent and growth phases of the YMC (Figure II-10). Thus, it can be predicted that newly

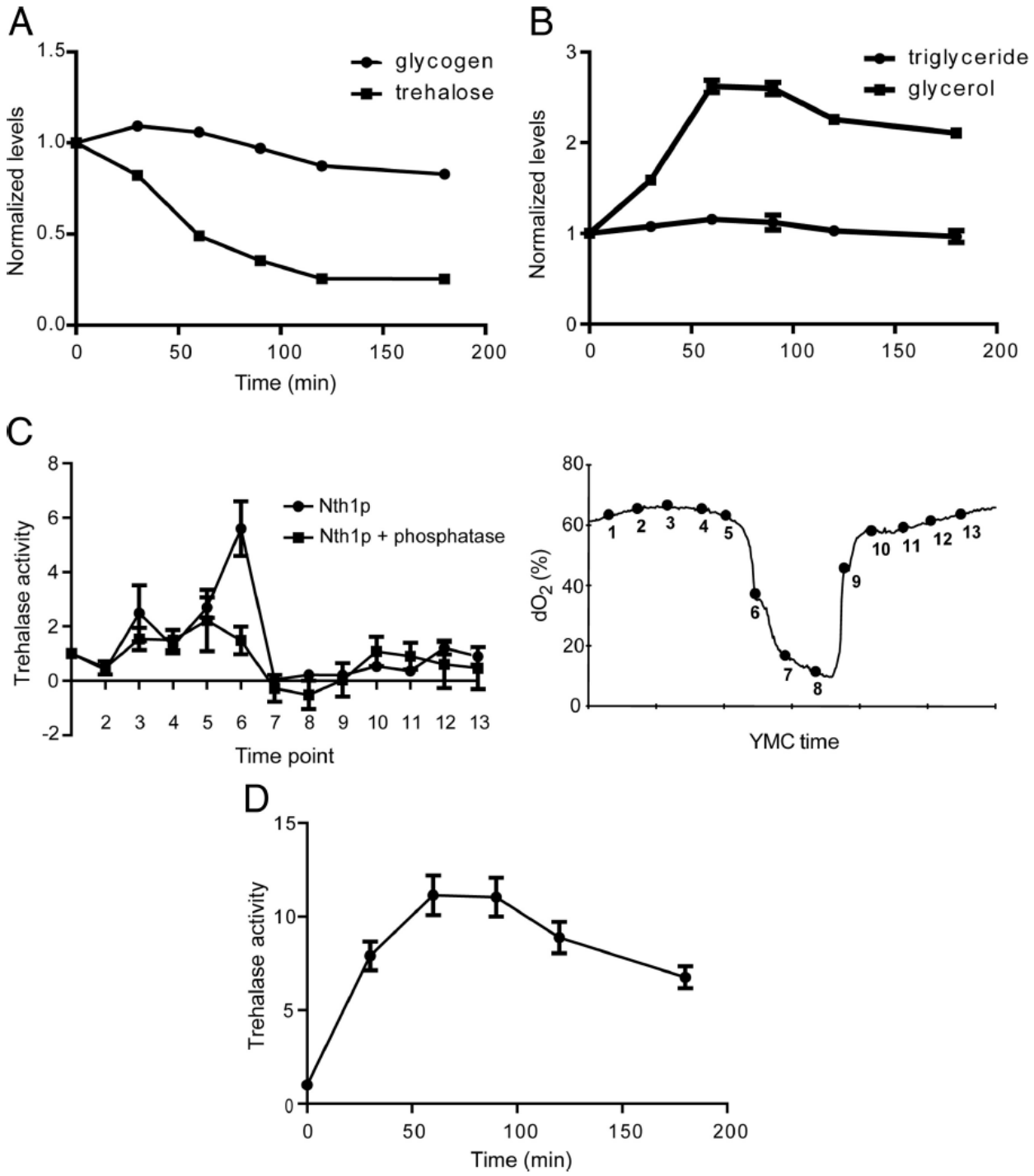

Figure II-8 Intracellular trehalose stores are rapidly metabolized as yeast cells exit quiescence. (A) Trehalose stores are metabolized before glycogen upon regrowth. WT cells were grown in YPGal minus trehalose medium for 168 h and diluted 10 times in volume with fresh prewarmed medium. Cell samples were collected quickly for 180 min thereafter. Samples were assayed for trehalose and glycogen content. Data are shown as mean ± SEM from three measurements in terms of glucose equivalents, normalized to levels before initiation of regrowth. (B) Total intracellular triglyceride levels do not decrease upon exit from quiescence. WT yeast cells were

grown, diluted into fresh medium, and samples were collected as described above. Samples were assayed for triglyceride and free glycerol levels. Results are shown as mean ± SEM from three measurements, normalized to levels present before regrowth. (C) Trehalase activity is up-regulated substantially during the switch to the OX growth phase. Cells expressing Nth1p-FLAG were harvested at 13 times points across one metabolic cycle. Nth1p was immunoprecipitated using FLAG epitope-conjugated beads and immediately assayed for trehalase activity with or without prior treatment with general phosphatases. Activity was normalized against the activity observed for time point 1. The x-axis tick marks denote 1-h time intervals. (D) Trehalase is rapidly activated upon exit from batch culture induced quiescence. Nth1p-FLAG was immunoprecipitated from cells at the same time points as in A after regrowth and assayed for trehalase activity. Activity was normalized against the activity observed just before initiation of regrowth.

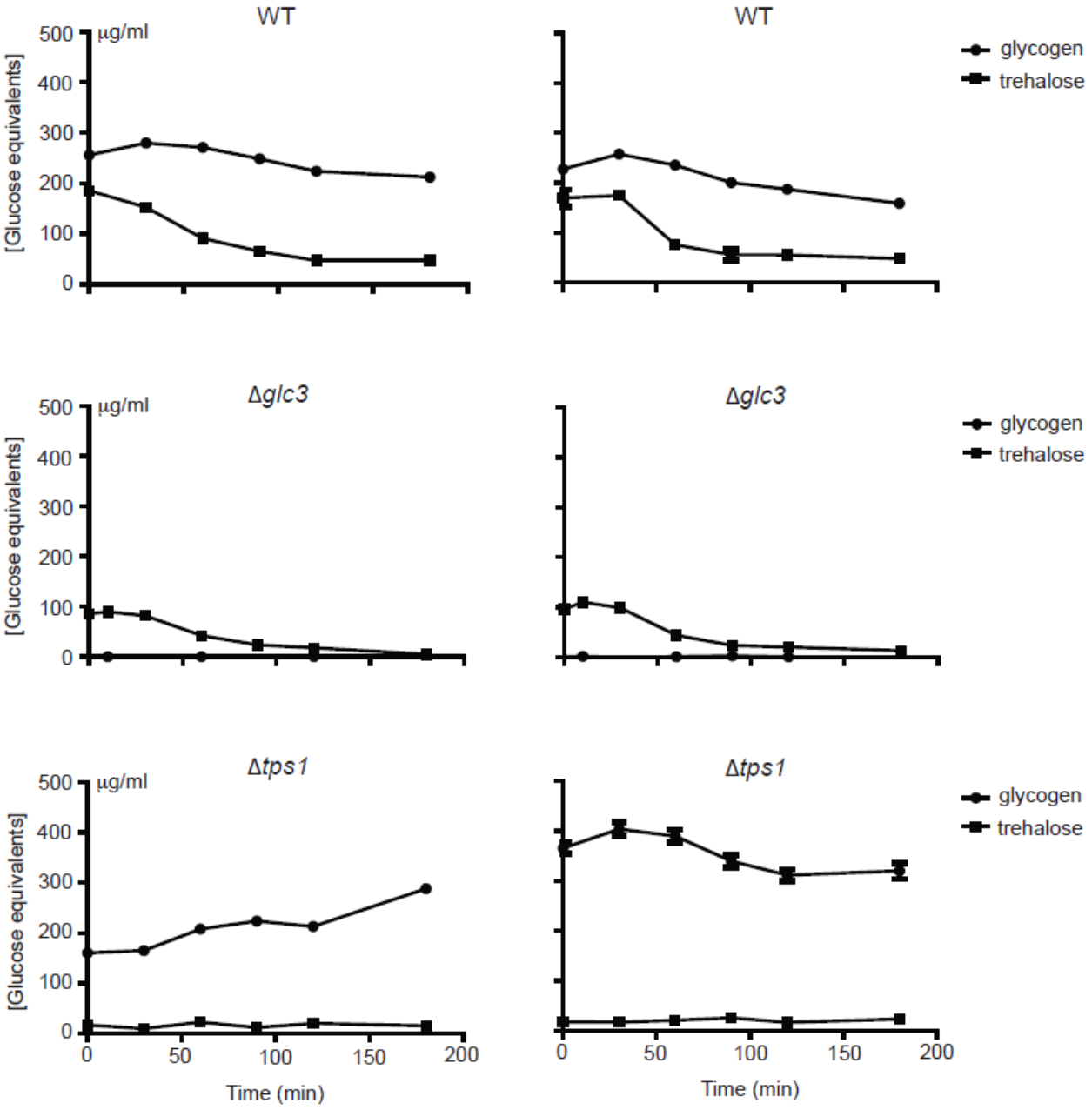

Figure II-9 Intracellular trehalose stores are rapidly metabolized in preference over glycogen upon regrowth. WT, Δglc3, Δtps1 yeast were grown in YPGal minus trehalose media for 168 hours and diluted 10 times in volume with fresh pre-warmed media. Cell samples were collected quickly at various time points until 180 minutes thereafter. Samples were assayed for trehalose and glycogen content and the quantities are shown as mean ± SEM from three measurements in terms of glucose equivalents. The results from two independent experiments are shown.

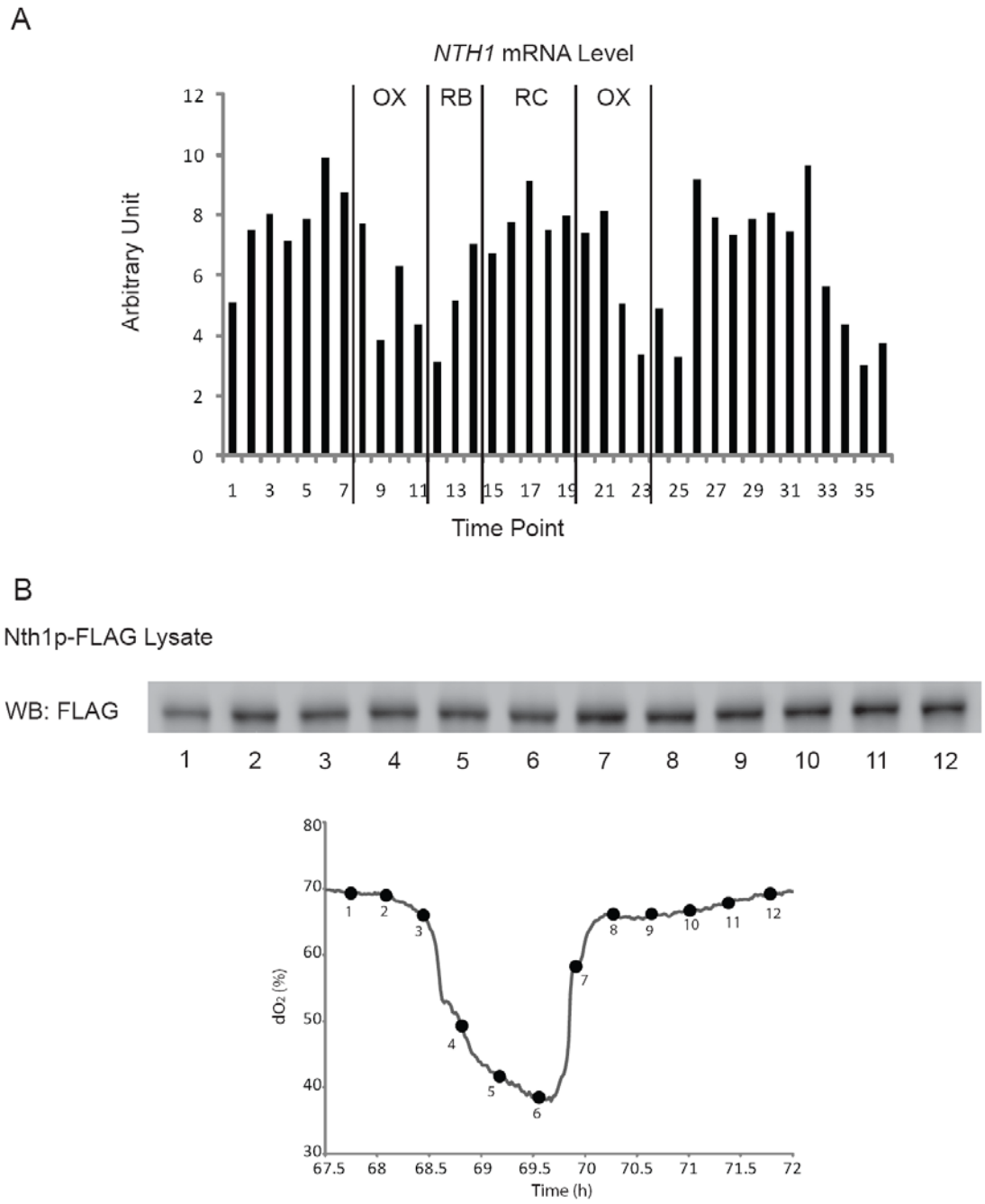

Figure II-10 Dynamics of *NTH1* mRNA and protein levels during the yeast metabolic cycle. (A) *NTH1* mRNA level peaks during the RC, quiescent phase of the yeast metabolic cycle (data obtained from Tu et al., Science 2005). (B) Nth1p protein levels do not change significantly during the yeast metabolic cycle. Cells expressing Nth1p-FLAG were collected at 12 time points through one yeast metabolic cycle as shown. The lysates of the 12 samples were subjected to western blot analysis using a FLAG antibody.

synthesized Nth1p protein accumulates during quiescence so that it may be rapidly activated by phosphorylation in response to appropriate metabolic or nutritional cues to help fuel regrowth of cells.

Lastly, our data predict that quiescent cells that contain less trehalose might recover more slowly and exhibit decreased survivability. To test this hypothesis, we determined the survivability of 7-d-old quiescent cells that were grown previously in either SGal or YPGal-T medium. We know that cells grown in SGal contain virtually no trehalose and small quantities of glycogen after 7 d, whereas cells grown in YPGal-T contain significant amounts of both trehalose and glycogen (Figures II-3 and II-4). We then tested the regrowth rates and survivability of these two populations of quiescent cells. Strikingly, the quiescent cells grown in SGal exhibited poor survivability and recovered much more slowly than quiescent cells grown in YPGal-T (Figure II-11). Thus, these observations suggest that intracellular trehalose stores could affect cell survivability and chronological life span.

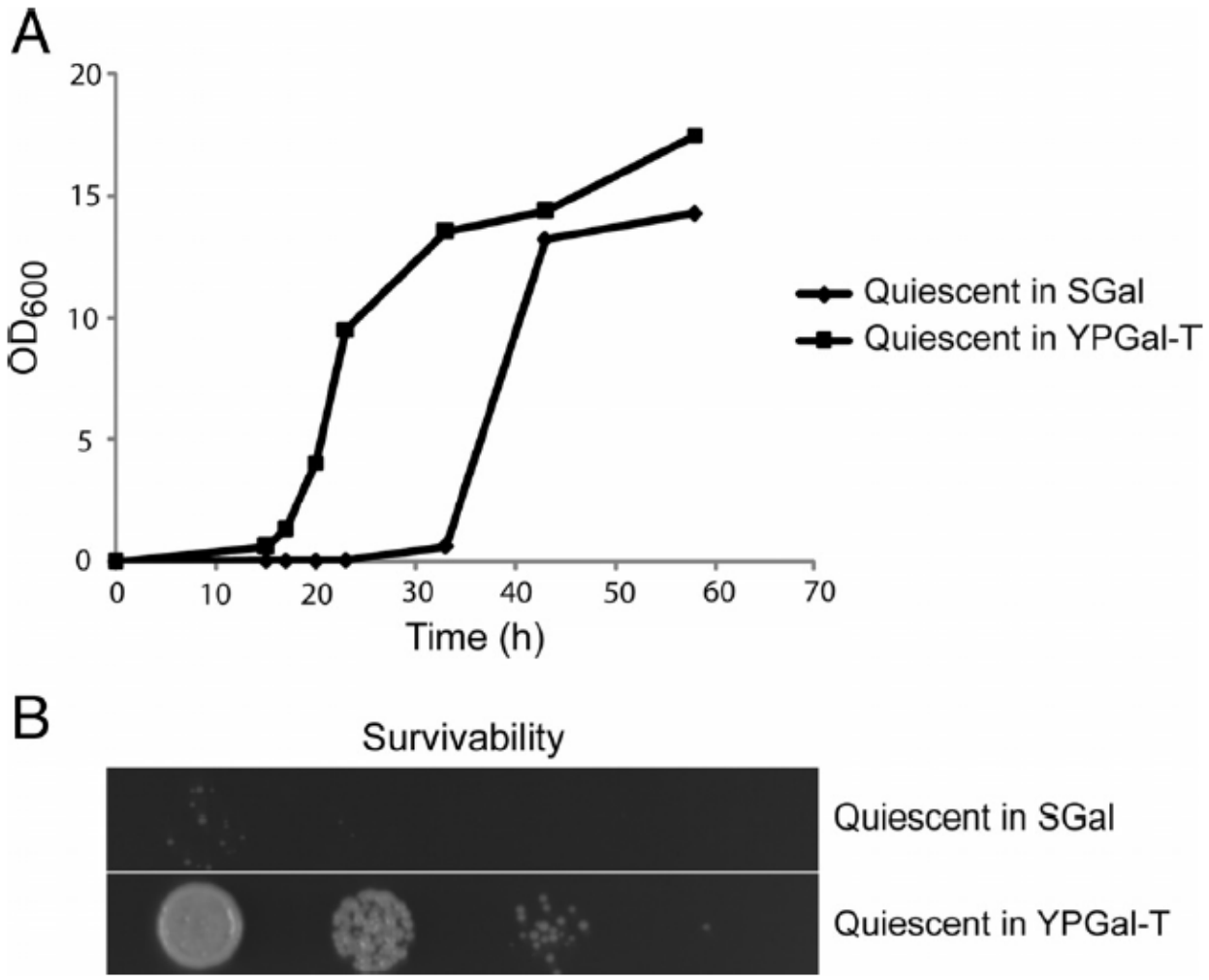

Figure II-11 Intracellular trehalose stores correlate with quiescent cell survivability. WT cells were inoculated into either SGal or YPGal minus trehalose medium and grown for 7 d. (A) Quiescent cells previously grown in SGal exhibit slower rates of regrowth. Cells from the two 7-d-old quiescent cultures were diluted into YPGal-T medium, and OD600 was monitored as a function of time. (B) Quiescent cells previously grown in SGal that contains virtually no trehalose exhibit poor survivability. As a measure of cell survivability, from left to right, 10,000, 1000, 100, and 10 cells from the quiescent cultures were spotted onto a YPGal agar plate. The plate was incubated at 30°C for 2 d to assess cell viability. Similar results were obtained in replicate experiments.

DISCUSSION

Here, our data strongly suggest that the primary reason quiescent cells observed during stationary phase become more dense is because these cells have accumulated more trehalose and glycogen stores. In turn, these cells can use these stored carbohydrates to help fuel cell cycle progression upon re-growth. This provides an explanation as to why these heavy, quiescent cells can begin division more readily than light, nonquiescent cells (Allen et al., 2006). However, we do not understand why only a fraction of cells in standard batch cultures become quiescent upon entry into stationary phase. Under such non–steady-state growth conditions, we speculate that certain nutrients or secreted metabolites might induce some cells to metabolize their trehalose and glycogen stores in an attempt to enter the cell cycle.

During continuous, steady-state growth conditions, cells in the RC phase of the YMC accumulate trehalose and glycogen in a manner similar to batch-cultured cells that enter stationary phase (Figures II-1 and II-3). Interestingly, the expression of many RC phase genes was found to be negatively correlated with increasing growth rate (Brauer et al., 2008). Thus, based on the criteria of gene expression and cell density, cells in the RC phase of the YMC are reminiscent of slow-growing cells that are about to enter quiescence. On entry into the OX growth phase, cells metabolize these carbohydrate stores and up-regulate numerous growth genes to fuel a round of growth and proliferation (Tu et al., 2005; Tu et al., 2007). Thus, there are continuous alternations between quiescent-like (RC) and growth (OX) phases during the YMC.

As cells enter prolonged stationary phase after growth in YP medium, trehalose levels tend to be maintained, whereas glycogen stores decrease (Figure II-2 and Figure II-3). Some of these glycogen and trehalose stores may be used to support basal metabolic activities as cells

persist in stationary phase; however, it is clear that trehalose is preferentially maintained over glycogen as the quiescent state progresses. On exit from quiescence, trehalose stores are metabolized before glycogen and reduced to levels typical of exponential phase growth (Figure II-8A).

Because mutants that cannot synthesize trehalose exhibit severe defects in the re-initiation of growth, and mutants that cannot synthesize glycogen do not, together our results suggest an important role for trehalose as a fuel reserve that enables yeast cells to survive starvation conditions and then rapidly proliferate upon return to favorable growth conditions. The rapid activation of the trehalase enzyme Nth1p during the switch to growth supports the idea that trehalose stores are quickly metabolized upon exit from quiescence to help fuel growth. Thus, the ability of a cell to accumulate sufficient trehalose stores is a key determinant of whether it can enter and exit quiescence successfully.

Trehalose has been widely reported to function as a stress protectant by acting as a chemical chaperone or osmolyte (Crowe et al., 1992; Singer and Lindquist, 1998b). Trehalose levels accrue under a variety of stress conditions, and increased levels of trehalose correlate with increased survivability after stresses such as heat shock, cold shock, and desiccation (Kandror et al., 2004; Singer and Lindquist, 1998a). We offer an additional interpretation to these previous observations in that trehalose stores in parallel might also function as an energy source that yeast cells initially utilize upon return to favorable growth conditions. Without sufficient trehalose stores, yeast cells would exhibit defects not only in their ability to persist in a quiescent state but also in their ability to exit the quiescent state induced by various stresses. Thus, although trehalose may directly function as a chaperone to help minimize protein aggregation or as an

osmolyte to minimize water loss (Crowe et al., 1992; Singer and Lindquist, 1998b), it may simultaneously serve as a critical energy reserve.

There are several significant reasons why trehalose might be a preferred energy source for survival of a variety of adverse conditions. Trehalose is a nonreducing disaccharide formed from two molecules of glucose. Because the glycosidic linkage exists between the 1-carbons of two glucose molecules, trehalose is more resistant than most carbohydrates to heat and acid-induced decomposition (Higashiyama, 2002). Thus, trehalose represents a source of energy that itself would endure a variety of harsh conditions that yeast might encounter in the wild. Moreover, cleavage of one glycosidic bond in trehalose would release two glucose equivalents that can be used for energy. In contrast, a glycogen polymer would liberate only one glucose equivalent per glycosidic bond cleaved. Trehalose is also an abundant component of plant seeds and fungal spores (Elbein et al., 2003; Higashiyama, 2002). In addition to protecting against desiccation, these trehalose stores also may be used as a source of energy to drive germination.

For these reasons, it becomes sensible as to why cells might favor the storage of trehalose over glycogen as time spent in the quiescent state increases. In many previous studies, a distinction between trehalose and glycogen in their roles as energy reserves has not been clear (Guillou et al., 2004; Lillie and Pringle, 1980; Sillje et al., 1999; Sillje et al., 1997). In the YMC system, both glycogen and trehalose accumulate to a similar extent during RC phase and both become degraded upon entry into OX growth phase (Figure II-1). However, the quiescent-like state in these situations persists on the order of hours, rather than days. As time spent in the quiescent state increases, cells may begin redirecting glucose equivalents from glycogen to trehalose to enhance survivability. Moreover, our data predict that trehalose synthesis may

induce other important aspects of the quiescence program and that trehalose metabolism will be coupled to cell cycle progression upon exit from quiescence. The precise mechanisms by which trehalose metabolism may be linked to the cell cycle, especially under nutrient-poor conditions, will be of great interest in future studies.

Lastly, our findings regarding trehalose and quiescence offer a slightly different perspective on chronological aging and life span in yeast. We speculate that the perturbation of pathways that negatively impact trehalose accumulation or metabolism might compromise the ability of a cell to rapidly exit the quiescent state, and thus its survivability (Figure II-11). Conversely, those that enhance trehalose storage or reduce trehalose metabolism while persisting in the quiescent state might improve survivability. In nature, yeast cells are more likely to undergo periodic bursts of rapid growth that alternate with long periods of quiescence, rather than continuous rapid growth that typically occurs under laboratory growth conditions (Lu et al., 2009; Sillje et al., 1999). Such conditions necessitate the accumulation of trehalose and other reserves (e.g., glycogen) so that cells can readily enter and exit quiescence when appropriate. The cycles of trehalose storage and breakdown that occur in yeast cell populations as a function of metabolic cycles during glucose-limited growth in essence depict such a strategy (Futcher, 2006; Tu et al., 2007; Xu and Tsurugi, 2006). We conclude that in addition to its numerous stress-protectant functions, a critical role for trehalose as an enduring energy reserve that in turn helps fuel rapid exit from quiescence cannot be discounted.

MATERIALS AND METHODS

Yeast Strains and Media

The prototrophic CEN.PK strain background was used for all experiments (van Dijken et al., 2000). Δ*glc3*, Δ*tps1*, and Δ*glc3*Δ*tps1* knockout strains were obtained by sporulation of a CEN.PK122 diploid strain in which one copy of the *GLC3* gene was replaced by a kan^R cassette and one copy of the *TPS1* gene was replaced by a nat^R cassette via homologous recombination. Sporulated haploid knockout strains were isolated by growth on YPD plates containing 200 μg/ml G418-sulfate (kan) or 100 μg/ml nourseothricin (Nat). The *NTH1*- FLAG strain was constructed by appending a FLAG epitope cassette to the C terminus of the endogenous chromosomal copy of *NTH1* by homologous recombination (Longtine et al., 1998). YPGal minus trehalose medium was made by treating YPGal medium (10 g/l yeast extract, 20 g/l peptone, and 2% galactose) with trehalase to deplete residual trehalose present in yeast extract and peptone. The treated medium was subsequently assayed for trehalose to ensure that it had been depleted of trehalose. SGal medium contained 6.7 g/l yeast nitrogen base without amino acids and 2% galactose. SGal plus trehalose medium contained 0.7 mg/ml trehalose (T9531; Sigma-Aldrich, St. Louis, MO) to mimic the concentration of trehalose present in YP medium.

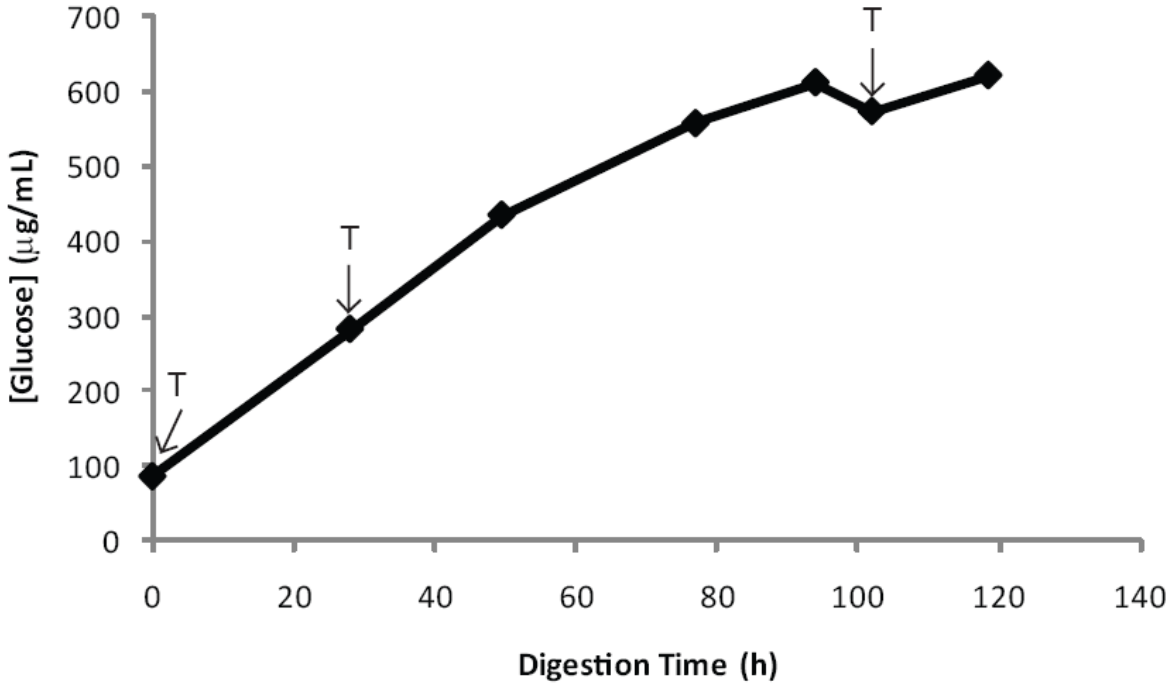

Figure II-12 Observed glucose increase during digestion of trehalose present in YPGal medium. 350 mL YPGal medium was treated with 50 μL trehalase solution at 37°C at the time points indicated and glucose concentration was monitored until a plateau was reached, which indicated the depletion of trehalose.

Production of Metabolic Cycles during Continuous Culture Growth

Continuous culture conditions used to observe yeast metabolic cycles were described previously (Tu et al., 2005). Briefly, each fermentor run was started by the addition of a 1- to 5-mL starter culture that had been grown overnight to saturation at 30 °C. The fermentors were operated at an agitation rate of ~500 rpm, an aeration rate of 1 L/min, a temperature of 30 °C, and a pH of 3.4, with a working volume of 0.5 or 1 L. Once the batch culture reached maximal density, the culture was starved for 8–10 h. Continuous culture was then initiated by the constant infusion of media containing 1% glucose at a dilution rate of ~0.09–0.1 h^{-1}. The growth media is a minimal

media consisting of 5 g/L $(NH4)_2SO_4$, 2 g/L KH_2PO_4, 0.5 g/L $MgSO_4 \cdot 7H_2O$, 0.1 g/L $CaCl_2 \cdot 2H_2O$, 0.02 g/L $FeSO_4 \cdot 7H_2O$, 0.01 g/L $ZnSO_4 \cdot 7H_2O$, 0.005 g/L $CuSO_4 \cdot 5H_2O$, 0.001 g/L $MnCl_2 \cdot 4H_2O$, 1 g/L yeast extract, 10 g/L glucose, 0.5 mL/L 70% (vol/vol) H_2SO_4, and 0.5 mL/L Antifoam 204 (Sigma).

Batch Culture Growth

Wild-type, Δ*glc3*, Δ*tps1*, and Δ*glc3*Δ*tps1* strains were grown in YPGal-T or SGal medium. Cells were first inoculated in 5 ml of the appropriate medium and grown at 30°C to saturation. Then, cultures were diluted into fresh medium and grown for several hours to OD_{600} = 0.7–2.0. These exponentially growing cultures were then diluted into 350 ml of YPGal-T or SGal medium to OD_{600} = 0.01 and grown at 30°C. Cell samples were then collected at indicated time points for density fractionation as well as trehalose and glycogen assays.

Density Fractionation

Fractionations of yeast cell cultures were performed as described previously, with minor modifications (Allen et al., 2006). Approximately 100 OD of yeast cells were collected for each sample and centrifuged at 3000 × *g* for 4 min at 4°C. After resuspension with 1 ml of ice-cold Tris buffer (50 mM Tris-HCl, pH 7.5), cell samples were kept on ice until they could be processed together. Such incubations on ice did not affect the density of cells within a span of 6 h. To make Percoll density gradients, Percoll PLUS (GE Healthcare, Little Chalfont, Buckinghamshire, United Kingdom) was diluted 10:1 (vol/vol) with 1.5 M NaCl. Then, 10 ml of the mixed solution was put into 15-ml tubes and centrifuged at either 19,310 × *g* (batch cultures) or 14,350 × *g* (continuous cultures) for 15 min at 20°C. Cells resuspended in Tris buffer were

overlaid carefully onto the pre-formed gradient and centrifuged at 400 × *g* for 30 min at 20°C. The fractionation of density standards was performed similarly using Density Marker Beads (GE Healthcare).

Estimation of Average Cell Density

Pictures of the density-fractionated cells were taken with a black background by using a Sony digital camera at 5-megapixel resolution under uniform lighting. Each gradient tube in the picture was individually cropped, resized, sorted, labeled with black background, converted to grayscale, and inverted in Photoshop (Adobe Systems, Mountain View, CA). To estimate the average density of each sample, intensities of every 2 pixels of each tube from the meniscus (top) to the bottom were measured using ImageJ (National Institutes of Health, Bethesda, MD). With the top pixels set as zero intensity, the remaining pixel data were converted to intensity percentages relative to the sum of the intensity of pixels for the entire tube. These intensity percentages can be used to estimate cell number percentages at each position in the tube relative to the meniscus. The exact density at each distance relative to the meniscus was estimated from the sedimentation position of density marker beads using Prism (GraphPad Software, San Diego, CA) to fit a dose-response curve with variable slope (four parameters). The average density of each cell sample was calculated by summing the products of the intensity percentage multiplied by density at each distance to the meniscus.

Glycogen and Trehalose Assays

Glycogen and trehalose assays were performed as described previously, with minor modifications (Parrou and Francois, 1997). Cell samples were collected and pelleted in parallel

with those used for density fractionations. Cell pellets were quickly washed with 1 ml of ice-cold H_2O and then resuspended in 0.25 ml of 0.25 M Na_2CO_3 and stored at −80°C until processed. For batch cultures, 20 OD total cells were collected. After resuspension in H_2O, 0.5 ml of cell suspensions was transferred to two capped Eppendorf tubes (one tube for glycogen assay and the other tube for trehalose assay). For continuous cultures, 10 OD total cells were collected twice directly into two capped Eppendorf tubes. When sample collections were complete, cell samples (in 0.25 M Na_2CO_3) were boiled at 95–98°C for 4 h, and then 0.15 ml of 1 M acetic acid and 0.6 ml of 0.2 M sodium acetate were added to each sample.

For controls, half of each sample was transferred to another Eppendorf tube, and the remaining half of the sample was incubated overnight with 1 U/ml amyloglucosidase (10115; Sigma-Aldrich) rotating at 57°C for the glycogen assay, or 0.025 U/ml trehalase (T8778; Sigma-Aldrich) at 37°C for the trehalose assay. Samples were then centrifuged at top speed for 3 min and assayed for glucose using a Glucose Assay kit (GAGO20; Sigma-Aldrich).

Glucose assays were done with modifications in a 96-well plate format. Samples were added into each well with or without dilution with H_2O to fit into the linear concentration range of the assay (20–80 μg/ml). The total volume of sample (with or without dilution) in each well was 40 μl. The plate was preincubated at 37°C for 5 min, and then 80 μl of the assay reagent from the kit was added into each well to start the colorimetric reaction. After 30-min incubation at 37°C, 80 μl of 12 N H_2SO_4 was added to stop the reaction. Absorbance at 540 nm was determined to assess the quantity of glucose liberated from either glycogen or trehalose.

Triglyceride and Free Glycerol Assays

Triglyceride and free glycerol levels were measured using the Serum Triglyceride Determination kit (TR0100; Sigma-Aldrich), with minor modifications. Cells (10 ODs) were collected at each time point and rapidly pelleted. The pellets were stored at –80°C until further processing. Cell pellets from each sample were resuspended with 500 µl of ice-cold H_2O and then broken open using bead-beating. After lysis, another 500 µl of H_2O was added.

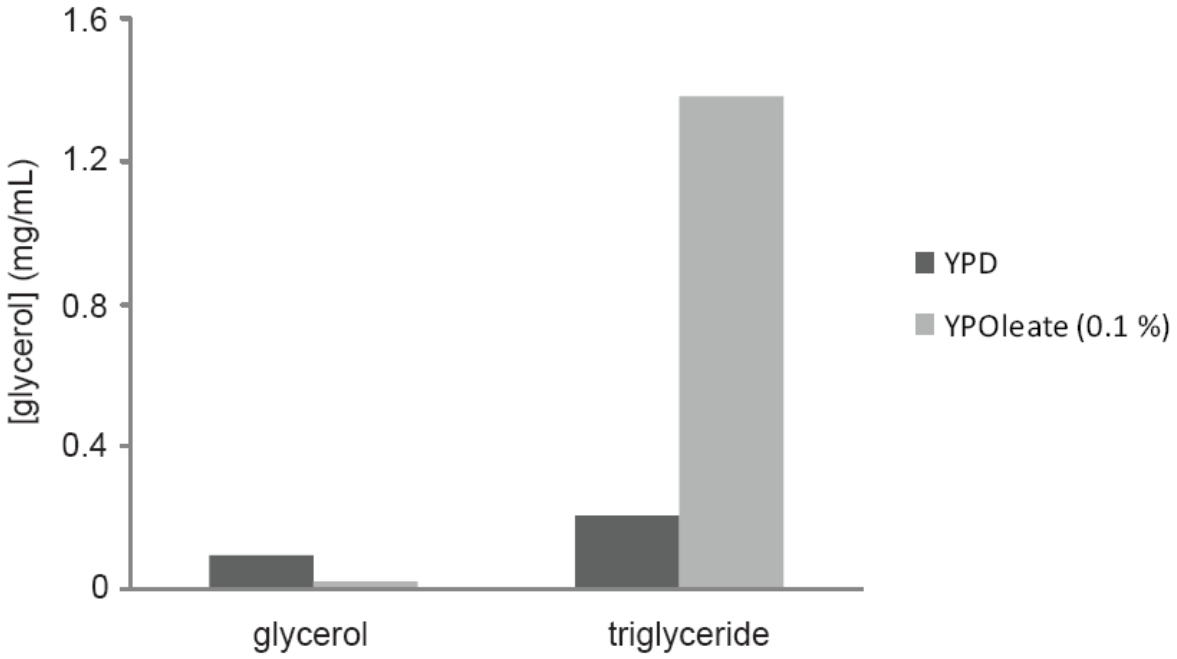

Figure II-13 Colorimetric triglyceride assay shows elevated levels of triglycerides in WT yeast grown in YPOleate (0.1 %) compared to YPD medium. WT yeast cells were grown in YPD and YPOleate (YP+0.1% oleate+0.2% Tween-20) to saturation. Triglyceride and glycerol levels were measured as described.

Triglyceride and free glycerol levels were then assayed largely as recommended: 4 parts of Free Glycerol Reagent was premixed with 1 part of water or 1 part of Triglyceride Reagent (contains lipoprotein lipase) to generate Triglyceride Reagent Blank and Triglyceride Working

Reagent, respectively. Then, 100 μl of each generated reagent was added into two separate wells for each sample in a 96-well plate and pre-warmed at 37°C for 5 min. The colorimetric reaction was started by adding 20 μl of each sample into two wells with different reagents. After 10-min incubation at 37°C, precipitate in each well was pelleted by centrifugation at top speed for 4 min, and then 80 μl of supernatant from each well was transferred to another plate and read at 540 nm.

Nth1p Immunoprecipitation and Activity Assay

Cells (50 ODs) were collected at each of 13 time points through one complete yeast metabolic cycle, or at various time points after regrowth in fresh medium. They were rapidly pelleted and stored at −80°C until further processing. Cell pellets were resuspended with 500 μl of lysis buffer (100 mM NaCl, 50 mM NaF, 100 mM Tris, pH 7.5, 1 mM EDTA, 1 mM EGTA, 0.1% Tween 20, 10% glycerol, 30 μM H-89, EMD Phosphatase Inhibitor Cocktail Set III [EMD Biosciences, San Diego, CA], Roche Protease Inhibitor Cocktail [Roche Diagnostics, Indianapolis, IN], 1 mM phenylmethylsulfonyl fluoride, and 14 mM β-mercaptoethanol), and then cells were broken open by bead- beating. After centrifugation, the supernatant was collected as cell lysate. The lysate was pre-cleared with ~15 μl of protein A/G agarose beads (Santa Cruz Biotechnology, Santa Cruz, CA). Another 25 μl of agarose beads were pre-conjugated with 2 μg of anti-FLAG antibody and then incubated with the pre-cleared lysate for 3 h at 4°C with rotation. The agarose beads were then washed four times with wash buffer (50 mM HEPES, pH 7.5, and 100 mM NaCl).

After resuspension in 100 μl of wash buffer, 20 μl of agarose beads suspension from each sample was transferred into two tubes containing Antarctic phosphatase buffer to generate two

sets of identical samples, one set for dephosphorylation of Nth1p and the other set as a control. Then, 1 μl of Antarctic phosphatase (New England Biolabs, Ipswich, MA) was added to one set of samples followed by 30-min incubation at 37°C. Nth1p activity was assayed by incubating with 180 μl of Trehalase Assay solution (50 mM imidazole, pH 7.0, and 50 mg/ml trehalose) at 30°C for 10 min. After the reaction was stopped by boiling for 5 min, the glucose generated in solution was assayed as described above.

III. ACETYL-COA INDUCES *CLN3* TRANSCRIPTION TO EXIT QUIESCENCE

In budding yeast cells, nutrient repletion induces rapid exit from quiescence and entry into a round of growth and division. The G1 cyclin *CLN3* is one of the earliest genes activated in response to nutrient repletion. Subsequent to its activation, hundreds of cell cycle genes can then be expressed, including the cyclins *CLN1/2* and *CLB5/6*. Although much is known regarding how *CLN3* functions to activate downstream targets, the mechanism through which nutrients activate *CLN3* transcription in the first place remains poorly understood. Here we show that a central metabolite of glucose catabolism, acetyl-CoA, induces *CLN3* transcription by promoting the acetylation of histones present in its regulatory region. The increase in acetyl-CoA production is sensed by the Gcn5p-containing SAGA transcriptional coactivator complex, which subsequently catalyzes histone acetylation at the *CLN3* locus alongside ribosomal and other growth genes to promote entry into the cell division cycle.

INTRODUCTION

The most basic building blocks of biological organisms are small molecule metabolites. In recent years, there has been renewed interest in understanding how the fundamental processes of cell growth and proliferation are coordinated with cellular metabolism. Nutrient-starved yeast cells arrest in a quiescent or G0 phase of the cell division cycle. Addition of nutrients stimulates exit from G0 and transition into G1 phase, and then ~800 genes are periodically transcribed as a function of the cell cycle (Cho et al., 1998; Spellman et al., 1998). *CLN3* is observed to be one of the earliest genes transcribed within this set (Cho et al., 1998; Rowicka et al., 2007; Spellman et al., 1998). Cln3p regulates G1 length by coordinating growth and division and may influence the critical cell size for passing START, the point at which cells commit to division (Cross, 1988; Jorgensen and Tyers, 2004; Nash et al., 1988; Turner et al., 2012). In *cln3*Δ mutants, cells become larger and stay in G1 phase longer, resulting in decreased growth and budding rates compared to wild type (Newcomb et al., 2003; Wu et al., 1999) (Figure III-1). Following *CLN3* activation, the G1 transcription complexes SBF and MBF can be activated by *CLN3*/*CDC28*-catalyzed phosphorylation of the SBF inhibitor Whi5p (Costanzo et al., 2004; de Bruin et al., 2004; Wijnen et al., 2002), and other unknown mechanisms, to enable transcription of over 200 downstream cell cycle genes (Ferrezuelo et al., 2010), including *CLN1/2* and *CLB5/6*. Cln1p and Cln2p can then further enhance SBF- and MBF-dependent G1 transcription through positive feedback mechanisms (Cross and Tinkelenberg, 1991; Dirick and Nasmyth, 1991; Doncic et al., 2011; Eser et al., 2011; Koch et al., 1993; Nasmyth and Dirick, 1991; Skotheim et al., 2008).

Although many studies have focused on the mechanisms by which Cln3p regulates G1 transcription, the mechanisms that lead to transcriptional activation of *CLN3* itself still remain

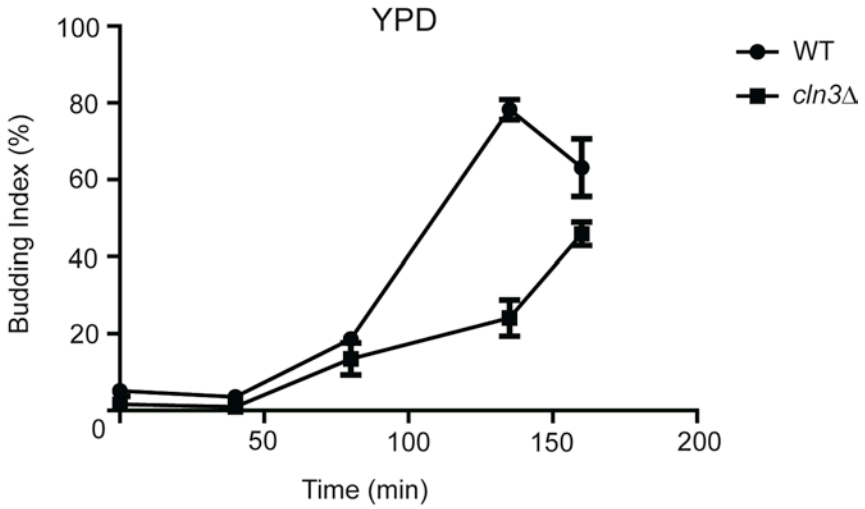

Figure III-1 *cln3Δ* mutant exhibits slower rates of budding upon nutrient repletion. Synchronized cells taken from the RC phase of the YMC were immediately washed and added to fresh YPD medium. Cell samples were collected from the indicated time points after repletion and fixed with 4% paraformaldehyde. Cells were observed with a light microscope to count percentage of cells with buds. At least 200 cells were counted per time point. Mean ± SD, n = 3

unresolved. Since the discovery of *CLN3* more than 20 years ago (Cross, 1988; Nash et al., 1988), the gene and its encoded protein have been reported to be regulated at multiple levels. At the transcriptional level, *CLN3* is activated by glucose (Parviz et al., 1998; Parviz and Heideman, 1998), which is reportedly mediated by Azf1p, a zinc-finger transcription factor (Newcomb et al., 2002). Following transcription, *CLN3* mRNA availability is regulated by a RNA-binding protein, Whi3p (Gari et al., 2001). At the translational level, *CLN3* is regulated by TOR (Target of Rapamycin) and cAMP-PKA pathways (Barbet et al., 1996; Hall et al., 1998), and repressed under various stress conditions (Gallego et al., 1997; Polymenis and Schmidt, 1997). Cln3p is thought to be a very unstable protein and subjected to ubiquitin-dependent proteolysis (Cross, 1990; Cross and Blake, 1993; Tyers et al., 1992; Yaglom et al., 1995). Finally, Cln3p protein localization has been reported to be regulated by molecular chaperone Ydj1p and Whi3p (Verges

et al., 2007; Wang et al., 2004). Cln3p also has a nuclear localization sequence on its C-terminus for nuclear import (Miller and Cross, 2001).

We have been utilizing the yeast metabolic cycle (YMC) to investigate the mechanisms that link cell growth and division to metabolism (Cai et al., 2011). In the YMC, a highly synchronized cell population undergoes robust oscillations in oxygen consumption and metabolism that are coupled to the cell cycle, during continuous glucose-limited growth (Tu et al., 2005; Tu et al., 2007). Microarray analysis of gene expression during the YMC has revealed that over half of all yeast genes are periodically expressed according to a specified logic. The YMC can be divided into three phases based on gene expression clustering – OX, RB and RC (Tu et al., 2005). In the OX phase, the vast majority of cellular growth genes are activated during a period of increased oxygen consumption. These include ribosomal protein (RP) and ribosome biogenesis (ribi) genes, amino acid biosynthetic genes, and numerous genes involved in increasing translational capacity. In the RB phase, the rate of oxygen consumption begins to decrease and a fraction of the cell population enters cell division. In this phase, many genes with roles in cell division are expressed, such as those encoding histone proteins, spindle pole body components, and proteins required for DNA replication. In the RC phase, a large cohort of genes associated with stress, survival, and stationary phase are induced. These expression data have also enabled the high-resolution timing of cell-cycle regulated transcripts to a resolution of ~2-3 minutes (Rowicka et al., 2007). The vast majority of “gold-standard” cell cycle genes, including all of the cyclins, are periodic and transcribed in their expected order in this YMC dataset (Rowicka et al., 2007). The accurate timing of cyclin and cell cycle gene expression as viewed in the YMC indicates that it faithfully recapitulates the order of events associated with cell cycle entry and progression. In this study, we used both the YMC and traditional batch cultures to

dissect the mechanism by which the transcription of the key G1 cyclin *CLN3* is activated in tune with metabolism to promote cell cycle entry.

RESULTS

Histone H3 is extensively acetylated at the promoter region of CLN3 upon its activation

In a recent study, we uncovered an important mechanism by which cellular growth genes are regulated in tune with metabolism. The acetylation of histones on multiple sites on H3 and H4 increases substantially during the OX growth phase of the YMC, precisely when intracellular levels of the metabolite acetyl-CoA increase (Cai et al., 2011). Subsequent ChIP-Seq analysis revealed that these acetylated histones were present almost exclusively at a set of over ~1,000 OX phase genes that are collectively rate-limiting for cell growth. These data reveal that acetyl-CoA induces the acetylation of histones at these growth genes to enable cell growth and proliferation (Cai et al., 2011; Cai and Tu, 2011).

Interestingly, we observed that *CLN3* belongs to this group of OX phase growth genes (Figure III-2A). *CLN3* is one of the earliest expressed genes specifically associated with the cell cycle (Cho et al., 1998; Rowicka et al., 2007; Spellman et al., 1998; Tu et al., 2005). Transcript levels of *CLN3* peak sharply in the OX phase along with ribosomal and other growth genes (Figure III-3). *CLN1* and *CLN2* expression immediately follow that of *CLN3* in the YMC (Figure III-2A). These data are consistent with previous reports showing that *CLN3* is expressed rapidly in response to fresh nutrients, and subsequently activates the other G1 cyclins, *CLN1* and *CLN2* (Dirick et al., 1995; Stuart and Wittenberg, 1995; Tyers et al., 1993). We therefore hypothesized that *CLN3* transcription might be similarly driven by the acetyl-CoA-induced acetylation of histones present in its regulatory region.

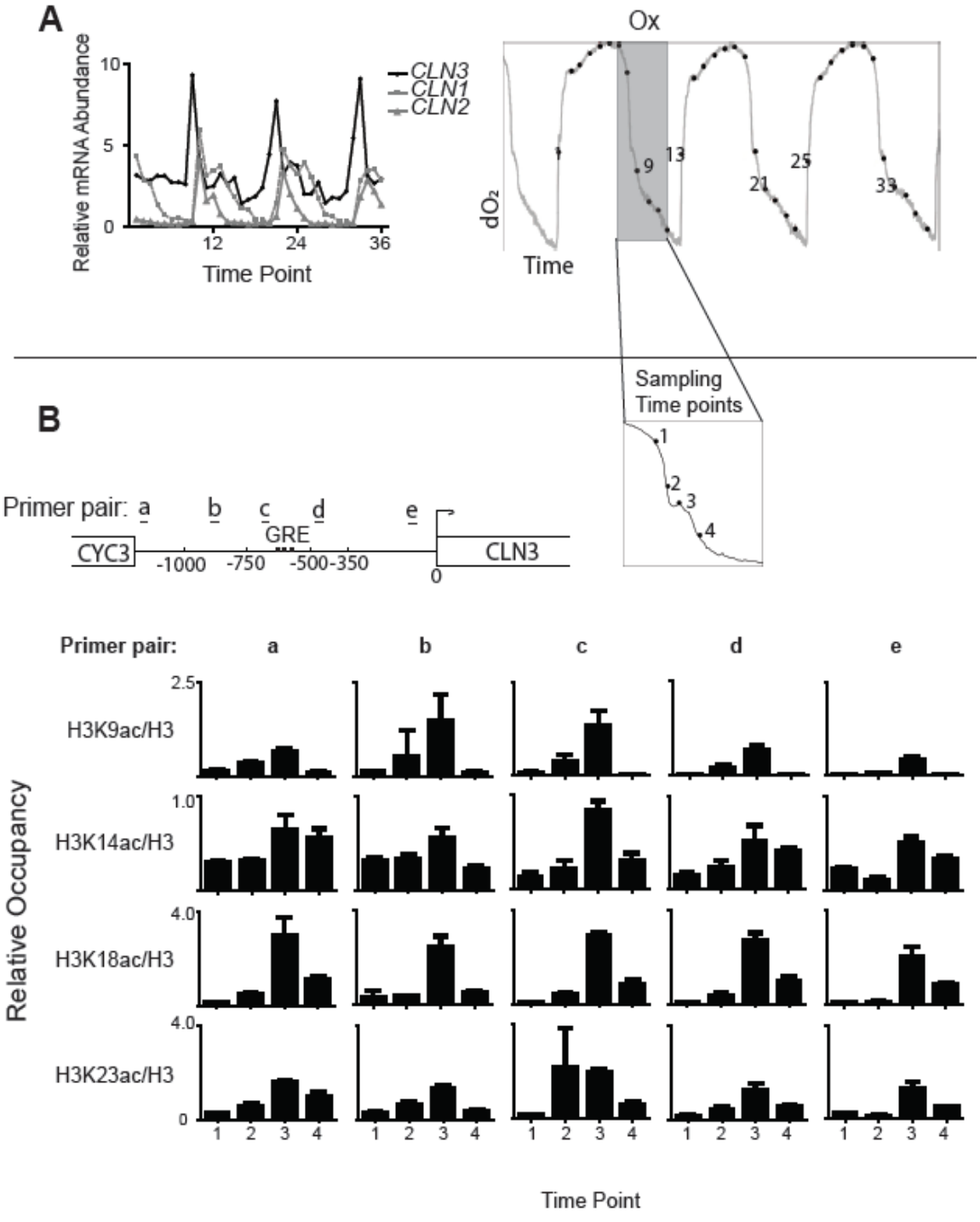

Figure III-2 *CLN3* transcription during the YMC is accompanied by histone acetylation in its promoter region. (A) *CLN3* transcript levels peak prior to *CLN1* and *CLN2* in the OX phase. Relative mRNA abundance (left) of *CLN3*, *CLN1* and *CLN2* at 36 time points across three consecutive metabolic cycles (right). Expression data are derived from the YMC microarray dataset (Tu et al., 2005). Each time point corresponds to ~25 min. (B) Histone H3 acetylation at

the *CLN3* locus correlates tightly with *CLN3* transcription. Histone acetylation was measured by ChIP with six primer pairs designed to span sequences upstream of the *CLN3* gene and its open reading frame. The Glucose Responsive Element (GRE) is marked (Parviz et al., 1998). Samples for ChIP were collected at the four time points 1-4, each ~5 min apart. Histone H3 acetylation signal was normalized to total histone H3 binding and expressed as "relative occupancy". Mean ± SD, n = 3

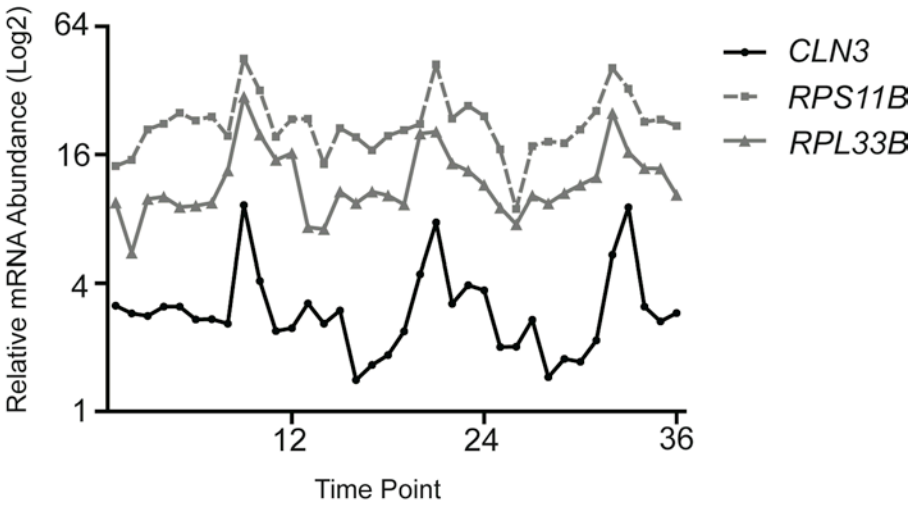

Figure III-3 *CLN3* expression is induced concurrently with ribosomal subunit genes. *CLN3* transcript levels increase in the same temporal window as *RPS11B* and *RPL33B* transcripts in the OX growth phase of the YMC. Expression data over three consecutive metabolic cycles were obtained previously (Tu et al., 2005).

In order to quantitate histone acetylation at the *CLN3* locus as cells transitioned into the OX growth phase of the YMC, we performed chromatin immunoprecipitation (ChIP) using antibodies that recognize specific acetylated sites on histone H3. We observed a significant increase in acetylation on multiple sites (H3K9, H3K14, H3K18, H3K23), during a time window precisely coinciding with the peak in *CLN3* mRNA levels (Figure III-2). The acetylated histones were detected in a region corresponding to the *CLN3* promoter proximal to a previously identified Glucose Responsive Element (GRE) (Newcomb et al., 2002; Parviz et al., 1998). These histones became rapidly deacetylated as cells proceeded further into the OX growth phase (Figure III-2B).

We next tested whether the dynamic acetylation of histones at the *CLN3* locus could also be observed in a batch culture model where cells exit quiescence and rapidly enter growth upon nutrient repletion (Figure III-4A). Following addition of fresh media containing glucose as the carbon source, we observed a substantial increase of histone acetylation on multiple sites in the same *CLN3* promoter region within 10 min (Figure III-4B), coinciding with the timing of *CLN3* mRNA induction (Figure III-5B). Taken together, these data indicate that histones on nucleosomes present at the upstream *CLN3* regulatory region are dynamically acetylated as yeast cells transition from a quiescent state into growth.

Acetyl-CoA induces CLN3 transcription via the Gcn5p-containing SAGA transcriptional coactivator

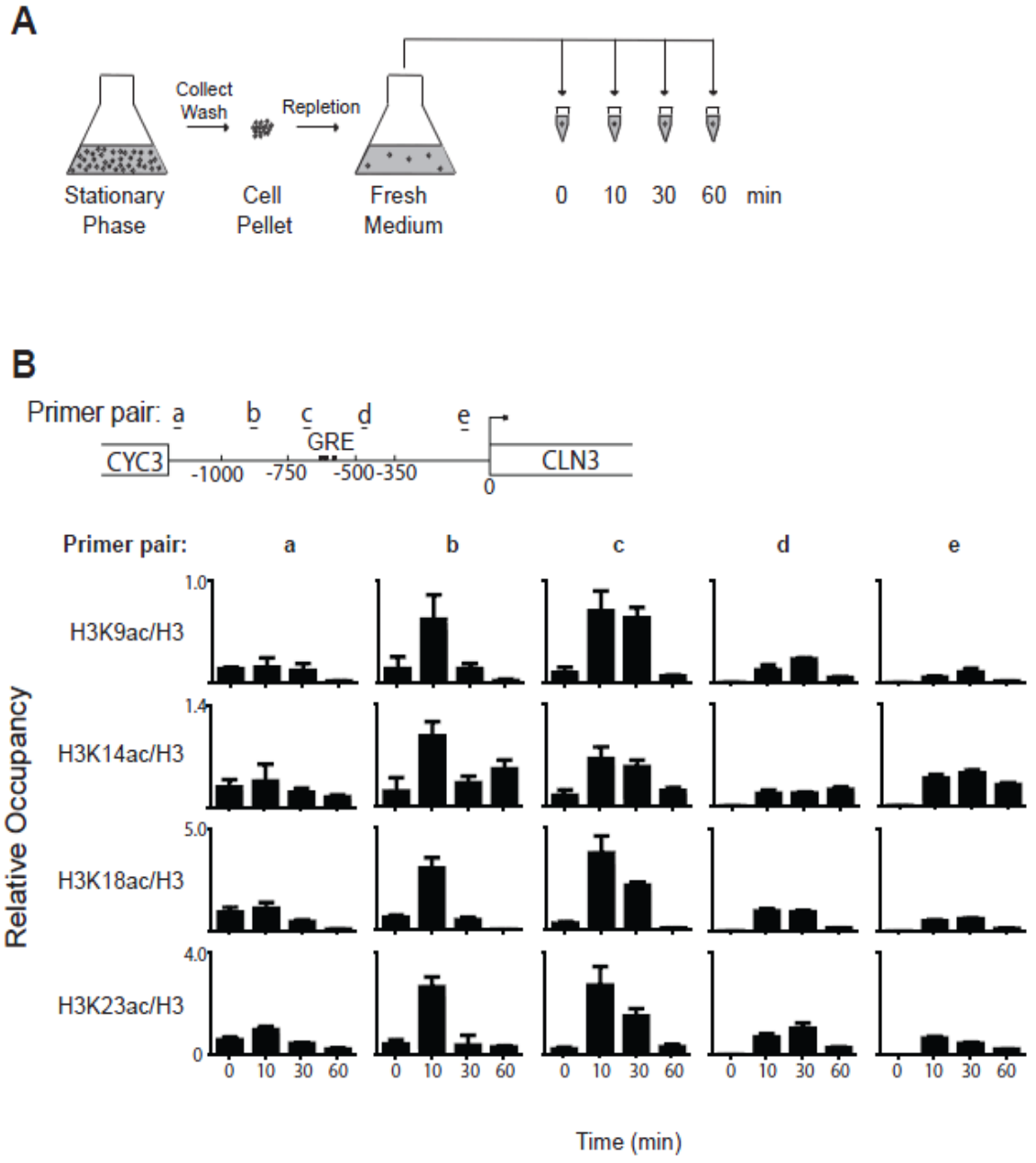

Figure III-4 *CLN3* induction following nutrient repletion in batch culture is accompanied by increased histone acetylation in its promoter region. (A) Schematic representation of experimental procedure for batch culture sampling (see also Materials and Methods). Samples for ChIP were collected at 0, 10, 30 and 60 min following addition of quiescent cells into fresh YPD medium. (B) Histone H3 acetylation following nutrient repletion was assayed as in Figure III-2.

Our observations thus far are entirely consistent with previous studies showing that glucose is a potent inducer of *CLN3* transcription (Parviz and Heideman, 1998). However, none of the well-known glucose or nutrient-signaling pathways including cAMP-PKA, TOR, and various glucose transporters, appears to be required for glucose-induced *CLN3* transcription (Hubler et al., 1993; Newcomb et al., 2003; Parviz and Heideman, 1998). In contrast, the inhibition of glycolysis compromises glucose-induced *CLN3* transcription, suggesting a downstream metabolite of glucose could be mediating its effects (Newcomb et al., 2003; Parviz and Heideman, 1998).

Recently, we observed that acetyl-CoA is a key metabolite of glucose and carbon sources that induces growth entry (Cai et al., 2011). Acetyl-CoA not only fuels the TCA cycle for ATP synthesis but is also used to synthesize fatty acids, sterols, and amino acids. Several simple carbon sources including ethanol, acetaldehyde, and acetate, each of which must be converted to acetyl-CoA for their assimilation (Figure III-5A), can effectively induce cycling cells to exit the quiescent-like RC phase and immediately enter the OX growth phase (Cai et al., 2011). The increased acetyl-CoA production upon entry into growth is sensed by the Gcn5p-containing SAGA acetyltransferase complex (Grant et al., 1997) and enables it to catalyze histone acetylation specifically at growth genes, the majority of which are transcribed during the OX phase of the YMC (Cai et al., 2011). Since *CLN3* transcription occurs during the OX phase alongside other growth genes and is coincident with a spike in acetyl-CoA levels and histone acetylation in its regulatory region, acetyl-CoA may also represent the key metabolic driver of *CLN3* transcription.

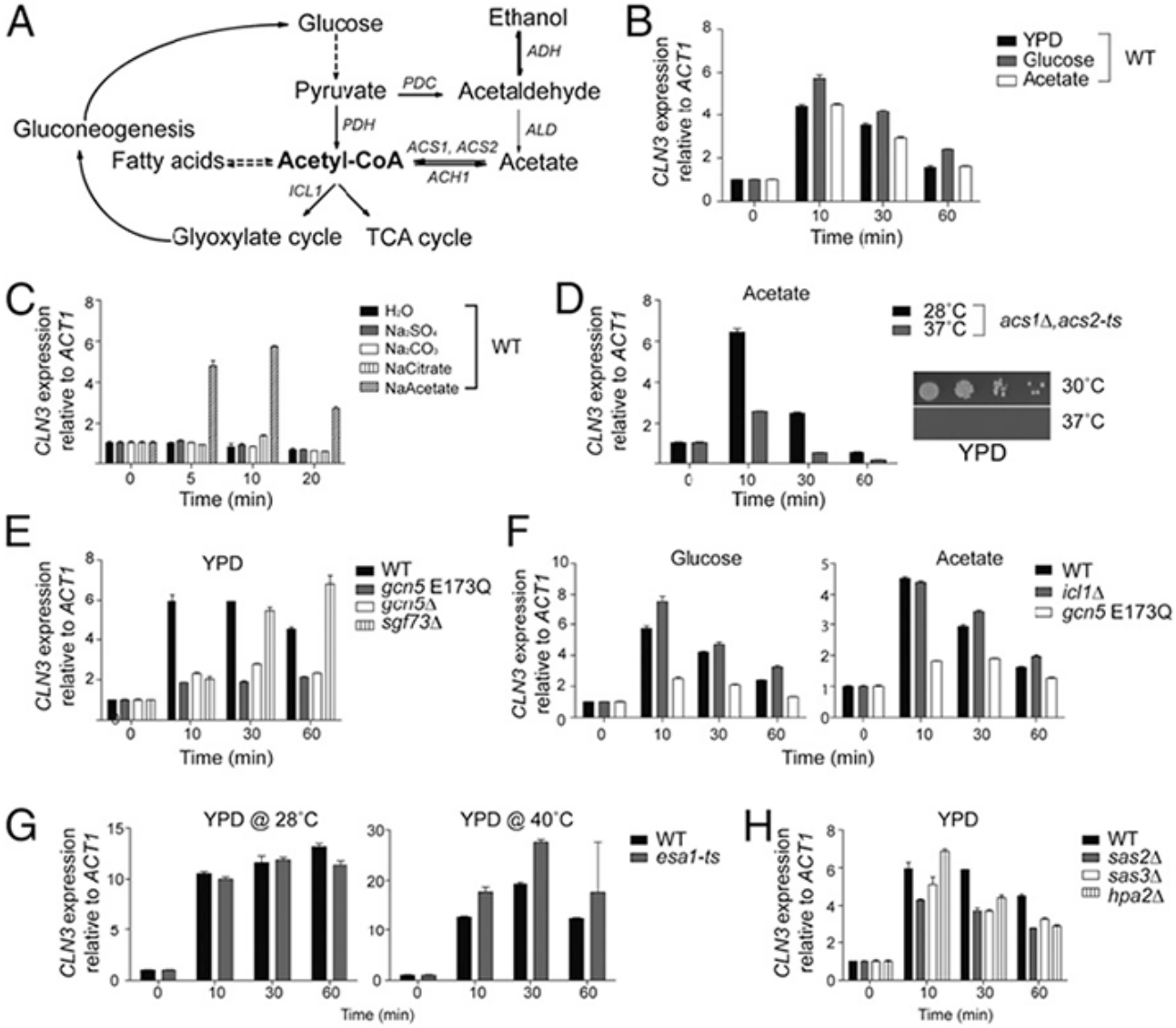

Figure III-5 Acetyl-CoA induces transcription of *CLN3* through the Gcn5p-containing SAGA transcriptional coactivator complex. (A) Metabolic pathways in yeast centered around acetyl-CoA. (B) *CLN3* transcription is induced by YPD, glucose, or acetate. *CLN3* transcription in batch culture was assayed by real-time qPCR at indicated times following exposure of quiescent cells to fresh YPD medium, 2% glucose alone, or 10 mM acetate alone. *CLN3* mRNA levels were normalized to *ACT1* mRNA levels and expressed as "*CLN3* expression relative to *ACT1*". Mean ± SD, n = 3. (C) *CLN3* transcription is specifically induced by acetate. *CLN3* transcription was measured as above in wild type following repletion with water, 0.1 mM sodium sulfate, sodium carbonate, sodium citrate, or sodium acetate. Mean ± SD, n = 3. (D) Acetate-induced *CLN3* transcription requires intact acetyl-CoA synthetase activity. *CLN3* transcription was measured as above in the temperature-sensitive mutant *acs1Δ, acs2-ts* at permissive and non-permissive temperatures upon repletion with 0.1 mM acetate. Mean ± SD, n = 3. The temperature-sensitive growth defect of this strain on YPD is shown in the inset. (E) *CLN3*

transcription is dependent on Gcn5p and components of SAGA. *CLN3* transcription was measured as above in wild type, *gcn5 E173Q* (catalytically inactive), *gcn5Δ*, and *sgf73Δ* strains following repletion with YPD. Mean ± SD, n = 3. (F) Acetyl-CoA-induced transcription of *CLN3* is dependent on the acetyltransferase activity of Gcn5p. *CLN3* transcription was measured as above in wild type, *icl1Δ* and *gcn5 E173Q* strains repleted with either 2% glucose or 10 mM acetate. *icl1*Δ mutants cannot convert acetyl-CoA to glucose. Mean ± SD, n = 3. (G) *CLN3* transcription is not dependent on the Esa1p-containing NuA4 H4 acetyltransferase complex. CLN3 transcription was measured as above in wild type and the *esa1-ts* mutant, following repletion with YPD at either the permissive (28ºC) or non-permissive temperature (40ºC). (H) *CLN3* transcription is not dependent on other acetyltransferases. *CLN3* transcription was measured as above in wild type, *sas2Δ*, *sas3Δ*, and *hpa2Δ* strains following repletion with YPD medium. Mean ± SD, n = 3

To investigate a possible role for acetyl-CoA in the regulation of *CLN3* transcription, we tested whether acetate can induce *CLN3* transcription in quiescent cells. Stationary phase cells were added to fresh media containing either YPD, glucose alone, or acetate alone, and *CLN3* transcription was monitored over several time points. Strikingly, *CLN3* transcription was induced in response to all three conditions with similar kinetics (Figure III-5B). To rule out the possibility that *CLN3* transcription by acetate repletion might be due to osmotic or ionic stress, *CLN3* induction was measured following repletion of other anionic salts such as sulfate, carbonate, or citrate, as well as water alone. Only acetate could potently induce *CLN3* transcription (Figure III-5C). As expected, the induction of *CLN3* transcription by acetate depends on functional acetyl-CoA synthetase enzymes (Figure III-5D). Since there is no other fate for acetate except its conversion to acetyl-CoA via the acetyl-CoA synthetase enzymes, these data suggest that acetyl-CoA derived from either glucose or acetate is sufficient to induce *CLN3* transcription. However, acetyl-CoA-derived from acetate can be used for gluconeogenesis through the glyoxylate pathway (Figure III-5A), thereby potentially contributing a source of glucose that could stimulate *CLN3* transcription through some as of yet unidentified glucose-specific pathway. To rule out this possibility, we tested whether acetate could still induce *CLN3* transcription in an *icl1Δ* mutant lacking the glyoxylate pathway (Fernandez et al., 1992). *CLN3* transcription was not compromised in this mutant, indicating that acetyl-CoA and not glucose is the key metabolite sufficient to activate *CLN3* transcription (Figure III-5F).

We next tested whether acetyl-CoA-induced *CLN3* transcription is likewise dependent on the Gcn5p acetyltransferase enzyme present within SAGA that catalyzes histone acetylation at growth genes (Cai et al., 2011). We assayed *CLN3* transcription following rich medium repletion

in a *gcn5Δ* or *gcn5 E173Q* mutant that is catalytically inactive (Trievel et al., 1999). In addition, we tested the *sgf73Δ* mutant which lacks an important subunit of SAGA that is dynamically acetylated in response to acetyl-CoA (Cai et al., 2011). Sgf73p is important for the histone acetyltransferase activity of SAGA and its recruitment to DNA (Cai et al., 2011; Shukla et al., 2006). *CLN3* induction was significantly compromised in each of these mutants, revealing the importance of Gcn5p and components of SAGA for activation of this gene (Figure III-5E). In *gcn5* mutants, *CLN3* induction was virtually eliminated, whereas the *sgf73*Δ mutant could still induce *CLN3* albeit with slower kinetics. Moreover, glucose or acetate alone could no longer induce *CLN3* transcription in the *gcn5 E173Q* mutant (Figure III-5F), and the acetate-induced histone acetylation in wild type quiescent cells was abolished in the *gcn5 E173Q* mutant (Figure III-6). These data clearly demonstrate that the effects of acetyl-CoA on *CLN3* induction are dependent on the acetyltransferase activity of Gcn5p, which consumes acetyl-CoA as a substrate.

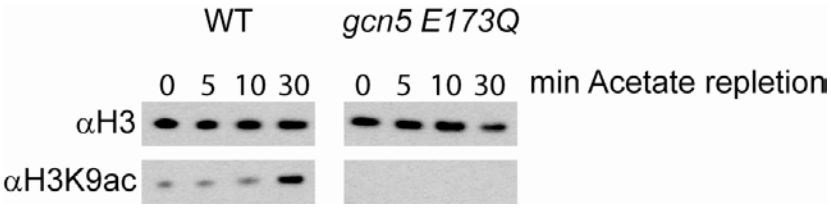

Figure III-6 Acetate induces acetylation of histone H3 in quiescent cells through Gcn5p H3K9 acetylation upon 0.1 mM acetate (pH 5.2) repletion in wild type and *gcn5 E173Q* catalytically inactive mutant strains was assayed by Western blot with αH3 and αH3K9ac antibodies at indicated time points.

To further investigate the possibility that Gcn5p activity is modulated by levels of acetyl-CoA, we constructed a *gcn5 A190T* mutant which was previously reported to have higher acetyl-CoA binding affinity *in vitro* (Langer et al., 2002). If this change to the enzyme is recapitulated

in vivo, CLN3 transcription in this mutant can be predicted to be more responsive to acetate repletion than wild type. However, *CLN3* induction in this *gcn5 A190T* mutant was sub-optimal at multiple acetate concentrations tested, contrary to our expectations (Figure III-7A). Furthermore, higher concentrations of acetate were needed to induce *gcn5 A190T* cells to enter the OX growth phase of the YMC, demonstrating that this mutant is actually less responsive to acetate than wild type (Figure III-7B). These phenotypes are consistent with our previous observation that the *gcn5 A190T* mutant is defective for growth on acetate as a carbon source (Cai et al., 2011)**.** Nonetheless, these data suggest the affinity of the Gcn5p acetyltransferase enzyme for acetyl-CoA can be neither too high nor too low, and that the wild type enzyme has been optimized to respond to a particular threshold of acetyl-CoA levels *in vivo.* The observation that a catalytically inactive mutant of Gcn5p is defective in *CLN3* induction, coupled with the observation that a mutation of Gcn5p that purportedly increases its affinity for acetyl-CoA *in vitro* is also sub-optimal for *CLN3* induction, argues that this acetyltransferase enzyme can respond to acetyl-CoA fluctuations *in vivo.*

We also tested other known histone acetyltransferases for possible contributions to *CLN3* transcription, including *ESA1*, the catalytic subunit of the NuA4 complex, *SAS2, SAS3* and *HPA2*. None of these other HATs had any effect on *CLN3* transcription following nutrient repletion (Figure III-5G, Figure III-5H), indicating that Gcn5p-containing SAGA is the major acetyltransferase that catalyzes histone acetylation at the *CLN3* locus to activate gene transcription.

To further investigate the regulation of *CLN3* transcription by SAGA, we examined whether SAGA is recruited to the *CLN3* promoter within the time frame of its transcription.

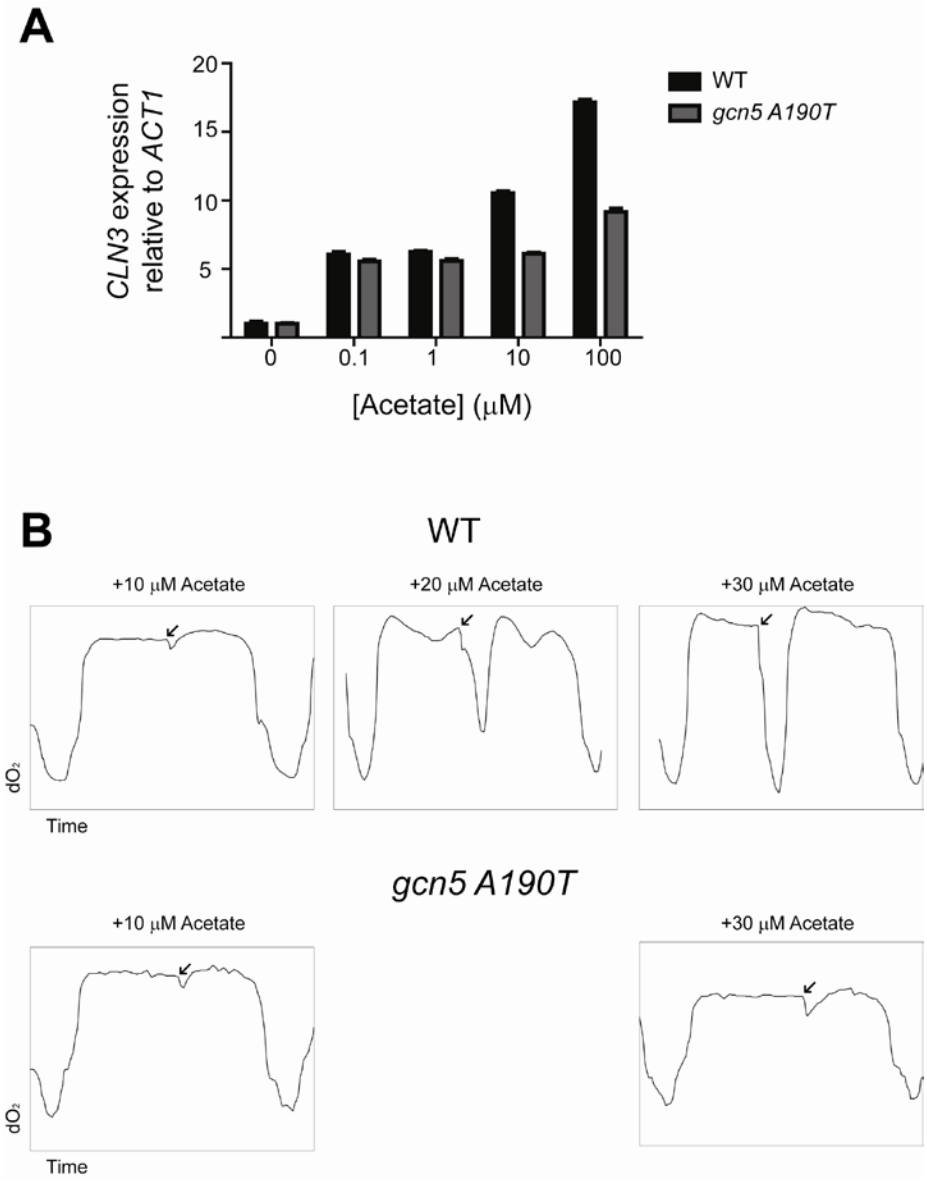

Figure III-7 The *gcn5 A190T* mutant exhibits less responsiveness to acetate than wild type. (A) *CLN3* transcription was measured as above in wild type and *gcn5 A190T* mutant strains repleted with different concentrations of acetate as indicated. The mRNA levels were normalized to *ACT1* mRNA levels and expressed as "*CLN3* expression relative to *ACT1*". Mean ± SD, n = 3. (B) Wild type and *gcn5 A190T* mutant strains were grown under continuous culture conditions to establish the YMC. The indicated concentrations of acetate were added directly into the chemostat at the indicated times in RC phase (arrows) to induce growth entry. Note that 30 μM acetate could induce wild type but not *gcn5 A190T* cells to enter growth.

Since *CLN3* transcription was observed in as early as 3 min immediately after nutrient repletion (Figure III-8), we tested for SAGA binding within this short time interval. SAGA binding was assessed by ChIP of strains expressing a flag epitope-tagged version of Spt7p, a scaffold protein important for integrity of the complex (Wu and Winston, 2002). SAGA binding at the *CLN3*

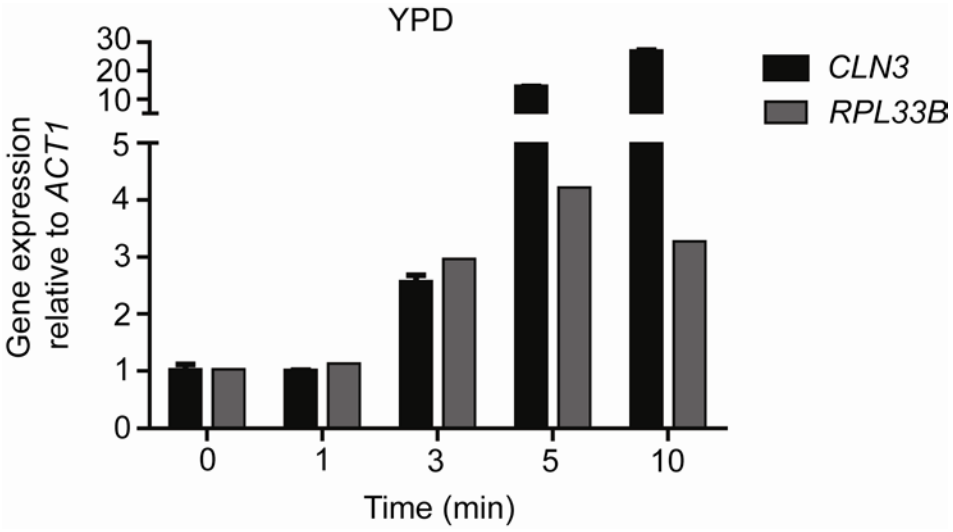

Figure III-8 *CLN3* transcription is induced in as early as 3 min following YPD repletion along with *RPL33B. CLN3* and *RPL33B* transcript levels were measured as above in wild type cells repleted with YPD. Their mRNA levels were normalized to *ACT1* mRNA levels and expressed as "Gene expression relative to *ACT1*". Mean ± SD, n = 3

regulatory region was observed in as early as 1 min after glucose repletion (Figure III-9). SAGA can auto-acetylate itself on several subunits (Cai et al., 2011; Rodriguez-Navarro et al., 2004), most notably on Sgf73p, which may mediate its recruitment to growth genes in response to acetyl-CoA (Cai et al., 2011). To test whether acetylation of SAGA might aid its recruitment to *CLN3,* we assayed SAGA binding in *gcn5 E173Q, gcn5Δ* and *sgf73Δ* mutants following nutrient repletion. SAGA recruitment to the *CLN3* promoter as well as ribosomal subunit gene promoters (*RPS11B* and *RPL33B*) was compromised by the absence of Gcn5p acetyltransferase activity

(Figure III-9). Moreover, in the *sgf73*Δ mutant, SAGA recruitment to *CLN3* and ribosomal genes was largely undetectable (Figure III-9), which was not due to lower amounts of Spt7p in the mutant whole cell lysates or immunoprecipitates (Figure III-10), suggesting that Sgf73p plays a key role in facilitating SAGA to bind growth gene targets. Although SAGA recruitment in the *sgf73*Δ mutant as assayed by Spt7p-ChIP was not detectable over a 60-min time period following glucose repletion (Figure III-10), *CLN3* induction could still occur, but at much slower rates (Figure III-5E).

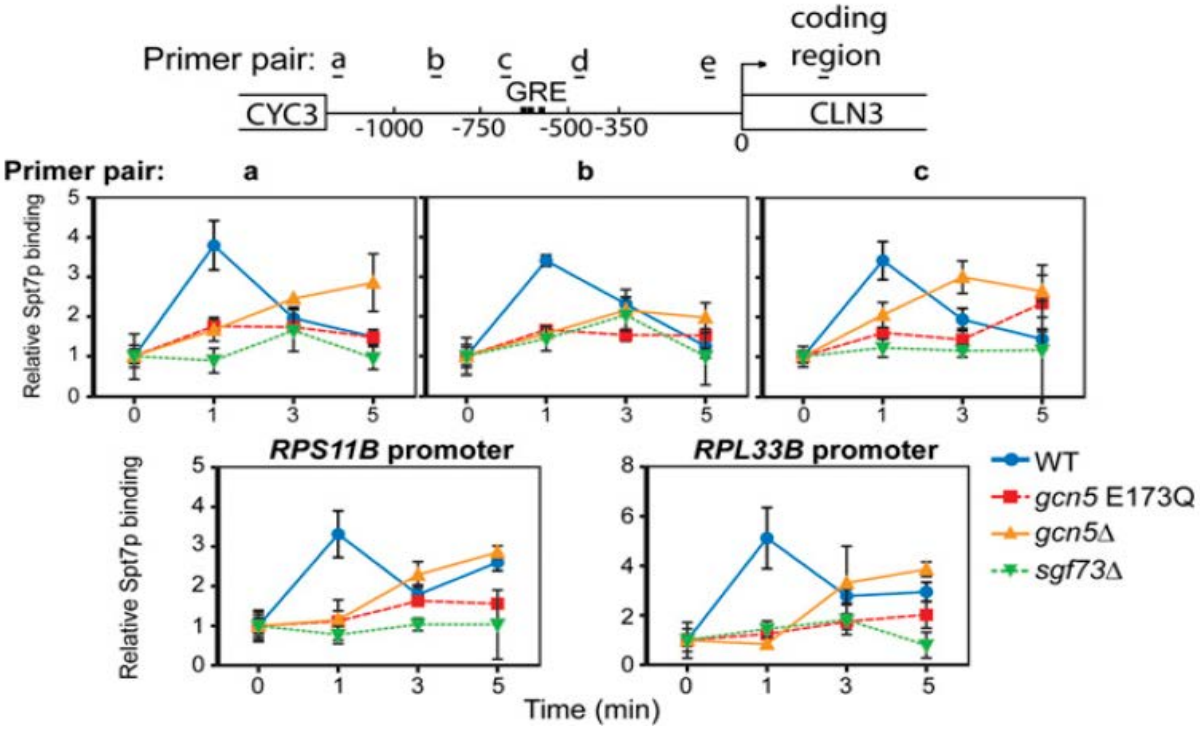

Figure III-9 Recruitment of SAGA to the *CLN3* promoter region depends on its acetyltransferase activity. SAGA binding at the *CLN3* promoter was assayed by ChIP in wild type, *gcn5 E173Q*, *gcn5Δ*, and *sgf73*Δ strains expressing *SPT7*-FLAG at 0, 1, 3 and 5 min immediately after repletion of quiescent cells with 2% glucose. Spt7p binding was normalized to the input DNA. Spt7p binding at promoters of ribosomal genes *RPS11B* and *RPL33B* is shown as control. Mean ± SD, n = 3. Spt7p binding spanned a larger region compared to acetylated histones (Figure III-2 and III-4).

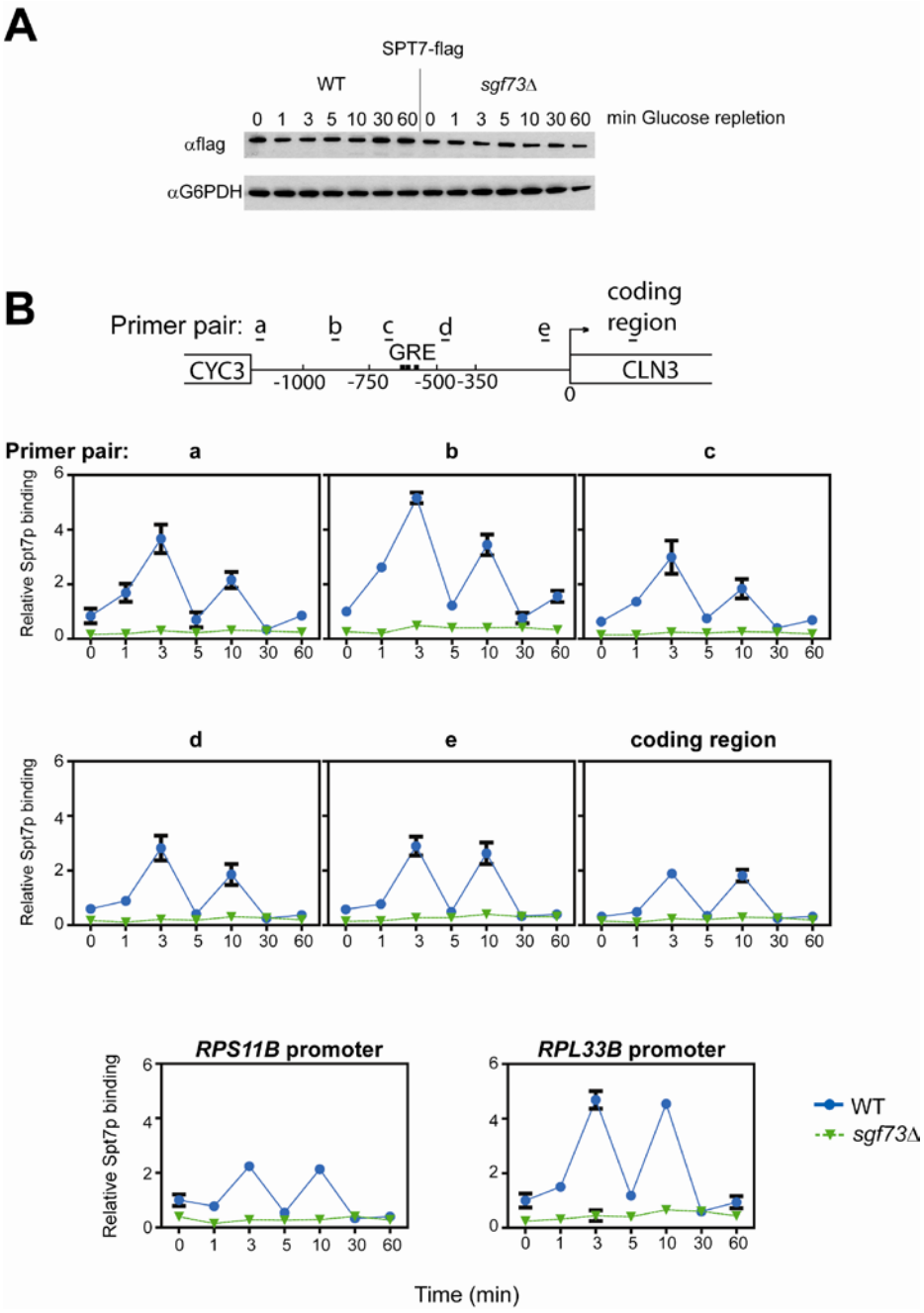

Figure III-10 Spt7p binding does not depend on the protein amount and is most significantly induced within 3 min after glucose repletion. (A) Proteins levels of Spt7p in wild type and *sgf73Δ* mutant after 2% glucose repletion were assayed by Western blot with an αflag antibody at indicated time points. The loading control is shown using an αG6PDH antibody. (B) SAGA binding at the *CLN3* promoter was assayed by ChIP in wild type and *sgf73Δ* mutant expressing *SPT7*-flag at indicated time points immediately following repletion of quiescent cells with 2% glucose. Spt7p binding was normalized to the input DNA. Spt7p binding throughout the entire

CLN3 locus, as well as at promoters of *RPS11B* and *RPL33B*, is shown. Spt7-binding appeared bimodal in the surveyed 60 minute period. Mean ± SD, n = 3

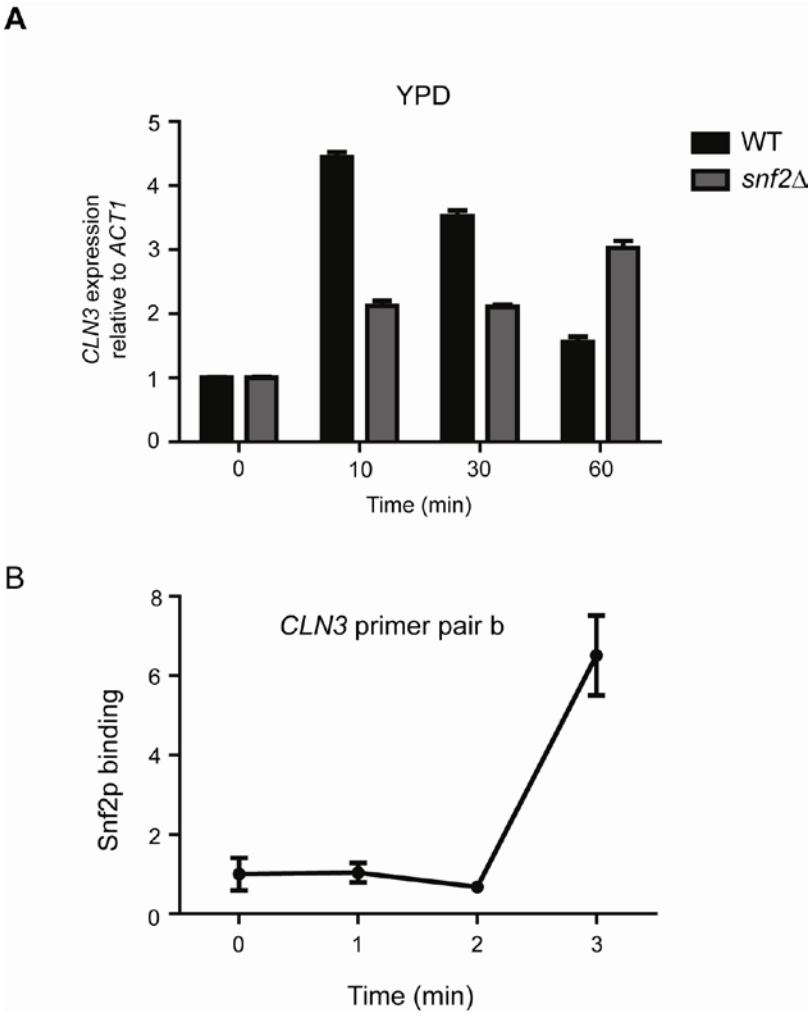

Figure III-11. Snf2p contributes to glucose-induced *CLN3* transcription. (A) *CLN3* transcription was measured as above in wild type and *snf2Δ* strains repleted with YPD. The mRNA levels were normalized to *ACT1* mRNA levels and expressed as "*CLN3* expression relative to *ACT1*". Mean ± SD, n = 3. (B) Snf2p binds the *CLN3* promoter upon repletion with YPD. Snf2p binding at the *CLN3* promoter was assayed by ChIP at 0, 1, 2 and 3 min immediately after repletion of quiescent cells with YPD. Snf2p binding was normalized to the input DNA. Only the primer pair b covered region is shown as it is the region with the most significant binding. Mean ± SD, n = 3

We speculated that other chromatin-modifying complexes might function to maintain the *CLN3* promoter region permissive for continued transcription. Since the Swi/Snf chromatin remodeling complex has been linked to SAGA and may have functions redundant with SAGA (Gregory et al., 1999; Kim et al., 2010; Sudarsanam et al., 1999), we tested whether the Swi/Snf complex might play a role in *CLN3* transcription. We observed Snf2p binding to the *CLN3* promoter region within 3 min following nutrient repletion, consistent with the time frame of SAGA binding and *CLN3* induction (Figure III-11). Furthermore, *CLN3* induction was compromised in the *snf2*Δ mutant, suggesting that the Swi/Snf complex is required to attain maximal levels of *CLN3* transcription (Figure III-11).

Rap1p and Fhl1p are transcription factors that may regulate CLN3 transcription

The SAGA transcriptional coactivator reportedly cannot bind DNA directly, so it must be recruited to its targets with the aid of particular transcription factors (Utley et al., 1998). The zinc-finger transcription factor Azf1p was previously reported to activate glucose-induced *CLN3* transcription by binding the GRE elements in its promoter (Newcomb et al., 2002; Parviz et al., 1998). Using an *azf1*Δ mutant strain, we confirmed the role for Azf1p in glucose-induced *CLN3* transcription and further showed its requirement for acetate-induced *CLN3* transcription (Figure III-12A). However, we were not able to observe significant Azf1p binding to the *CLN3* locus following nutrient repletion after many exhaustive trials. Consistent with our results, Azf1p binding was not observed at the *CLN3* promoter in a genome-wide survey of transcription factor binding (Harbison et al., 2004). We then assayed Azf1p binding to the *CLN3* promoter using the YMC where cells synchronously transition between different metabolic states. Surprisingly,

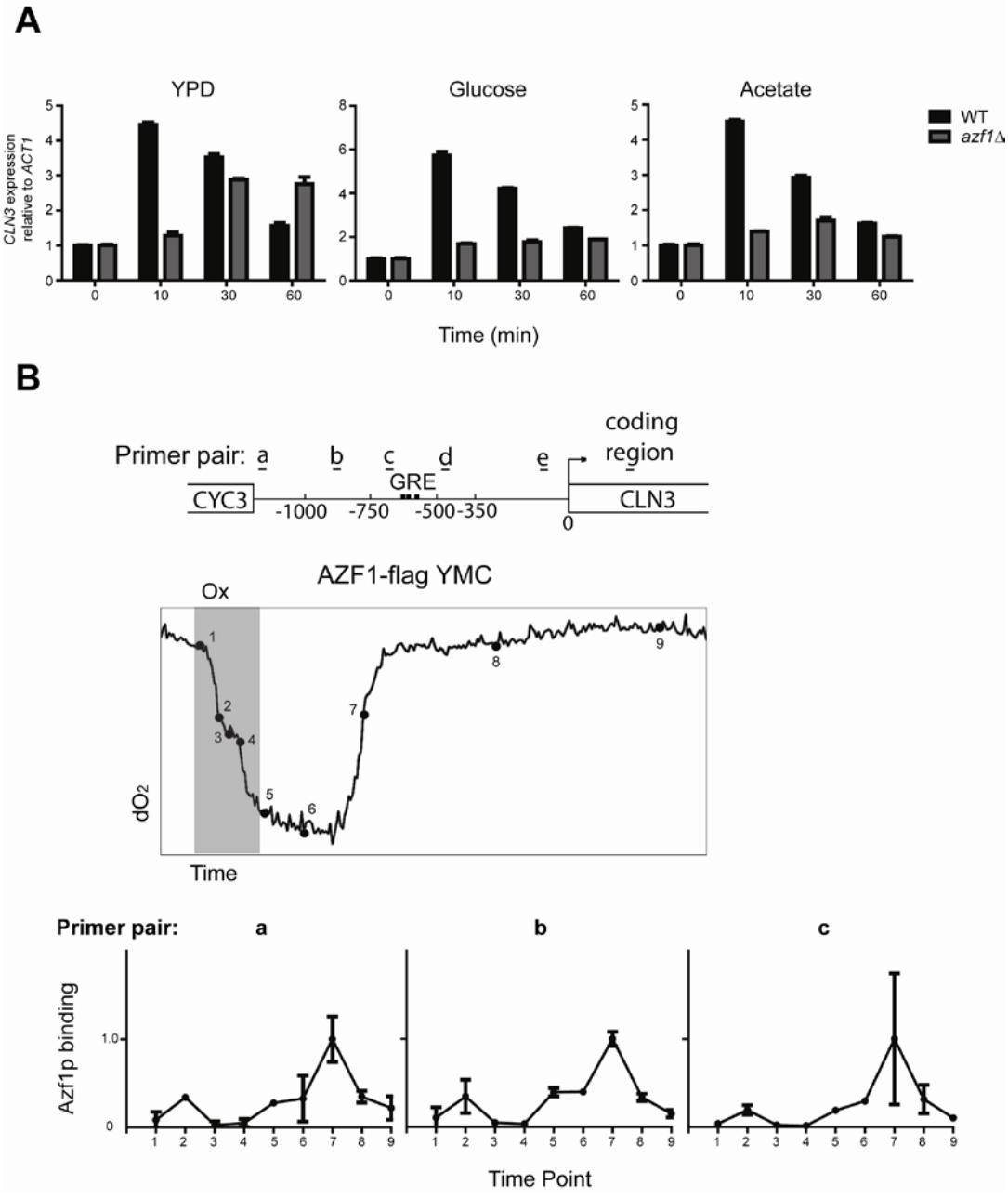

Figure III-12 On the role of Azf1p in the regulation of *CLN3* transcription. (A) Azf1p is required for optimal *CLN3* transcription following YPD, glucose or acetate repletion. *CLN3* transcription was measured as above in wild type and *azf1Δ* strains repleted with YPD, 2% glucose and 10 mM acetate. Mean ± SD, n = 3. (B) Azf1p binding at *CLN3* regulatory region does not correlate with active *CLN3* transcription in the YMC. Azf1p binding at the *CLN3* locus was assayed by ChIP at 9 time points across one YMC. Azf1p binding was normalized to the input DNA. Mean ± SD, n = 3

Azf1p binding to the *CLN3* regulatory region was observed in the RB phase, whereas *CLN3* transcript levels peak much earlier in the OX phase (Figure III-12B). A transcription factor that mediates the recruitment of SAGA to the *CLN3* locus would be expected to bind specifically during the OX phase. Thus, how Azf1p contributes to the regulation of *CLN3* transcription may be more complicated than expected and requires further investigation.

Mcm1p is another transcription factor reported to mediate *CLN3* transcription in a cell-cycle dependent manner (Kuo and Grayhack, 1994; MacKay et al., 2001; Mai et al., 2002; McInerny et al., 1997). We tested the binding of Mcm1p to the *CLN3* promoter across the YMC. Surprisingly, Mcm1p binding at the *CLN3* promoter was observed in the RB phase and did not correlate with the temporal window of active *CLN3* transcription (Figure III-13B), although we observed correlation of Mcm1p binding and *CLN3* transcription in batch culture (Figure III-13A). The same disconnect between the timing of Mcm1p-binding and transcription was observed for two ribosomal subunit genes, *RPS11B* and *RPL33B* (Figure III-13B). Moreover, a *mcm1-ts* mutant did not compromise *CLN3* transcription (Parviz et al., 1998). As with Azf1p, a direct role for Mcm1p in activating *CLN3* transcription remains uncertain. Since Mcm1p can serve as either a transcriptional activator or repressor, it may play a repressive role at *CLN3* and ribosomal genes.

To determine whether other transcription factors might regulate *CLN3*, we mined a list of possible candidates that have been reported to bind its regulatory region using YEASTRACT (Teixeira et al., 2006). We constructed individual deletion strains for non-essential transcription factors on this list. None of these except Azf1p displayed a compromising effect on glucose-induced *CLN3* transcription (Figure III-12A). Besides Mcm1p, Rap1p and Fhl1p are two

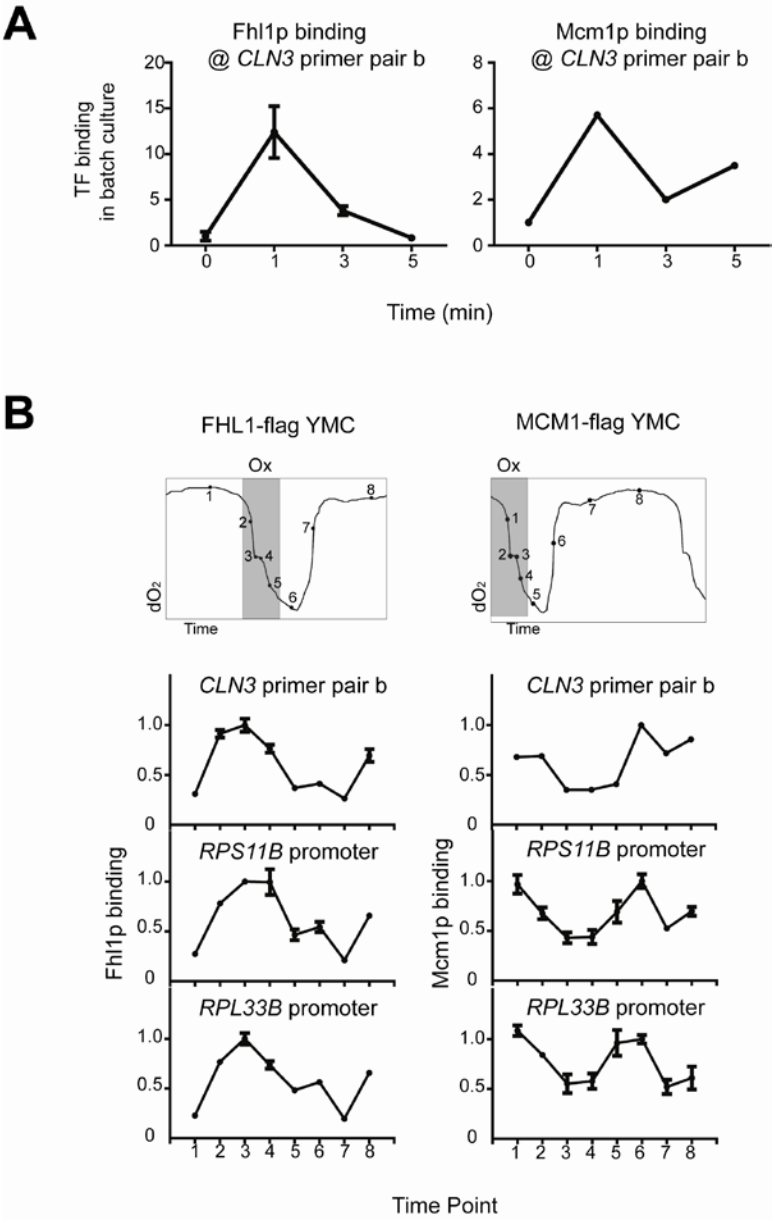

Figure III-13 Fhl1p and Mcm1p binding at *CLN3* and ribosomal gene promoters in the YMC. (A) Fhl1p and Mcm1p binding at *CLN3* promoter was assayed by ChIP in batch culture at indicated time points immediately following 2% glucose repletion. The binding was normalized to the input DNA. Mean ± SD, n = 3. (B) Fhl1p and Mcm1p binding at *CLN3*, *RPS11B* and *RPL33B* promoters was assayed by ChIP at 8 time points across one YMC. Their binding was normalized to the input DNA. Mean ± SD, n = 3

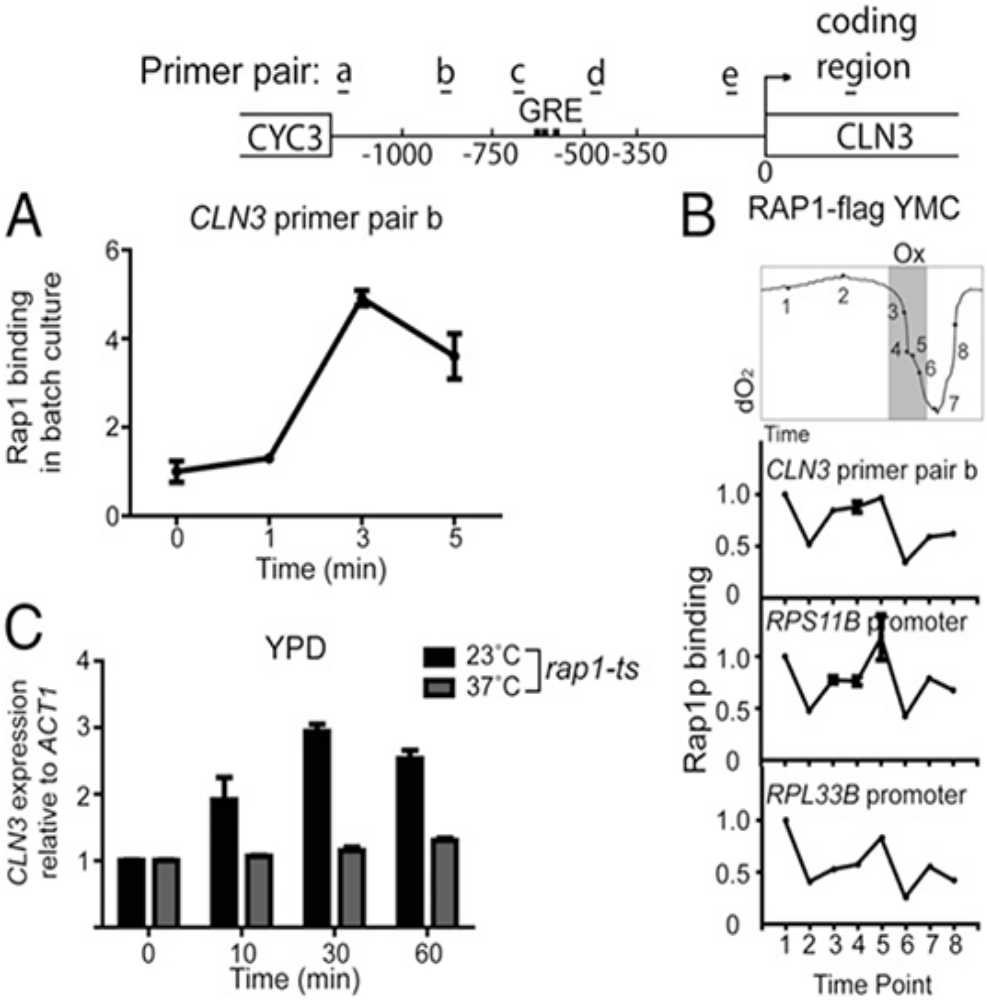

Figure III-14 Ribosomal protein gene transcription factor Rap1p regulates *CLN3* transcription. (A) Rap1p is recruited to the *CLN3* promoter upon repletion with glucose in batch culture. Rap1p binding at the *CLN3* promoter was assayed by ChIP at 0, 1, 3 and 5 min immediately after repletion of quiescent cells with 2% glucose. Binding was normalized to the input DNA. Binding was observed primarily in the region covered by primer pair b. Mean ± SD, n = 3. (B) Rap1p is recruited to the *CLN3* promoter, as well as ribosomal gene promoters, during the OX growth phase of the YMC. Rap1p binding at the indicated gene promoter regions was assayed by ChIP at 8 unequally spaced time points across one metabolic cycle. Mean ± SD, n = 3. (C) *CLN3* transcription requires Rap1p. *CLN3* transcription was measured in batch culture by real-time qPCR at 0, 10, 30 and 60 min following exposure of *rap1-ts* quiescent cells to fresh YPD medium at the permissive and non-permissive temperature. Mean ± SD, n = 3

essential transcription factors that have been reported to bind the *CLN3* regulatory region in genome-wide studies (Kasahara et al., 2007; Lavoie et al., 2010; Lee et al., 2002; Rhee and Pugh, 2011). Rap1p and Fhl1p in complex with other transcription factors are known to regulate ribosomal gene expression (Rudra et al., 2005; Schawalder et al., 2004; Tareen et al., 2004; Wade et al., 2004). In both the YMC and batch cultures, we observed the tight co-regulation of *CLN3* transcription with ribosomal subunit gene transcription (Figure III-3 and Figure III-8). We then observed that both Rap1p and Fhl1p bound the *CLN3* promoter region immediately following nutrient repletion (Figure III-14A and Figure III-13A). In the YMC, in contrast to Azf1p and Mcm1p, Rap1p and Fhl1p bound the *CLN3* regulatory region as well as *RPS11B* and *RPL33B* precisely in the OX growth phase, which is the time of active *CLN3* transcription (Figure III-14B and Figure III-13B). Furthermore, we tested a temperature-sensitive mutant *rap1-ts* for its ability to induce *CLN3* expression. *CLN3* transcription in this mutant was compromised only at the non-permissive temperature, further suggestive of an active role for Rap1p in *CLN3* transcription (Figure III-14C). Thus, our findings suggest that Rap1p, and possibly Fhl1p, may represent the transcription factors that together with SAGA, induce the transcription of *CLN3* and ribosomal genes in response to acetyl-CoA.

DISCUSSION

How cell growth and division are coordinated with metabolism and the metabolic state of a cell has remained a critical unresolved question in the cell cycle field. While many previous studies of the yeast cell cycle have focused on transcriptional events downstream of the G1 cyclin *CLN3,* it has remained unclear what drives the transcription of *CLN3* in the first place upon exit from quiescence to set subsequent events of the cell cycle in motion. *CLN3* has been proposed to be subjected to multiple forms of regulation, at the transcriptional, post-transcriptional, and post-translational levels. Moreover, although glucose is known to be a potent inducer of *CLN3* transcription (Parviz et al., 1998; Parviz and Heideman, 1998), how the glucose signal might be relayed to the transcriptional machinery to activate the *CLN3* gene has remained poorly understood.

In this study, we provide evidence that acetyl-CoA is most likely the key metabolite of glucose and carbon sources that drives the transcription of *CLN3,* thereby linking cellular metabolism to a critical regulator of cell cycle progression. As revealed by the high synchrony and temporal resolution offered by the YMC, *CLN3* is co-expressed along with ribosomal and other growth genes as cells exit the quiescent-like RC phase and transition into the OX growth phase (Figure III-3). We previously discovered that acetyl-CoA induces the acetylation of histones present at these growth genes to enable their activation (Cai et al., 2011). Acetyl-CoA production increases during growth and enables the Gcn5p acetyltransferase present within SAGA to catalyze histone acetylation precisely at these genes. Since *CLN3* is expressed at the same time as these other growth genes, it became predictable that *CLN3* might also be regulated by acetyl-CoA-driven histone acetylation. We now show that this is indeed the case using two

different but complementary culturing methods in the YMC and batch culture. Just like ribosomal and other growth genes, acetyl-CoA enables Gcn5p present within SAGA to catalyze the acetylation of histones present at the *CLN3* regulatory region. Recruitment of SAGA to the *CLN3* locus is dependent on the catalytic activity of Gcn5p, suggesting that the acetylation of particular subunits within SAGA (Spt7p, Ada3p, and Sgf73p), induced by acetyl-CoA, may be a key event that facilitates its recruitment to all of its growth gene targets. The role of SAGA and histone acetylation in mediating activation of *CLN3* is further supported by a previous report showing that *CLN3* mRNA levels are reduced in *ada2* and *ngg1* mutants within SAGA, and derepressed in *rpd3* histone deacetylase mutants (Wu et al., 1999). It remains possible that acetyl-CoA could also indirectly promote transcription of *CLN3* through additional mechanisms, for example via induction of glucose transporters that mediate glucose uptake, or via other downstream metabolites.

Since SAGA cannot bind DNA directly, it is most likely recruited to gene regulatory regions by transcription factors. Although Azf1p and Mcm1p are transcription factors that have been previously reported to regulate *CLN3* transcription, we did not observe their binding to the *CLN3* locus at the correct time of its activation in the YMC. By screening other transcription factors with potential binding sites in the *CLN3* regulatory region, we observed that the ribosomal transcription factors Rap1p and Fhl1p also bound the *CLN3* regulatory region at the correct time of its activation in the YMC as well as following glucose repletion. Moreover, a *rap1-ts* mutant at the non-permissive temperature exhibited compromised *CLN3* transcription (Figure III-14C). Thus, these transcription factors may coordinate with SAGA to activate *CLN3* in addition to ribosomal genes, in response to increased acetyl-CoA production. As the binding of Azf1p and Mcm1p to *CLN3* occurs subsequent to its activation in the YMC, these

transcription factors may function as repressors to help maintain the gene in a silent state. Future work will be required to elucidate the role of these transcription factors in the regulation of *CLN3* transcription.

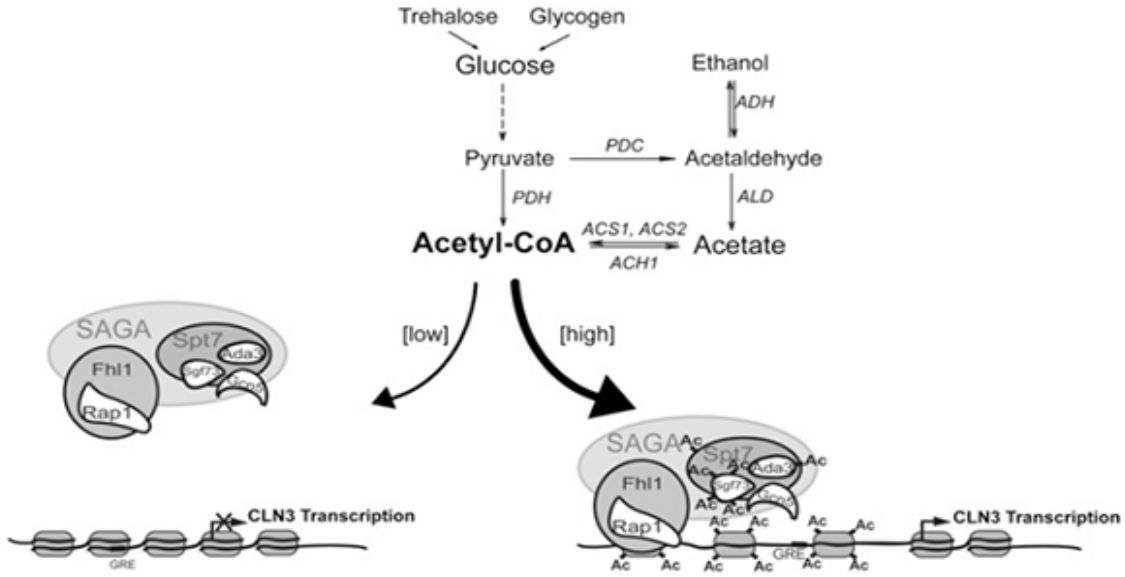

Figure III-15 Model linking glucose to *CLN3* transcription through the metabolite acetyl-CoA and the SAGA transcriptional coactivator complex. A key output of glucose catabolism is the production of acetyl-CoA. Increased acetyl-CoA synthesis enables Gcn5p-containing SAGA to catalyze the acetylation of histones at the *CLN3* locus for transcription of this key G1 cyclin. Glucose can also be derived from the storage carbohydrates trehalose and glycogen. Acetate is also a source of acetyl-CoA.

Budding yeast cells accumulate substantial amounts of the storage carbohydrates trehalose and glycogen upon entry into stationary phase or quiescence (Shi et al., 2010; Sillje et al., 1999). They then break down these carbohydrate stores to produce glucose, providing a "finishing kick to START" for re-entry into growth (Futcher, 2006; Sillje et al., 1999). In summary, our studies indicate that a key output of glucose metabolism critical for cell proliferation is an increase in acetyl-CoA production. Indeed, we observed that intracellular

acetyl-CoA levels increase substantially during the OX growth phase of the YMC as well as in exponential growth, compared to stationary phase (Cai et al., 2011). The burst of acetyl-CoA production, most easily fueled by glucose, then enables Gcn5p-containing SAGA to acetylate histones at a set of more than 1,000 growth genes, as well as *CLN3*, enabling activation of these genes and thereby setting the cellular growth program in motion (Figure III-15). Thus, acetyl-CoA may represent the metabolic basis of the elusive "finishing kick" and "growth rate threshold" that gates entry into the START of the cell division cycle by regulating access to these growth genes in the chromatin. As such, our results strongly suggest that the very molecule that is used to stitch together cellular building blocks such as fatty acids, sterols, and amino acids, is a critical metabolite that is monitored by yeast cells in the decision to proliferate.

MATERIALS AND METHODS

Yeast Strains and Media

The prototrophic CEN.PK strain background was used for all experiments (van Dijken et al., 2000). All knockout strains in this study were made by gene replacement using KanR/NatR/HygroR cassettes via homologous recombination (Longtine et al., 1998). The temperature-sensitive mutant *acs2-ts* was made by complementing the *acs2* null CEN.PK strain with a cloned p417 plasmid containing the *acs2-ts* construct (Takahashi et al., 2006) (a gift from Jef Boeke, The Johns Hopkins University School of Medicine, Baltimore). The temperature-sensitive mutant *esa1-ts* was made by replacing the genomic *ESA1* in CEN.PK strain with the *esa1-531-ts* construct (Lin et al., 2009) (a gift from Jef Boeke). The temperature sensitive mutant *rap1-ts* was made by mutation of proline 694 to leucine according to a previous *rap1-ts* screen (Kurtz and Shore, 1991). For ChIP, the gene of interest was C-terminally tagged at its endogenous chromosomal locus with a 3× FLAG epitope via homologous recombination. Strains used in this study are listed below.

Table III-1 Strains used in this study

Strain name	**Genotype**
WT	CEN.PK, MATa
acs1Δ, acs2-ts	MATa, acs1Δ::phleoR, acs2Δ::NatR, p417-acs2-ts-KanR
azf1Δ	MATa, azf1Δ::KanR
cln3Δ	MATa, cln3Δ::NatR
esa1-ts	MATa, esa1-531-KanR
gcn5Δ	MATa, gcn5Δ::KanR
gcn5 A190T	MATa, gcn5 A190T-KanR
gcn5 E173Q	MATa, gcn5 E173Q-NatR
hpa2Δ	MATa, hpa2Δ::NatR

icl1Δ	MATa, icl1Δ::NatR
rap1-ts	MATa, rap1 P694L-flag-NatR
sas2Δ	MATa, sas2Δ::KanR
sas3Δ	MATa, sas3Δ::NatR
sgf73Δ	MATa, sgf73Δ::NatR
snf2Δ	MATa, snf2Δ::KanR
AZF1-flag	MATa, AZF1-flag-KanR
FHL1-flag	MATa, FHL1-flag-NatR
MCM1-flag	MATa, MCM1-flag-NatR
RAP1-flag	MATa, RAP1-flag-NatR
SNF2-flag	MATa, SNF2-flag-NatR
SPT7-flag	MATa, SPT7-flag-KanR
SPT7-flag, gcn5Δ	MATa, SPT7-flag-KanR, gcn5Δ::NatR
SPT7-flag, gcn5 E173Q	MATa, SPT7-flag-KanR, gcn5 E173Q-NatR
SPT7-flag, sgf73Δ	MATa, SPT7-flag-KanR, sgf73Δ::NatR

Yeast Metabolic Cycles

Continuous culture conditions used to observe yeast metabolic cycles were described previously (Tu et al., 2005). Briefly, each fermentor run was started by the addition of a 1- to 5-mL starter culture that had been grown overnight to saturation at 30 °C. The fermentors were operated at an agitation rate of ~500 rpm, an aeration rate of 1 L/min, a temperature of 30 °C, and a pH of 3.4, with a working volume of 0.5 or 1 L. Once the batch culture reached maximal density, the culture was starved for 8–10 h. Continuous culture was then initiated by the constant infusion of media containing 1% glucose at a dilution rate of ~0.09–0.1 h^{-1}. The growth media is a minimal media consisting of 5 g/L $(NH4)_2SO_4$, 2 g/L KH_2PO_4, 0.5 g/L $MgSO_4 \cdot 7H_2O$, 0.1 g/L $CaCl_2 \cdot 2H_2O$, 0.02 g/L $FeSO_4 \cdot 7H_2O$, 0.01 g/L $ZnSO_4 \cdot 7H_2O$, 0.005 g/L $CuSO_4 \cdot 5H_2O$, 0.001 g/L $MnCl_2 \cdot 4H_2O$, 1 g/L yeast extract, 10 g/L glucose, 0.5 mL/L 70% (vol/vol) H_2SO_4, and 0.5 mL/L Antifoam 204 (Sigma).

Batch Culture Growth

Strains were grown in Yeast Extract Peptone Dextrose (YPD) or Synthetic Defined media at 30 °C to stationary phase for 2 or 3 d. Cells were collected, washed with PBS once, and added to either a pre-warmed YPD, 2% glucose solution, or sodium acetate solution (pH 5.2) as indicated in the figure legend to a final OD600 = 0.5 and grown at 30 °C. Cell samples were collected at indicated time points for specific assays. The temperature-sensitive mutants *acs1Δ, acs2-ts,* and *esa1-ts* were grown in YPD at the permissive temperature 28 °C for 2 or 3 d. The *rap1-ts* temperature-sensitive mutant was grown in YPD at the permissive temperature 23 °C for 4 d owing to its significantly slower growth rate than WT.

mRNA Expression Analysis

Samples for mRNA extraction (5 OD cells) were collected, washed with diethylpyrocarbonate (DEPC)-treated water and stored at −80 °C. Frozen cell pellets were resuspended in 1 mL RNA STAT-60 (CS-110; Tel-Test, Inc.).Whole cell lysis was achieved by minibead beating. Total mRNA from each cell sample were extracted with 0.2 mL of chloroform and then precipitated by mixing the aqueous phase from chloroform extraction with 0.5 mL of isopropanol. mRNA was then washed with ethanol, dissolved in DEPC water, treated with DNase I (M0303; NEB), and reverse-transcribed to cDNA (18064-014; Invitrogen). Total cDNA was analyzed for levels of *CLN3*, *RPL33B,* or *ACT1* as indicated by real-time quantitative PCR with corresponding primer pairs listed below. *CLN3* expression was typically normalized against *ACT1*. The optimal transcript for normalization was not obvious because mRNA for *ACT1* as well as 16 other candidate normalization genes increased gradually upon nutrient repletion. Regardless, through many trials we verified that *CLN3* is transcriptionally induced to a

significant extent upon nutrient repletion, and this correlates well with its significant induction in the OX growth phase of the YMC (Rowicka et al., 2007).

Chromatin Immunoprecipitation

ChIP was performed as previously described (Cai et al., 2011) with minor modifications. Cell samples were collected and fixed with fresh 0.7% formaldehyde. After decrosslinking, the immunoprecipitated DNA fragments were purified by either 0.4 mL phenol–chloroform followed by precipitating DNA fragments with 44 μL of 3 M sodium acetate (pH 5.2) and 1 μL of 20 mg/mL glycogen, or QIAquick PCR Purification Kit (Qiagen). The purified DNA was dissolved in TE [1 mM Tris (pH 8.0) and 0.1 mM EDTA] and analyzed by real-time quantitative PCR with corresponding primer pairs (shown in the Table III-2).

Table III-2 Real-time qPCR primer pair sequences

Primer Pair	**Forward Sequence**	**Reverse Sequence**
CLN3 ORF	TCAGCGCTGCCTCATGTC	ATGGCCCGCCTCTTTTG
ACT1 ORF	TCGTTCCAATTTACGCTGGTT	CGGCCAAATCGATTCTCAA
RPL33B ORF	GCCGTGGAATAGGCTGATTC	GGCCCCAACTATAACACATGTTTT
CLN3 a	CAGCCAGCGTAAGTACGTGTAAA	ATTGATTGTGGCTGCACTAGGA
CLN3 b	TCGGCGGGTTTTCTTGAC	GGCCAAGCGTTCAAACGA
CLN3 c	CCCTCCCCAGCCAAAGAG	GCGTTTGGTTGCGACACTT
CLN3 d	GGGTTTTTGCCCTCATCTTTT	GCTCGAGGAAAGTACAGATATACAAATTAT
CLN3 e	CCGAGTCCCAGTCGCAAT	ACCGAATGAGGAAATGCAATG
RPS11B promoter	GTTCCACGCCAACCTTTCA	GCAGCAGAGAAGGGAAACGT
RPL33B promoter	GCCTGGAGACCGCTTCTCTT	GCAGTGACGCTCTGTTGCA

IV. DISCUSSION AND FUTURE DIRECTIONS

In my graduate work, I have attempted to understand the regulation of quiescence in the budding yeast Saccharomyces *cerevisiae* from the aspect of cellular metabolism. Quiescence is the state where cells encounter stress and arrest their growth until conditions improve. Quiescence was not considered important because of its seemingly inactive or dying status. However, it is the most common state for organisms on earth. Around 60% of microbes on earth remain in quiescence. For multicellular eukaryotes, most of their cells stay in a quiescent-like state after differentiation. The budding yeast is a simple eukaryote but has highly conserved basic biological processes found in multicellular organisms, including mammals. Thus, the study of yeast quiescence has the potential to offer fundamental insights into understanding how post-mitotic differentiated cells or even quiescent stem cells are maintained.

TREHALOSE IS A KEY DETERMINANT OF QUIESCENCE

Yeast quiescence is usually acquired by growing cells in rich media to starvation. After all carbon sources are exhausted, yeast cells will enter quiescence without dividing further. During the establishment of quiescence, two populations of yeast cells could be separated by density fractionation (Allen et al., 2006). The low density cell population contained mixed cell types – unbudded and budded. They were less resistant to stresses and did not readily restart growth upon repletion of nutrients, so they were termed non-quiescent (nonQ) cells. In contrast, the high density cell population contained uniformly unbudded cells that were more resistant to stresses and were more viable. Thus, the dense cell population was considered as the real

quiescent (Q) cells. The discovery of the two cell populations from stationary phase culture may constitute a milestone in understanding yeast quiescence. It reveals the stationary phase culture previously used in quiescence studies is a mixture of different cell types. Furthermore, with the ability to purify quiescent cells, subsequent studies would be less obscured and more straightforward. To study yeast quiescence, I first wondered what could cause the increased density of yeast cells during quiescence entry. Did the density change promote quiescence or was it simply a consequence of quiescence? The increased density of Q cells may be a key to further understand how quiescence was regulated.

Glycogen and trehalose have been known to accumulate in quiescent cells (Francois and Parrou, 2001). Strikingly, Q cells contained large amount of glycogen granules, revealed by electron microscopy (Allen et al., 2006). Similarly during the YMC, cells in the quiescent-like RC phase contained higher content of glycogen and trehalose (Tu et al., 2005; Tu et al., 2007). Thus, the separation of two populations by cellular density may as well be considered as the separation of cells containing low and high content of glycogen and trehalose. Indeed, my data showed that during the quiescence establishment in either batch culture or YMC, glycogen and trehalose gradually accumulated and correlated with the cell density increase. This observation strongly supports the hypothesis that carbon reserves constitute the density change of Q cells. Furthermore, this idea is further supported by the abolished density change of mutant cells lacking glycogen and trehalose synthesis.

Then, why do yeast cells accumulate glycogen and trehalose? Are they important in quiescence regulation? Interestingly, trehalose-ablated cells significantly delayed the regrowth in fresh nutrients. Moreover, they yielded much less Q cells than WT by density fractionation.

These observations indicate trehalose is indispensible in quiescence regulation. Trehalose has been well-known to function as an intracellular stress protectant. Although trehalose can chaperone proteins and lipids to preserve their integrity, it may also serve as an energy source. Trehalose, as a chemically stable disaccharide, might endure the harsh conditions experienced during quiescence and provide a critical supply of energy when cells re-enter growth upon nutrient repletion. I now show that trehalose was preferentially retained over glycogen and degraded immediately upon nutrient repletion, concomitant with the activation of the trehalase. Altogether, my data suggest that glycogen and trehalose constitute the density change of Q cells and trehalose is a key determinant of quiescence in its establishment, maintenance and exit.

After establishing trehalose as a key determinant of quiescence, further questions remain regarding the specific mechanisms of trehalose in promoting quiescence as well as other mechanisms of quiescence regulation. Here I would like to summarize new evidence in the field that links trehalose to metabolism, mitochondria and protein-RNA granule formation.

Trehalose may influence metabolism in regulation of quiescence

In my experiments, a trehalose-ablated mutant – *tps1Δ* strain had significant problem in adapting and re-initiating growth in fresh media. Although lack of the immediate product of Tps1p – trehalose 6-phosphate has been proposed to impact the regulation of glucose uptake and metabolism (Thevelein and Hohmann, 1995), yeast cells fed on galactose still showed growth defect. With the following evidence, I propose that trehalose accumulation correlates with and may contribute to the tightly regulated metabolism in Q cells.

The yeast vacuole is critical for various cellular processes, including nutrient and metabolite storage, cellular growth control (e.g. TORC1 regulation), and autophagic degradation of various cellular constituents. Interestingly, Q cells contained a single electron-dense vacuole in comparison to nonQ cells (Allen et al., 2006). Without dye staining, electron-dense vacuole usually infers significant accumulation of mass. It is predictable that Q cells accumulate resources to resist stress conditions. Therefore, what is accumulated in the vacuole could be of significant interest. Candidate metabolite includes amino acids that accumulated during the quiescent-like RC phase of the YMC (Tu et al., 2007). Upon quiescence exit, metabolites stored in the vacuole may quickly signal to TORC1 for initiation of the growth program. Alternatively, the storage of metabolites in the vacuole may prevent deleterious effects of such metabolites to cellular organelles. During yeast replicative aging, mitochondrial membrane potential decreased, which led to defective mitochondrial functions (Veatch et al., 2009). Strikingly, the defective mitochondrial membrane potential was rescued by enhanced maintenance of vacuolar acidity that promotes vacuolar storage of metabolites (Hughes and Gottschling, 2012). Consistently, enhanced vacuolar storage of neutral amino acids partially restored the mitochondrial membrane potential and extended replicative lifespan. Thus, vacuolar storage is important to keep certain metabolites from affecting other cellular organelles. Beside the critical role in replicative aging, mitochondria has also been found essential for quiescent cells (Allen et al., 2006; Friis et al., 2014; Lai et al., 2002; Ocampo et al., 2012). Vacuolar storage is likely to be noteworthy in maintaining mitochondrial functions during quiescence. How vacuolar storage of metabolites regulates quiescence and whether trehalose has any role in facilitating the vacuolar storage could be potentially revealing.

What is a quiescent cell doing metabolically? Is it really in quiescence? “Quiescence” usually refers to such cells because in nutrient-limited or stress conditions, they don’t divide and produce progeny. However, in higher eukaryotes, quiescent differentiated cells did not divide but maintained high metabolic activity similar to proliferating cells (Lemons et al., 2010). In yeast, a similar phenomenon was observed (Davidson et al., 2011). In SP culture, although yeast cells stopped dividing in the absence of glucose, they accumulated various provisions to prepare for quiescence. Remarkably, purified yeast Q cells exhibited high respiratory activity, perhaps by metabolizing the carbon reserves. Furthermore, work from two decades ago showed yeast cells in stationary phase produced similar groups of proteins with those produced in growth phase, albeit at 0.2 % rate (Fuge et al., 1994). With a similar set of proteins available, quiescent cells may maintain some metabolic activity and readily restart cell division upon nutrient repletion. Accordingly, it is of significant interest to ask questions as: what metabolic activity is crucial in maintaining quiescent cells? Can the cellular viability be altered? Why do quiescent cells need to maintain particular metabolic activities? Will quiescent cells eventually die because they run out of their intracellular nutrient reserves? Existing evidence reveals the importance of several metabolic pathways in Q cells, such as fatty acid oxidation, carbohydrate metabolism and coenzyme metabolism (Allen et al., 2006). However, the underlying logic of the quiescent metabolic network is still mostly unresolved. Perhaps metabolite profiling during the log phase to stationary phase transition, and metabolic flux analysis during quiescence can help answer some of the above questions.

Trehalose holds intimate relationship with mitochondria

Mitochondria have been known for providing efficient energy to meet the needs for cell growth and proliferation. Mitochondria are also pleiotropic in their contribution to human health (Barrientos, 2003; Steinmetz et al., 2002). Although still under debate, mitochondria were noted to play an important role in opposing yeast replicative aging by synthesizing iron-sulfur clusters to antagonize genomic instability (Veatch et al., 2009). Accumulating evidence has recently started to reveal a critical role for mitochondria in quiescence regulation.

During the post-diauxic shift, yeast cells exhaust glucose and start to use non-fermentable carbon sources. They usually divide once before entry into quiescence. Interestingly, the last round of cell division was found to be highly asymmetric and critically important in establishing the Q cell population (Li et al., 2013). Yeast cellular replicative age can be counted by the number of bud scars that accumulate after each cell division. Based on the number of bud scars on each cell, nearly the entire Q cell population was comprised of virgin daughter cells, while cells of all ages could be found in the nonQ cell population (Allen et al., 2006). Importantly, mitochondria are also distributed between two cell populations in a highly asymmetric manner. Multiple mitochondria localized proteins were observed more in Q cells than in nonQ cells, including enzymes in TCA cycle and components of the electron transport chain (Davidson et al., 2011). Strikingly, mtDNA content may be better maintained in Q cells based on the observation that the mtDNA packaging protein Abf2p localized more to Q cells than nonQ cells (Li et al., 2013). Consistent with the enriched mitochondrial proteins in Q cells, high respiratory activity was found in Q cells, while nonQ cells displayed minimal respiration (Davidson et al., 2011). In the absence of functional mitochondria, yeast cells form significantly smaller colonies called petites on glucose containing plates. When nonQ cells were regrown on glucose containing plates, 40% of the cells formed petites compared to 6% from Q cells (Aragon et al.,

2008). The differentiation and isolation of two cell populations may as well be the separation of cell populations containing functional and dysfunctional mitochondria. Collectively, these data suggest highly functional mitochondria are asymmetrically distributed into the daughter cells that constitute almost the entire Q cell population.

While Q cells contain highly functional mitochondria, most nonQ cells accumulated dysfunctional mitochondria during entry into quiescence. Although budding yeast cells have recently been reported to asymmetrically maintain functional mitochondria in daughter cells (Higuchi et al., 2013; Hughes and Gottschling, 2012), the asymmetric distribution of mitochondria in quiescence may represent an extreme case in which respiration in mother (nonQ) cells is severely compromised. It is intriguing how this extremely asymmetric distribution of mitochondria may be accomplished during the last round of cell division before quiescence entry. Is it due to vacuolar acidity (Hughes and Gottschling, 2012) or retrograde actin cable flow (Higuchi et al., 2013)? Is it *de novo* mitochondria biogenesis? The investigations on the asymmetric distribution of mitochondria during quiescence establishment may lead to the understanding of quiescence regulation.

The asymmetric distribution of mitochondria can be a fundamental factor in determining the longevity of Q cells. A missense mutation in *ATP2* - component of ATP synthase complex, caused loss of asymmetric segregation of mitochondria during mitotic divisions and led to rapid clonal senescence of daughter cells (Lai et al., 2002). Furthermore, multiple mitochondria protein deletion mutants were not able to form the Q cell population, including *atp1*, *qcr7*, *rip1*, *sdh4*, *kgd1* and *cor1* (Allen et al., 2006). Thus, asymmetric distribution of mitochondria may promote quiescence in daughter cells during the last round of cell division.

I have shown that glycogen and trehalose accumulation increased cell density in quiescence. Recently, Breeden and colleagues confirmed this finding by showing distinct accumulation of glycogen and trehalose between Q and nonQ cells (Li et al., 2013). Interestingly, the asymmetric distribution of glycogen and trehalose seems to correlate with the asymmetric distribution of mitochondria. Thus, trehalose and glycogen accumulation may play reciprocal roles with mitochondria maintenance. Dysfunctional mitochondria mutants have been found to impact intracellular trehalose and glycogen accumulation. mtDNA ablated mutant, also called rho0 mutant, accumulated minimal amounts of trehalose and glycogen in entering quiescence (Enjalbert et al., 2000; Friis et al., 2014; Ocampo et al., 2012). Notably, the same mitochondria mutant had much shorter lifespan in quiescence (Ocampo et al., 2012). Trehalose supplementation to this mutant extended significantly the lifespan beyond that of the isogenic WT. This suggests trehalose and glycogen accumulation are tightly regulated by mitochondrial function, both of which contribute to the longevity of cells in quiescence. However, the mechanism of how mitochondria regulate carbon reserves remains completely unknown. Here, I propose that retrograde pathway may be activated by the dysfunctional mitochondria in nonQ cells and may contribute to the depletion of trehalose and glycogen storage during establishment of quiescence.

Retrograde signaling pathway is activated by dysfunctional mitochondria (Butow and Avadhani, 2004; Jazwinski, 2013). Beside ATP production, TCA cycle in mitochondria also provide intermediate metabolites for the synthesis of glutamine and aspartate. Glutamine is the favorite nitrogen source for eukaryotes. It not only is one of the amino acids for protein synthesis but also fuels the nucleotides pool for DNA replication. In the absence of extracellular glutamine, mitochondria are the only source of glutamine by *de novo* synthesis. Thus, mutants

with dysfunctional mitochondria must activate retrograde signaling pathway to complement the production of glutamine from carbon sources. In establishing quiescence, nonQ cells may activate retrograde signaling due to the presence of dysfunctional mitochondria. Activated retrograde pathway increases the expression of enzymes for glutamine synthesis that consume trehalose and glycogen storage and lead to the formation of low-density nonQ cell population.

Conversely, trehalose may regulate mitochondrial function. Trehalose synthesis mutants compared to WT displayed decreased respiration in the presence of glucose (Noubhani et al., 2009). Furthermore, trehalose may chaperone mitochondria to prevent loss of their integrity and function. Trehalose has been shown to chaperone proteins and membrane lipids to prevent aggregation in dehydration condition (Crowe et al., 1992). Trehalose is also implicated in maintaining cell viability in cold temperature (Kandror et al., 2004). Recently, trehalose has been used widely as an *in vitro* conservant for biological materials in desiccation and cryo-protection, including preserving *in vitro* membrane integrity and function of extracted mammalian mitochondria (Liu et al., 2005; Yamaguchi et al., 2007). Thus, it may be plausible to hypothesize that trehalose can also preserve mitochondrial function *in vivo* under stress conditions.

Altogether, mitochondria may play critical roles in cellular quiescence. The asymmetric distribution of functional mitochondria in daughter cells during the last round of mitosis during quiescence entry may facilitate the differentiation of the two cell populations. While functional mitochondria in Q cells may promote the accumulation of trehalose and glycogen, dysfunctional mitochondria in nonQ cells may drive the depletion of trehalose and glycogen storage by activating retrograde signaling pathway. It is tempting to test in the future whether this

hypothesis holds up. Furthermore, whether the high respiration observed in Q cells helps maintain quiescence and how it maintains quiescence remain to be examined in the future.

Trehalose correlates with protein-RNA granule formation

When glucose levels drop to 0.6%, there is a rapid drop in global translation initiation (Castelli et al., 2011). Accompanying events include the formation of mRNA-protein granules, such as P-bodies and stress granules (Decker and Parker, 2012). These mRNP complexes sequester or degrade mRNAs. The accumulated mRNAs in the granules can reportedly return to translation (Brengues et al., 2005) due to the interaction with translation initiation factors (Brengues and Parker, 2007; Hoyle et al., 2007). In addition, Igo1 and Igo2, downstream of the stress kinase Rim15, inhibit degradation of mRNAs critical for the transition to quiescence (Talarek et al., 2010).

Previously, a large group of mRNAs was detected in a manner dependent on protease treatment in stationary phase cells (Aragon et al., 2006), suggesting these mRNAs were sequestered in mRNP granules. The same authors then examined categories of mRNAs released by protease treatment in differentiated Q cells and nonQ cells (Aragon et al., 2008). Strikingly, Q cells contained thousands of mRNAs residing in protein-RNA granules while nonQ cells had minimal sequestered mRNAs. Interestingly, half of the protease-released mRNAs in Q cells corresponded to those freely available in nonQ cells, such as gene products in Ty element transposition and DNA recombination. It suggests that Q cells sequester growth-related mRNAs into mRNP complexes to repress their translation during entry into quiescence.

Multiple RNA binding proteins have been found to impact quiescent cell survival at various degrees. Ssd1p is a RNA binding protein that is induced in stress conditions, such as oxidative stress, heat shock and nutrient starvation. It is polymorphic among laboratory and wild yeast strains and partially determines their diversified longevity in stress conditions. The WT allele *SSD1-V* supported longer lifespan in both replicative aging and chronological aging (Kaeberlein et al., 2004; Li et al., 2009). WT *SSD1-V* strain yielded more Q cells than *ssd1-d* mutant (Li et al., 2009). Ssd1p has been found to increase longevity gene transcripts involved in cell wall biogenesis and salt response. It also promoted accumulation of iron homeostasis gene transcripts that may facilitate the maintenance of mitochondrial function. Conversely, Ssd1p repressed ribosome biogenesis mRNAs so that cells could keep the growth arrested in quiescence. Mpt5, a RNA binding protein, plays overlapping roles with Ssd1 in promoting quiescence. It is also polymorphic among yeast strains like Ssd1. Notably, the double deletion mutant of ssd1 and mpt5 abolished trehalose and glycogen storage and did not form any Q cell population (Li et al., 2013). Lsm1, the decapping enzyme for mRNA degradation in P-bodies (Coller and Parker, 2005; Holmes et al., 2004), is also critical for the longevity of Q cells. Strikingly, purified Q cells of *lsm1* deletion mutant had a half life of 4 weeks compared to 11 weeks for WT Q cells (Li et al., 2013). The *lsm1* mutant was further exacerbated by *mpt5* and *ssd1* deletion in carbohydrate accumulation, cell wall modification and Q cell yield. Thus, there may be a correlation between carbon reserve and mRNP granules during quiescence. It will be tempting to examine the relationship between the accumulation of trehalose and glycogen and mRNP granules for quiescence regulation.

ACETYL-COA INDUCES *CLN3* TRANSCRIPTION TO EXIT QUIESCENCE AND INITIATE CELL CYCLE PROGRESSION

Quiescence is the resting state that is commonly observed in organisms on earth. Around 60% of microbes on earth remain in a quiescent state that usually appears unculturable in current laboratory conditions (Lewis, 2007). In multicellular eukaryotes, most cells spend the majority of their life in a quiescent-like state after differentiation. Beyond contributing to a more rounded view of a cell's life cycle, understanding quiescence can potentially aid in the development of novel interventions against diverse processes including aging, infection and cancer. Most of the world's microorganisms have yet to be cultured. Among these organisms are likely to be many novel microbes that stay in quiescence and may produce medically useful natural products. An understanding of how to stimulate these microorganisms to exit quiescence may aid in the culturing of them and lead to profound discoveries.

I showed in my first project that trehalose was a key determinant of quiescence and might fuel the initial cell cycle progression upon quiescence exit. To investigate the mechanism of quiescence exit, I started my second project by asking how trehalose might contribute to the exit of quiescence. Trehalose is a disaccharide comprised of two glucose moieties. The immediate activation of trehalase and degradation of trehalose upon nutrient repletion to quiescent yeast cells suggest a surge of intracellular glucose may occur and trigger the activation of cellular growth program. Indeed, glucose is the favored carbon source for all organisms that have evolutionarily developed multiple glucose sensing and signaling pathways to allow rapid and optimal utilization of glucose in re-growth and proliferation (Santangelo, 2006). Consistently, when yeast cells in the YMC transition from the RC phase to the OX phase, trehalose and

glycogen storage decreased with a concomitant glucose peak during the midst of the OX phase (Tu et al., 2007). In search of additional metabolites that also accumulated during the OX phase, acetyl-CoA turned out to be a strong candidate. Acetyl-CoA is the downstream metabolite of glycolysis from glucose and fuels many intermediate metabolism for cell growth and proliferation, such as TCA cycle, amino acid synthesis, fatty acid synthesis and protein acetylation. Interestingly, the acetyl-CoA peak correlated well with the induction of *CLN3* transcription – the first activated G1 cyclin to initiate cell cycle (Tu et al., 2005; Tu et al., 2007). Thus, *CLN3* transcription could be a key cellular response to nutrients for quiescence exit.

Acetyl-CoA had recently been found in our lab to trigger yeast growth entry (Cai et al., 2011). My colleague Ling showed that acetyl-CoA served as the substrate for extensive histone acetylation that induced a total of ~1000 growth gene transcription (e.g. ribosome biogenesis) from a quiescent-like state. *CLN3* mRNA peak correlated with the numerous ribosome mRNA peaks during the OX phase of YMC (Tu et al., 2005). It has been shown that *CLN3* transcription depended on glucose. However, the transcription did not require canonical glucose signaling pathways, including PKA, TOR and Snf3/Rgt2 glucose transporters (Newcomb et al., 2003; Parviz and Heideman, 1998). Instead, glycolysis was found to be essential for the induction of *CLN3* transcription by glucose (Newcomb et al., 2003). Thus, I hypothesized that *CLN3* transcription was induced by the glycolysis product – acetyl-CoA, which could trigger the acetylation of histones at *CLN3* promoter.

In my experiments, I was able to induce *CLN3* transcription with acetate in quiescent cells as potently as glucose or rich media. Acetate produces acetyl-CoA through acetyl-CoA synthetases. Consistent with my hypothesis, a temperature-sensitive mutant of acetyl-CoA

synthetases did not respond to acetate at non-permissive temperature. Upon repletion of acetate, histone H3 acetylation increased which was dependent on the activity of the SAGA complex, the histone H3 acetyltransferase complex. Previously, Azf1p, an asparagine-rich zinc finger transcription factor, was implicated in mediating glucose induced *CLN3* transcription (Newcomb et al., 2002). For acetate-induced *CLN3* transcription, I found Azf1p was also crucial, supporting the idea that acetyl-CoA was the metabolite from glucose catabolism that induced *CLN3* transcription. Furthermore, the SAGA complex bound to the *CLN3* promoter immediately upon glucose repletion. Histone H3 acetylation sites known to support active transcription were subsequently acetylated, suggestive of the role of acetyl-CoA in transcription induction by acetylating histones. These data may suggest common cellular strategies in coping with altering environmental perturbations. Beside potent gene-specific activation by transcription factors, altering histone acetylation as a function of nutrient availability may facilitate the temporal coordination of large numbers of genes with similar functions for rapid cellular adaptation and growth initiation.

The rapid growth and division of yeast cells can be likened to those of mammalian cancer cells. Terminally differentiated mammalian cells usually enter a quiescent-like state and are not able to divide. However, these non-dividing cells can transform into an uncontrolled dividing state that is usually associated with genomic lesions, such as aneuploidy (Pfau and Amon, 2012). These cells modify their metabolic strategies to support invasive growth in nutrient-challenging conditions that are usually found *in vivo*. Thus, it may be intriguing to understand the metabolic strategies of cancer cells to exit the quiescent-like state. Evidence has hinted at acetyl-CoA as the key metabolite cancer cells rely on. Under nutrient-rich conditions, actively dividing mammalian cells undergo glycolysis to produce pyruvate that is transported into mitochondria and converted

to acetyl-CoA. Then, citrate derived from acetyl-CoA is transported back into cytosol and releases acetyl-CoA there for the purposes of histone acetylation and fatty acid synthesis (Wellen et al., 2009). However, under nutrient-poor conditions, normal mammalian cells might survive on the energy from fatty acid oxidation and mitochondrial respiration. Acetyl-CoA in these cells is not sufficient in cytosol to support histone acetylation and fatty acid synthesis that are crucial for growth and proliferation. Then how do mammalian cancer cells obtain their nucleo-cytosolic pools of acetyl-CoA to grow under the nutrient-challenging conditions? Interestingly, numerous clinical PET-imaging studies have indicated that a wide spectrum of human tumors avidly uptake [11C]-acetate (Grassi et al., 2012). These observations not only support the essential role of acetyl-CoA in cancer cell growth, but also indicate that acetate may serve as an alternative source of acetyl-CoA during the nutrient-challenging conditions. Thus, it will be of significant interest to investigate how acetyl-CoA might regulate the cancer cell metabolism and lead to cell growth and proliferation.

Yeast is the simplest unicellular eukaryote but does share many basic cellular mechanisms among eukaryotes. Often, yeast studies can offer fundamental insights to aid in understanding complex mammalian cellular processes. I and other colleagues in the lab have found that acetyl-CoA is a key metabolite that triggered the exit of quiescence and the initiation of cell cycle progression upon nutrient repletion. Although extension of this idea onto mammalian systems is of interest, continued mechanistic studies in yeast may nevertheless hold the key to rapidly uncover additional insights on the role of acetyl-CoA in the regulation of quiescence exit and other cellular processes.

V. BIBLIOGRAPHY

Allen, C., Buttner, S., Aragon, A.D., Thomas, J.A., Meirelles, O., Jaetao, J.E., Benn, D., Ruby, S.W., Veenhuis, M., Madeo, F., *et al.* (2006). Isolation of quiescent and nonquiescent cells from yeast stationary-phase cultures. The Journal of cell biology *174*, 89-100.

Aragon, A.D., Quinones, G.A., Thomas, E.V., Roy, S., and Werner-Washburne, M. (2006). Release of extraction-resistant mRNA in stationary phase Saccharomyces cerevisiae produces a massive increase in transcript abundance in response to stress. Genome biology *7*, R9.

Aragon, A.D., Rodriguez, A.L., Meirelles, O., Roy, S., Davidson, G.S., Tapia, P.H., Allen, C., Joe, R., Benn, D., and Werner-Washburne, M. (2008). Characterization of differentiated quiescent and nonquiescent cells in yeast stationary-phase cultures. Molecular biology of the cell *19*, 1271-1280.

Barbet, N.C., Schneider, U., Helliwell, S.B., Stansfield, I., Tuite, M.F., and Hall, M.N. (1996). TOR controls translation initiation and early G1 progression in yeast. Mol Biol Cell *7*, 25-42.

Barrientos, A. (2003). Yeast models of human mitochondrial diseases. IUBMB life *55*, 83-95.

Becker, A., Schloder, P., Steele, J.E., and Wegener, G. (1996). The regulation of trehalose metabolism in insects. Experientia *52*, 433-439.

Benaroudj, N., Lee, D.H., and Goldberg, A.L. (2001). Trehalose accumulation during cellular stress protects cells and cellular proteins from damage by oxygen radicals. The Journal of biological chemistry *276*, 24261-24267.

Boer, V.M., Crutchfield, C.A., Bradley, P.H., Botstein, D., and Rabinowitz, J.D. (2010). Growth-limiting intracellular metabolites in yeast growing under diverse nutrient limitations. Molecular biology of the cell *21*, 198-211.

Brauer, M.J., Huttenhower, C., Airoldi, E.M., Rosenstein, R., Matese, J.C., Gresham, D., Boer, V.M., Troyanskaya, O.G., and Botstein, D. (2008). Coordination of growth rate, cell cycle, stress response, and metabolic activity in yeast. Molecular biology of the cell *19*, 352-367.

Brengues, M., and Parker, R. (2007). Accumulation of polyadenylated mRNA, Pab1p, eIF4E, and eIF4G with P-bodies in Saccharomyces cerevisiae. Molecular biology of the cell *18*, 2592-2602.

Brengues, M., Teixeira, D., and Parker, R. (2005). Movement of eukaryotic mRNAs between polysomes and cytoplasmic processing bodies. Science *310*, 486-489.

Butow, R.A., and Avadhani, N.G. (2004). Mitochondrial signaling: the retrograde response. Molecular cell *14*, 1-15.

Cai, L., McCormick, M.A., Kennedy, B.K., and Tu, B.P. (2013). Integration of multiple nutrient cues and regulation of lifespan by ribosomal transcription factor Ifh1. Cell Rep *4*, 1063-1071.

Cai, L., Sutter, B.M., Li, B., and Tu, B.P. (2011). Acetyl-CoA induces cell growth and proliferation by promoting the acetylation of histones at growth genes. Mol Cell *42*, 426-437.

Cai, L., and Tu, B.P. (2011). On Acetyl-CoA as a Gauge of Cellular Metabolic State. Cold Spring Harb Symp Quant Biol *76*, 195-202.

Castelli, L.M., Lui, J., Campbell, S.G., Rowe, W., Zeef, L.A., Holmes, L.E., Hoyle, N.P., Bone, J., Selley, J.N., Sims, P.F., *et al.* (2011). Glucose depletion inhibits translation initiation via eIF4A loss and subsequent 48S preinitiation complex accumulation, while the pentose phosphate pathway is coordinately up-regulated. Molecular biology of the cell *22*, 3379-3393.

Chang, E., Yang, J., Nagavarapu, U., and Herron, G.S. (2002). Aging and survival of cutaneous microvasculature. The Journal of investigative dermatology *118*, 752-758.

Chen, Z., Odstrcil, E.A., Tu, B.P., and McKnight, S.L. (2007). Restriction of DNA replication to the reductive phase of the metabolic cycle protects genome integrity. Science *316*, 1916-1919.

Cho, R.J., Campbell, M.J., Winzeler, E.A., Steinmetz, L., Conway, A., Wodicka, L., Wolfsberg, T.G., Gabrielian, A.E., Landsman, D., Lockhart, D.J., *et al.* (1998). A genome-wide transcriptional analysis of the mitotic cell cycle. Mol Cell *2*, 65-73.

Choder, M. (1991). A general topoisomerase I-dependent transcriptional repression in the stationary phase in yeast. Genes & development *5*, 2315-2326.

Coller, J., and Parker, R. (2005). General translational repression by activators of mRNA decapping. Cell *122*, 875-886.

Costanzo, M., Nishikawa, J.L., Tang, X., Millman, J.S., Schub, O., Breitkreuz, K., Dewar, D., Rupes, I., Andrews, B., and Tyers, M. (2004). CDK activity antagonizes Whi5, an inhibitor of G1/S transcription in yeast. Cell *117*, 899-913.

Cross, F.R. (1988). DAF1, a mutant gene affecting size control, pheromone arrest, and cell cycle kinetics of Saccharomyces cerevisiae. Mol Cell Biol *8*, 4675-4684.

Cross, F.R. (1990). Cell cycle arrest caused by CLN gene deficiency in Saccharomyces cerevisiae resembles START-I arrest and is independent of the mating-pheromone signalling pathway. Mol Cell Biol *10*, 6482-6490.

Cross, F.R., and Blake, C.M. (1993). The yeast Cln3 protein is an unstable activator of Cdc28. Mol Cell Biol *13*, 3266-3271.

Cross, F.R., and Tinkelenberg, A.H. (1991). A potential positive feedback loop controlling CLN1 and CLN2 gene expression at the start of the yeast cell cycle. Cell *65*, 875-883.

Crowe, J.H., Hoekstra, F.A., and Crowe, L.M. (1992). Anhydrobiosis. Annual review of physiology *54*, 579-599.

Davidson, G.S., Joe, R.M., Roy, S., Meirelles, O., Allen, C.P., Wilson, M.R., Tapia, P.H., Manzanilla, E.E., Dodson, A.E., Chakraborty, S., *et al.* (2011). The proteomics of quiescent and nonquiescent cell differentiation in yeast stationary-phase cultures. Molecular biology of the cell *22*, 988-998.

de Bruin, R.A., McDonald, W.H., Kalashnikova, T.I., Yates, J., 3rd, and Wittenberg, C. (2004). Cln3 activates G1-specific transcription via phosphorylation of the SBF bound repressor Whi5. Cell *117*, 887-898.

De Virgilio, C. (2012). The essence of yeast quiescence. FEMS microbiology reviews *36*, 306-339.

De Virgilio, C., Hottiger, T., Dominguez, J., Boller, T., and Wiemken, A. (1994). The role of trehalose synthesis for the acquisition of thermotolerance in yeast. I. Genetic evidence that trehalose is a thermoprotectant. European journal of biochemistry / FEBS *219*, 179-186.

Decker, C.J., and Parker, R. (2012). P-bodies and stress granules: possible roles in the control of translation and mRNA degradation. Cold Spring Harbor perspectives in biology *4*, a012286.

Dirick, L., Bohm, T., and Nasmyth, K. (1995). Roles and regulation of Cln-Cdc28 kinases at the start of the cell cycle of Saccharomyces cerevisiae. EMBO J *14*, 4803-4813.

Dirick, L., and Nasmyth, K. (1991). Positive feedback in the activation of G1 cyclins in yeast. Nature *351*, 754-757.

Doncic, A., Falleur-Fettig, M., and Skotheim, J.M. (2011). Distinct interactions select and maintain a specific cell fate. Mol Cell *43*, 528-539.

Elbein, A.D., Pan, Y.T., Pastuszak, I., and Carroll, D. (2003). New insights on trehalose: a multifunctional molecule. Glycobiology *13*, 17R-27R.

Enjalbert, B., Parrou, J.L., Vincent, O., and Francois, J. (2000). Mitochondrial respiratory mutants of Saccharomyces cerevisiae accumulate glycogen and readily mobilize it in a glucose-depleted medium. Microbiology *146 (Pt 10)*, 2685-2694.

Erdag, G., Eroglu, A., Morgan, J., and Toner, M. (2002). Cryopreservation of fetal skin is improved by extracellular trehalose. Cryobiology *44*, 218-228.

Eser, U., Falleur-Fettig, M., Johnson, A., and Skotheim, J.M. (2011). Commitment to a cellular transition precedes genome-wide transcriptional change. Mol Cell *43*, 515-527.

Fabrizio, P., and Longo, V.D. (2007). The chronological life span of Saccharomyces cerevisiae. Methods in molecular biology *371*, 89-95.

Fernandez, E., Moreno, F., and Rodicio, R. (1992). The ICL1 gene from Saccharomyces cerevisiae. European journal of biochemistry / FEBS *204*, 983-990.

Ferrezuelo, F., Colomina, N., Futcher, B., and Aldea, M. (2010). The transcriptional network activated by Cln3 cyclin at the G1-to-S transition of the yeast cell cycle. Genome Biol *11*, R67.

Fleck, C.B., and Brock, M. (2009). Re-characterisation of Saccharomyces cerevisiae Ach1p: fungal CoA-transferases are involved in acetic acid detoxification. Fungal Genet Biol *46*, 473-485.

Francois, J., and Parrou, J.L. (2001). Reserve carbohydrates metabolism in the yeast Saccharomyces cerevisiae. FEMS microbiology reviews *25*, 125-145.

Friis, R.M., Glaves, J.P., Huan, T., Li, L., Sykes, B.D., and Schultz, M.C. (2014). Rewiring AMPK and mitochondrial retrograde signaling for metabolic control of aging and histone acetylation in respiratory-defective cells. Cell reports *7*, 565-574.

Fuge, E.K., Braun, E.L., and Werner-Washburne, M. (1994). Protein synthesis in long-term stationary-phase cultures of Saccharomyces cerevisiae. Journal of bacteriology *176*, 5802-5813.

Fujino, T., Kondo, J., Ishikawa, M., Morikawa, K., and Yamamoto, T.T. (2001). Acetyl-CoA synthetase 2, a mitochondrial matrix enzyme involved in the oxidation of acetate. J Biol Chem *276*, 11420-11426.

Futcher, B. (2006). Metabolic cycle, cell cycle, and the finishing kick to Start. Genome biology *7*, 107.

Gadd, G.M., Chalmers, K., and Reed, R.H. (1987). The role of trehalose in dehydration resistance of Saccharomyces cerevisiae. FEMS microbiology letters *48*, 249-254.

Gallego, C., Gari, E., Colomina, N., Herrero, E., and Aldea, M. (1997). The Cln3 cyclin is down-regulated by translational repression and degradation during the G1 arrest caused by nitrogen deprivation in budding yeast. EMBO J *16*, 7196-7206.

Gari, E., Volpe, T., Wang, H., Gallego, C., Futcher, B., and Aldea, M. (2001). Whi3 binds the mRNA of the G1 cyclin CLN3 to modulate cell fate in budding yeast. Genes Dev *15*, 2803-2808.

Gendron, C.M., Minois, N., Fabrizio, P., Longo, V.D., Pletcher, S.D., and Vaupel, J.W. (2003). Biodemographic trajectories of age-specific reproliferation from stationary phase in the yeast Saccharomyces cerevisiae seem multiphasic. Mech Ageing Dev *124*, 1059-1063.

Grant, P.A., Duggan, L., Cote, J., Roberts, S.M., Brownell, J.E., Candau, R., Ohba, R., Owen-Hughes, T., Allis, C.D., Winston, F., *et al.* (1997). Yeast Gcn5 functions in two multisubunit complexes to acetylate nucleosomal histones: characterization of an Ada complex and the SAGA (Spt/Ada) complex. Genes Dev *11*, 1640-1650.

Grant, P.A., Eberharter, A., John, S., Cook, R.G., Turner, B.M., and Workman, J.L. (1999). Expanded lysine acetylation specificity of Gcn5 in native complexes. J Biol Chem *274*, 5895-5900.

Grassi, I., Nanni, C., Allegri, V., Morigi, J.J., Montini, G.C., Castellucci, P., and Fanti, S. (2012). The clinical use of PET with (11)C-acetate. American journal of nuclear medicine and molecular imaging *2*, 33-47.

Gregory, P.D., Schmid, A., Zavari, M., Munsterkotter, M., and Horz, W. (1999). Chromatin remodelling at the PHO8 promoter requires SWI-SNF and SAGA at a step subsequent to activator binding. EMBO J *18*, 6407-6414.

Guillou, V., Plourde-Owobi, L., Parrou, J.L., Goma, G., and Francois, J. (2004). Role of reserve carbohydrates in the growth dynamics of Saccharomyces cerevisiae. FEMS yeast research *4*, 773-787.

Hall, D.D., Markwardt, D.D., Parviz, F., and Heideman, W. (1998). Regulation of the Cln3-Cdc28 kinase by cAMP in Saccharomyces cerevisiae. EMBO J *17*, 4370-4378.

Harbison, C.T., Gordon, D.B., Lee, T.I., Rinaldi, N.J., Macisaac, K.D., Danford, T.W., Hannett, N.M., Tagne, J.B., Reynolds, D.B., Yoo, J., *et al.* (2004). Transcriptional regulatory code of a eukaryotic genome. Nature *431*, 99-104.

Hengherr, S., Heyer, A.G., Kohler, H.R., and Schill, R.O. (2008). Trehalose and anhydrobiosis in tardigrades--evidence for divergence in responses to dehydration. The FEBS journal *275*, 281-288.

Hensley, C.T., Wasti, A.T., and DeBerardinis, R.J. (2013). Glutamine and cancer: cell biology, physiology, and clinical opportunities. J Clin Invest *123*, 3678-3684.

Higashiyama, T. (2002). Novel functions and applications of trehalose. Pure Appl Chem *74*, 1263-1269.

Higuchi, R., Vevea, J.D., Swayne, T.C., Chojnowski, R., Hill, V., Boldogh, I.R., and Pon, L.A. (2013). Actin dynamics affect mitochondrial quality control and aging in budding yeast. Current biology : CB *23*, 2417-2422.

Holmes, L.E., Campbell, S.G., De Long, S.K., Sachs, A.B., and Ashe, M.P. (2004). Loss of translational control in yeast compromised for the major mRNA decay pathway. Molecular and cellular biology *24*, 2998-3010.

Hottiger, T., De Virgilio, C., Hall, M.N., Boller, T., and Wiemken, A. (1994). The role of trehalose synthesis for the acquisition of thermotolerance in yeast. II. Physiological concentrations of trehalose increase the thermal stability of proteins in vitro. European journal of biochemistry / FEBS *219*, 187-193.

Hoyle, N.P., Castelli, L.M., Campbell, S.G., Holmes, L.E., and Ashe, M.P. (2007). Stress-dependent relocalization of translationally primed mRNPs to cytoplasmic granules that are kinetically and spatially distinct from P-bodies. The Journal of cell biology *179*, 65-74.

Hubler, L., Bradshaw-Rouse, J., and Heideman, W. (1993). Connections between the Ras-cyclic AMP pathway and G1 cyclin expression in the budding yeast Saccharomyces cerevisiae. Mol Cell Biol *13*, 6274-6282.

Hughes, A.L., and Gottschling, D.E. (2012). An early age increase in vacuolar pH limits mitochondrial function and lifespan in yeast. Nature *492*, 261-265.

Jazwinski, S.M. (2013). The retrograde response: when mitochondrial quality control is not enough. Biochimica et biophysica acta *1833*, 400-409.

Jorgensen, P., and Tyers, M. (2004). How cells coordinate growth and division. Curr Biol *14*, R1014-1027.

Kaeberlein, M., Andalis, A.A., Liszt, G.B., Fink, G.R., and Guarente, L. (2004). Saccharomyces cerevisiae SSD1-V confers longevity by a Sir2p-independent mechanism. Genetics *166*, 1661-1672.

Kandror, O., Bretschneider, N., Kreydin, E., Cavalieri, D., and Goldberg, A.L. (2004). Yeast adapt to near-freezing temperatures by STRE/Msn2,4-dependent induction of trehalose synthesis and certain molecular chaperones. Molecular cell *13*, 771-781.

Kasahara, K., Ohtsuki, K., Ki, S., Aoyama, K., Takahashi, H., Kobayashi, T., Shirahige, K., and Kokubo, T. (2007). Assembly of regulatory factors on rRNA and ribosomal protein genes in Saccharomyces cerevisiae. Mol Cell Biol *27*, 6686-6705.

Kaspar von Meyenburg, H. (1969). Energetics of the budding cycle of Saccharomyces cerevisiae during glucose limited aerobic growth. Archiv fur Mikrobiologie *66*, 289-303.

Kim, J.H., Saraf, A., Florens, L., Washburn, M., and Workman, J.L. (2010). Gcn5 regulates the dissociation of SWI/SNF from chromatin by acetylation of Swi2/Snf2. Genes Dev *24*, 2766-2771.

Koch, C., Moll, T., Neuberg, M., Ahorn, H., and Nasmyth, K. (1993). A role for the transcription factors Mbp1 and Swi4 in progression from G1 to S phase. Science *261*, 1551-1557.

Kuo, M.H., and Grayhack, E. (1994). A library of yeast genomic MCM1 binding sites contains genes involved in cell cycle control, cell wall and membrane structure, and metabolism. Mol Cell Biol *14*, 348-359.

Kurtz, S., and Shore, D. (1991). RAP1 protein activates and silences transcription of mating-type genes in yeast. Genes & development *5*, 616-628.

Lai, C.Y., Jaruga, E., Borghouts, C., and Jazwinski, S.M. (2002). A mutation in the ATP2 gene abrogates the age asymmetry between mother and daughter cells of the yeast Saccharomyces cerevisiae. Genetics *162*, 73-87.

Langer, M.R., Fry, C.J., Peterson, C.L., and Denu, J.M. (2002). Modulating acetyl-CoA binding in the GCN5 family of histone acetyltransferases. J Biol Chem *277*, 27337-27344.

Lavoie, H., Hogues, H., Mallick, J., Sellam, A., Nantel, A., and Whiteway, M. (2010). Evolutionary tinkering with conserved components of a transcriptional regulatory network. PLoS Biol *8*, e1000329.

Lee, T.I., Rinaldi, N.J., Robert, F., Odom, D.T., Bar-Joseph, Z., Gerber, G.K., Hannett, N.M., Harbison, C.T., Thompson, C.M., Simon, I., *et al.* (2002). Transcriptional regulatory networks in Saccharomyces cerevisiae. Science *298*, 799-804.

Lemons, J.M., Feng, X.J., Bennett, B.D., Legesse-Miller, A., Johnson, E.L., Raitman, I., Pollina, E.A., Rabitz, H.A., Rabinowitz, J.D., and Coller, H.A. (2010). Quiescent fibroblasts exhibit high metabolic activity. PLoS biology *8*, e1000514.

Lewis, K. (2007). Persister cells, dormancy and infectious disease. Nature reviews Microbiology *5*, 48-56.

Li, L., Lu, Y., Qin, L.X., Bar-Joseph, Z., Werner-Washburne, M., and Breeden, L.L. (2009). Budding yeast SSD1-V regulates transcript levels of many longevity genes and extends chronological life span in purified quiescent cells. Molecular biology of the cell *20*, 3851-3864.

Li, L., Miles, S., Melville, Z., Prasad, A., Bradley, G., and Breeden, L.L. (2013). Key events during the transition from rapid growth to quiescence in budding yeast require posttranscriptional regulators. Molecular biology of the cell *24*, 3697-3709.

Lillie, S.H., and Pringle, J.R. (1980). Reserve carbohydrate metabolism in Saccharomyces cerevisiae: responses to nutrient limitation. Journal of bacteriology *143*, 1384-1394.

Lin, Y.Y., Lu, J.Y., Zhang, J., Walter, W., Dang, W., Wan, J., Tao, S.C., Qian, J., Zhao, Y., Boeke, J.D., *et al.* (2009). Protein acetylation microarray reveals that NuA4 controls key metabolic target regulating gluconeogenesis. Cell *136*, 1073-1084.

Liu, X.H., Aksan, A., Menze, M.A., Hand, S.C., and Toner, M. (2005). Trehalose loading through the mitochondrial permeability transition pore enhances desiccation tolerance in rat liver mitochondria. Biochimica et biophysica acta *1717*, 21-26.

Longtine, M.S., McKenzie, A., 3rd, Demarini, D.J., Shah, N.G., Wach, A., Brachat, A., Philippsen, P., and Pringle, J.R. (1998). Additional modules for versatile and economical PCR-based gene deletion and modification in Saccharomyces cerevisiae. Yeast *14*, 953-961.

Lu, C., Brauer, M.J., and Botstein, D. (2009). Slow growth induces heat-shock resistance in normal and respiratory-deficient yeast. Molecular biology of the cell *20*, 891-903.

Luong, A., Hannah, V.C., Brown, M.S., and Goldstein, J.L. (2000). Molecular characterization of human acetyl-CoA synthetase, an enzyme regulated by sterol regulatory element-binding proteins. J Biol Chem *275*, 26458-26466.

MacKay, V.L., Mai, B., Waters, L., and Breeden, L.L. (2001). Early cell cycle box-mediated transcription of CLN3 and SWI4 contributes to the proper timing of the G(1)-to-S transition in budding yeast. Mol Cell Biol *21*, 4140-4148.

Mai, B., Miles, S., and Breeden, L.L. (2002). Characterization of the ECB binding complex responsible for the M/G(1)-specific transcription of CLN3 and SWI4. Mol Cell Biol *22*, 430-441.

McInerny, C.J., Partridge, J.F., Mikesell, G.E., Creemer, D.P., and Breeden, L.L. (1997). A novel Mcm1-dependent element in the SWI4, CLN3, CDC6, and CDC47 promoters activates M/G1-specific transcription. Genes Dev *11*, 1277-1288.

Miller, M.E., and Cross, F.R. (2001). Mechanisms controlling subcellular localization of the G(1) cyclins Cln2p and Cln3p in budding yeast. Mol Cell Biol *21*, 6292-6311.

Nash, R., Tokiwa, G., Anand, S., Erickson, K., and Futcher, A.B. (1988). The WHI1+ gene of Saccharomyces cerevisiae tethers cell division to cell size and is a cyclin homolog. EMBO J *7*, 4335-4346.

Nasmyth, K., and Dirick, L. (1991). The role of SWI4 and SWI6 in the activity of G1 cyclins in yeast. Cell *66*, 995-1013.

Newcomb, L.L., Diderich, J.A., Slattery, M.G., and Heideman, W. (2003). Glucose regulation of Saccharomyces cerevisiae cell cycle genes. Eukaryot Cell *2*, 143-149.

Newcomb, L.L., Hall, D.D., and Heideman, W. (2002). AZF1 is a glucose-dependent positive regulator of CLN3 transcription in Saccharomyces cerevisiae. Mol Cell Biol *22*, 1607-1614.

Noubhani, A., Bunoust, O., Bonini, B.M., Thevelein, J.M., Devin, A., and Rigoulet, M. (2009). The trehalose pathway regulates mitochondrial respiratory chain content through hexokinase 2 and cAMP in Saccharomyces cerevisiae. The Journal of biological chemistry *284*, 27229-27234.

Ocampo, A., Liu, J., Schroeder, E.A., Shadel, G.S., and Barrientos, A. (2012). Mitochondrial respiratory thresholds regulate yeast chronological life span and its extension by caloric restriction. Cell metabolism *16*, 55-67.

Parrou, J.L., and Francois, J. (1997). A simplified procedure for a rapid and reliable assay of both glycogen and trehalose in whole yeast cells. Analytical biochemistry *248*, 186-188.

Parulekar, S.J., Semones, G.B., Rolf, M.J., Lievense, J.C., and Lim, H.C. (1986). Induction and elimination of oscillations in continuous cultures of Saccharomyces cerevisiae. Biotechnology and bioengineering *28*, 700-710.

Parviz, F., Hall, D.D., Markwardt, D.D., and Heideman, W. (1998). Transcriptional regulation of CLN3 expression by glucose in Saccharomyces cerevisiae. J Bacteriol *180*, 4508-4515.

Parviz, F., and Heideman, W. (1998). Growth-independent regulation of CLN3 mRNA levels by nutrients in Saccharomyces cerevisiae. J Bacteriol *180*, 225-230.

Perez-Chacon, G., Astudillo, A.M., Balgoma, D., Balboa, M.A., and Balsinde, J. (2009). Control of free arachidonic acid levels by phospholipases A2 and lysophospholipid acyltransferases. Biochim Biophys Acta *1791*, 1103-1113.

Pfau, S.J., and Amon, A. (2012). Chromosomal instability and aneuploidy in cancer: from yeast to man. EMBO reports *13*, 515-527.

Pinon, R. (1978). Folded chromosomes in non-cycling yeast cells: evidence for a characteristic g0 form. Chromosoma *67*, 263-274.

Polymenis, M., and Schmidt, E.V. (1997). Coupling of cell division to cell growth by translational control of the G1 cyclin CLN3 in yeast. Genes Dev *11*, 2522-2531.

Porro, D., Martegani, E., Ranzi, B.M., and Alberghina, L. (1988). Oscillations in continuous cultures of budding yeast: a segregated parameter analysis. Biotechnology and bioengineering *32*, 411-417.

Powers, R.W., 3rd, Kaeberlein, M., Caldwell, S.D., Kennedy, B.K., and Fields, S. (2006). Extension of chronological life span in yeast by decreased TOR pathway signaling. Genes & development *20*, 174-184.

Rhee, H.S., and Pugh, B.F. (2011). Comprehensive genome-wide protein-DNA interactions detected at single-nucleotide resolution. Cell *147*, 1408-1419.

Ribeiro, M.J., Reinders, A., Boller, T., Wiemken, A., and De Virgilio, C. (1997). Trehalose synthesis is important for the acquisition of thermotolerance in Schizosaccharomyces pombe. Molecular microbiology *25*, 571-581.

Rodriguez-Navarro, S., Fischer, T., Luo, M.J., Antunez, O., Brettschneider, S., Lechner, J., Perez-Ortin, J.E., Reed, R., and Hurt, E. (2004). Sus1, a functional component of the SAGA histone acetylase complex and the nuclear pore-associated mRNA export machinery. Cell *116*, 75-86.

Rowicka, M., Kudlicki, A., Tu, B.P., and Otwinowski, Z. (2007). High-resolution timing of cell cycle-regulated gene expression. Proc Natl Acad Sci U S A *104*, 16892-16897.

Rudra, D., Zhao, Y., and Warner, J.R. (2005). Central role of Ifh1p-Fhl1p interaction in the synthesis of yeast ribosomal proteins. EMBO J *24*, 533-542.

Santangelo, G.M. (2006). Glucose signaling in Saccharomyces cerevisiae. Microbiology and molecular biology reviews : MMBR *70*, 253-282.

Satroutdinov, A.D., Kuriyama, H., and Kobayashi, H. (1992). Oscillatory metabolism of Saccharomyces cerevisiae in continuous culture. FEMS microbiology letters *77*, 261-267.

Schawalder, S.B., Kabani, M., Howald, I., Choudhury, U., Werner, M., and Shore, D. (2004). Growth-regulated recruitment of the essential yeast ribosomal protein gene activator Ifh1. Nature *432*, 1058-1061.

Shi, L., Sutter, B.M., Ye, X., and Tu, B.P. (2010). Trehalose is a key determinant of the quiescent metabolic state that fuels cell cycle progression upon return to growth. Molecular biology of the cell *21*, 1982-1990.

Shukla, A., Bajwa, P., and Bhaumik, S.R. (2006). SAGA-associated Sgf73p facilitates formation of the preinitiation complex assembly at the promoters either in a HAT-dependent or independent manner in vivo. Nucleic Acids Res *34*, 6225-6232.

Sillje, H.H., Paalman, J.W., ter Schure, E.G., Olsthoorn, S.Q., Verkleij, A.J., Boonstra, J., and Verrips, C.T. (1999). Function of trehalose and glycogen in cell cycle progression and cell viability in Saccharomyces cerevisiae. Journal of bacteriology *181*, 396-400.

Sillje, H.H., ter Schure, E.G., Rommens, A.J., Huls, P.G., Woldringh, C.L., Verkleij, A.J., Boonstra, J., and Verrips, C.T. (1997). Effects of different carbon fluxes on G1 phase duration, cyclin expression, and reserve carbohydrate metabolism in Saccharomyces cerevisiae. Journal of bacteriology *179*, 6560-6565.

Singer, M.A., and Lindquist, S. (1998a). Multiple effects of trehalose on protein folding in vitro and in vivo. Molecular cell *1*, 639-648.

Singer, M.A., and Lindquist, S. (1998b). Thermotolerance in Saccharomyces cerevisiae: the Yin and Yang of trehalose. Trends in biotechnology *16*, 460-468.

Skotheim, J.M., Di Talia, S., Siggia, E.D., and Cross, F.R. (2008). Positive feedback of G1 cyclins ensures coherent cell cycle entry. Nature *454*, 291-296.

Spellman, P.T., Sherlock, G., Zhang, M.Q., Iyer, V.R., Anders, K., Eisen, M.B., Brown, P.O., Botstein, D., and Futcher, B. (1998). Comprehensive identification of cell cycle-regulated genes of the yeast Saccharomyces cerevisiae by microarray hybridization. Mol Biol Cell *9*, 3273-3297.

Steinmetz, L.M., Scharfe, C., Deutschbauer, A.M., Mokranjac, D., Herman, Z.S., Jones, T., Chu, A.M., Giaever, G., Prokisch, H., Oefner, P.J., *et al.* (2002). Systematic screen for human disease genes in yeast. Nature genetics *31*, 400-404.

Stuart, D., and Wittenberg, C. (1995). CLN3, not positive feedback, determines the timing of CLN2 transcription in cycling cells. Genes Dev *9*, 2780-2794.

Suda, T., Arai, F., and Hirao, A. (2005). Hematopoietic stem cells and their niche. Trends in immunology *26*, 426-433.

Sudarsanam, P., Cao, Y., Wu, L., Laurent, B.C., and Winston, F. (1999). The nucleosome remodeling complex, Snf/Swi, is required for the maintenance of transcription in vivo and is partially redundant with the histone acetyltransferase, Gcn5. EMBO J *18*, 3101-3106.

Takahashi, H., McCaffery, J.M., Irizarry, R.A., and Boeke, J.D. (2006). Nucleocytosolic acetyl-coenzyme a synthetase is required for histone acetylation and global transcription. Mol Cell *23*, 207-217.

Talarek, N., Cameroni, E., Jaquenoud, M., Luo, X., Bontron, S., Lippman, S., Devgan, G., Snyder, M., Broach, J.R., and De Virgilio, C. (2010). Initiation of the TORC1-regulated G0 program requires Igo1/2, which license specific mRNAs to evade degradation via the 5'-3' mRNA decay pathway. Molecular cell *38*, 345-355.

Tareen, N., Zadshir, A., Martins, D., Nagami, G., Levine, B., and Norris, K.C. (2004). Alterations in acid-base homeostasis with aging. J Natl Med Assoc *96*, 921-925; quiz 925-926.

Teixeira, M.C., Monteiro, P., Jain, P., Tenreiro, S., Fernandes, A.R., Mira, N.P., Alenquer, M., Freitas, A.T., Oliveira, A.L., and Sa-Correia, I. (2006). The YEASTRACT database: a tool for the analysis of transcription regulatory associations in Saccharomyces cerevisiae. Nucleic acids research *34*, D446-451.

Thevelein, J.M., and Hohmann, S. (1995). Trehalose synthase: guard to the gate of glycolysis in yeast? Trends in biochemical sciences *20*, 3-10.

Trievel, R.C., Rojas, J.R., Sterner, D.E., Venkataramani, R.N., Wang, L., Zhou, J., Allis, C.D., Berger, S.L., and Marmorstein, R. (1999). Crystal structure and mechanism of histone acetylation of the yeast GCN5 transcriptional coactivator. Proc Natl Acad Sci U S A *96*, 8931-8936.

Tu, B.P., Kudlicki, A., Rowicka, M., and McKnight, S.L. (2005). Logic of the yeast metabolic cycle: temporal compartmentalization of cellular processes. Science *310*, 1152-1158.

Tu, B.P., and McKnight, S.L. (2006). Metabolic cycles as an underlying basis of biological oscillations. Nature reviews Molecular cell biology *7*, 696-701.

Tu, B.P., and McKnight, S.L. (2007). The yeast metabolic cycle: insights into the life of a eukaryotic cell. Cold Spring Harbor symposia on quantitative biology *72*, 339-343.

Tu, B.P., Mohler, R.E., Liu, J.C., Dombek, K.M., Young, E.T., Synovec, R.E., and McKnight, S.L. (2007). Cyclic changes in metabolic state during the life of a yeast cell. Proceedings of the National Academy of Sciences of the United States of America *104*, 16886-16891.

Turner, J.J., Ewald, J.C., and Skotheim, J.M. (2012). Cell size control in yeast. Curr Biol *22*, R350-359.

Tyers, M., Tokiwa, G., and Futcher, B. (1993). Comparison of the Saccharomyces cerevisiae G1 cyclins: Cln3 may be an upstream activator of Cln1, Cln2 and other cyclins. EMBO J *12*, 1955-1968.

Tyers, M., Tokiwa, G., Nash, R., and Futcher, B. (1992). The Cln3-Cdc28 kinase complex of S. cerevisiae is regulated by proteolysis and phosphorylation. EMBO J *11*, 1773-1784.

Uno, I., Matsumoto, K., Adachi, K., and Ishikawa, T. (1983). Genetic and biochemical evidence that trehalase is a substrate of cAMP-dependent protein kinase in yeast. The Journal of biological chemistry *258*, 10867-10872.

Utley, R.T., Ikeda, K., Grant, P.A., Cote, J., Steger, D.J., Eberharter, A., John, S., and Workman, J.L. (1998). Transcriptional activators direct histone acetyltransferase complexes to nucleosomes. Nature *394*, 498-502.

van der Plaat, J.B. (1974). Cyclic 3',5'-adenosine monophosphate stimulates trehalose degradation in baker's yeast. Biochemical and biophysical research communications *56*, 580-587.

van Dijken, J.P., Bauer, J., Brambilla, L., Duboc, P., Francois, J.M., Gancedo, C., Giuseppin, M.L., Heijnen, J.J., Hoare, M., Lange, H.C., *et al.* (2000). An interlaboratory comparison of physiological and genetic properties of four Saccharomyces cerevisiae strains. Enzyme and microbial technology *26*, 706-714.

Veatch, J.R., McMurray, M.A., Nelson, Z.W., and Gottschling, D.E. (2009). Mitochondrial dysfunction leads to nuclear genome instability via an iron-sulfur cluster defect. Cell *137*, 1247-1258.

Verges, E., Colomina, N., Gari, E., Gallego, C., and Aldea, M. (2007). Cyclin Cln3 is retained at the ER and released by the J chaperone Ydj1 in late G1 to trigger cell cycle entry. Mol Cell *26*, 649-662.

Wade, J.T., Hall, D.B., and Struhl, K. (2004). The transcription factor Ifh1 is a key regulator of yeast ribosomal protein genes. Nature *432*, 1054-1058.

Wang, H., Gari, E., Verges, E., Gallego, C., and Aldea, M. (2004). Recruitment of Cdc28 by Whi3 restricts nuclear accumulation of the G1 cyclin-Cdk complex to late G1. EMBO J *23*, 180-190.

Wang, Q., Zhang, Y., Yang, C., Xiong, H., Lin, Y., Yao, J., Li, H., Xie, L., Zhao, W., Yao, Y., *et al.* (2010). Acetylation of metabolic enzymes coordinates carbon source utilization and metabolic flux. Science *327*, 1004-1007.

Wellen, K.E., Hatzivassiliou, G., Sachdeva, U.M., Bui, T.V., Cross, J.R., and Thompson, C.B. (2009). ATP-citrate lyase links cellular metabolism to histone acetylation. Science *324*, 1076-1080.

Werner-Washburne, M., Braun, E., Johnston, G.C., and Singer, R.A. (1993). Stationary phase in the yeast Saccharomyces cerevisiae. Microbiological reviews *57*, 383-401.

Werner-Washburne, M., Wylie, B., Boyack, K., Fuge, E., Galbraith, J., Weber, J., and Davidson, G. (2002). Comparative analysis of multiple genome-scale data sets. Genome Res *12*, 1564-1573.

Wijnen, H., Landman, A., and Futcher, B. (2002). The G(1) cyclin Cln3 promotes cell cycle entry via the transcription factor Swi6. Mol Cell Biol *22*, 4402-4418.

Wu, M., Newcomb, L., and Heideman, W. (1999). Regulation of gene expression by glucose in Saccharomyces cerevisiae: a role for ADA2 and ADA3/NGG1. J Bacteriol *181*, 4755-4760.

Wu, P.Y., and Winston, F. (2002). Analysis of Spt7 function in the Saccharomyces cerevisiae SAGA coactivator complex. Mol Cell Biol *22*, 5367-5379.

Xu, Z., and Tsurugi, K. (2006). A potential mechanism of energy-metabolism oscillation in an aerobic chemostat culture of the yeast Saccharomyces cerevisiae. The FEBS journal *273*, 1696-1709.

Yaglom, J., Linskens, M.H., Sadis, S., Rubin, D.M., Futcher, B., and Finley, D. (1995). p34Cdc28-mediated control of Cln3 cyclin degradation. Mol Cell Biol *15*, 731-741.

Yamaguchi, R., Andreyev, A., Murphy, A.N., Perkins, G.A., Ellisman, M.H., and Newmeyer, D.D. (2007). Mitochondria frozen with trehalose retain a number of biological functions and preserve outer membrane integrity. Cell death and differentiation *14*, 616-624.

Zhao, S., Xu, W., Jiang, W., Yu, W., Lin, Y., Zhang, T., Yao, J., Zhou, L., Zeng, Y., Li, H., *et al.* (2010). Regulation of cellular metabolism by protein lysine acetylation. Science *327*, 1000-1004.

Zhou, X., Yuan, J., Liu, J., and Liu, B. (2010). Loading trehalose into red blood cells by electroporation and its application in freeze-drying. Cryo letters *31*, 147-156.